University of Alberta

Copyrolysis of bitumen and oxygenate containing materials at low temperature

by

Elaheh Toosi

A thesis submitted to the Faculty of Graduate Studies and Research
in partial fulfillment of the requirements for the degree of

Master of Science

in

Chemical Engineering

Department of Chemical and Materials Engineering

©Elaheh Toosi
Fall 2013
Edmonton, Alberta

DEDICATION

To whom I never can exist spiritually without, who taught me what love and life are, whose true generosities are obvious even in their eyes, my lovely mom, my lovely dad and my lovely sister.

Abstract

Bitumen, as one of the most important unconventional sources of energy, has long been an attractive source for production of liquid fuels. It is important to improve the yield and quality of the useful products resulting from bitumen upgrading processes so that the best outcome can be achieved with the least capital cost. It has been shown in literature that if the thermal upgrading processes are performed at lower temperature (below 400 °C), the obtained liquid yield can be improved. However, the low temperature slows down the rates and in general low temperature processes are less likely to be economical in industry. If this rate-challenge can be overcome, it is more beneficial to operate the bitumen upgrading processes at lower temperature. The working hypothesis was that oxygenate containing compounds, which are more reactive for thermal conversion, can be used to increase the overall reaction rate of bitumen conversion at lower temperature. This thesis studied the effect of co-processing some oxygenate containing materials with bitumen, namely, different coal and biomass derived materials.

Acknowledgments

Firstly, I would like to say great thanks to my supervisor, Dr. Arno De Klerk for his great support and guidance during my entire master program. I will always remember his admirable patience and his nice attitude to me. And I really appreciate for all the time he has given to my project. Also, I would like to thank my co-supervisor, Dr. William McCaffrey for his support and guidance. Without their both kind supervisory this study could not be done.

Secondly, I would like to thank Dr. Shaofeng Yang and Lisa Brandt for their guidance.

Thirdly, I would like to give great thanks to my dear friend Korel Dawkins for her great help in revising my thesis and to my friend Ladan Shamaei in helping me with the gas analysis.

The last but not the least, I should say that thanks would be nothing in comparison to the love that my mother, father and my sister have given to me. In every moment, in all the successes and failures, they were them who lightened the pass of my life with their honest bright love .Their incredible magic motivation has always fulfilled me with an enjoyable strength which warms my heart and lets me keep trying hard. I owe my sincerest gratitude to my mother, father and Parisa (my sister) whose kind supports have been always with me.

Table of Contents

List of Tables

List of Figures

1.   CHAPTER 1: INTRODUCTION

1.1   Background

1.1.1   Oil sand derived bitumen

The need for unconventional resources of energy increases every day and as a result much attention is focused on unconventional energy resources. One of the resources that has a great impact on the North American economy is bitumen. It is notable that more than 95% of the world's bitumen resources are in North America (Hein 2006a). There are about fifteen oil sand sources in Alberta. These are located in three regions: Athabasca, Cold Lake and Peace River. The largest oil sand reserve is in Athabasca (Hein 2006b). Today, about half of Canada's crude oil comes from oil sand. This includes bitumen and synthetic crude oil.

Oil sand is a mixture of clay, sand and some amount of petroleum called bitumen. Bitumen can be extracted from oil sand or by in situ extraction methods such as Steam Assisted Gravity Drainage (SAGD) and Cyclic Steam Stimulation (CSS). The SAGD method uses two horizontal wells. One sits on top of the other. The top well stimulates the steam, causing oil to reduce its viscosity and enabling it to be pumped from the bottom well to the surface. In CSS, steam is injected through a vertical well into an oil reservoir. This process makes the oil less viscous, which allows it to be collected from the same vertical well to the surface.

After coke (coke is a solid residue obtained from petroleum materials), bitumen has the highest average molecular weight of crude oil products. It is dense and rich in heteroatoms such as nitrogen, oxygen, sulphur (NOS) and metals (Strausz, et al. 2003). Bitumen has properties which make it different from other

materials; it is highly viscous and it is hard to pump. Also, it is dense and its fractions have high boiling points. Bitumen is mainly used for pavement construction (Carrera, et al. 2010). The petroleum industry uses it as a feed stock to produce synthetic products. Bitumen on its own might not be useful, plus its viscosity is too high, making it difficult to pump; therefore, some characteristics of bitumen must change by some reactions. Generally, upgrading is used to change the original feed to more profitable products such as synthetic crude oil.

1.1.2   Bitumen upgrading and its transportation

Because of its specifications, the raw bitumen is not as useful as bitumen upgrading final products.For example, its carbon-to-hydrogen ratio content is too high and its boiling point is relatively higher than regular fuels used in industry. However, it has the potential to be converted to lighter fractions with a lower carbon-to-hydrogen ratio. Upgraing is the term used to describe the methods used to change bitumen to more advantageous products. Upgrading has two main goals: to produce compounds whose boiling points are lower than that of bitumen; and to improve the hydrogen-to-carbon ratio by rejecting carbon (coking) or increasing the hydrogen content (Speight 1998).

The mixture of bitumen and crude oils are transported through pipelines. Bitumen`s high viscosity makes it difficult to transport through pipelines; a diluent is usually added to aid the process. The diluent (which is also added to heavy oil) is usually a natural gas condensate or a petroleum-derived light hydrocarbon.

1.1.3 Bitumen thermal cracking

The most common upgrading method is thermal cracking. It is used in many industries to upgrade bitumen to more valuable products. In thermal cracking, thermal energy is used to break bitumen's large molecules into smaller ones. Petroleum residue on its own does not have much value; however, its value increases when it is converted to a product with lower viscosity and lighter materials. The liquid products of the cracking reactions are mainly naphtha, motor gasoline, jet fuel and diesel fuel. These have lower boiling points than the residue feed.

Bitumen consists of a large fraction of atmospheric residue. Petroleum residue contains heteroatoms and some metal content and has a high Conradson Carbon Residue (CCR). CCR is a parameter determined by a standard method. It shows the percentage of the coked materials that remains after the specific standard method is applied. CCR is an indication which shows the oil's ability to form solids (coke) during thermal processing. For bitumen to produce more valuable products, its boiling point distribution must decrease. The most suitable thermal conversion technologies that change bitumen's undesirable characteristics to more valuable products are visbreaking, coking and residue hydroconversion. Brief descriptions of the reasons these technologies are used for bitumen upgrading are discussed in the following paragraphs.

Visbreaking deals with the molecular mass of the feed. It provides a mild thermal cracking and finally lowers the residue's viscosity until it can be used as a fuel oil. The basis of the coking process is carbon rejection. The main reaction that happens in coking is the aromatization in which metals and some heteroatoms are trapped in the solid product (coke). The solid byproduct is undesirable and contains high molecular weight products with much amount of minerals; therefore coke must be separated from the rest of the products. Removing the coke causes the remaining liquid product to have a higher H/C

ratio which is an advantage because increasing H/C ratio is one of the targets in upgrading. Coking also has another positive point which is capturing the carbon dioxide. When a large amount of carbon is rejected in the coke format, there is not much chance of CO_2 production.

In the residue hydroconversion process, hydrogen is added to the residue while the residue is being cracked. Residue fractions have the highest heteroatom amounts, and as the boiling point decreases, the fraction's heteroatom content also decreases (Wauquier 1995). The main goal in residue hydroconversion is to lower the residue's heteroatom content by cracking it to light fractions with the addition of hydrogen.

Catalytic residue conversion is another thermal conversion technology which is less suitable for direct bitumen upgrading because the presence of metals cause fouling. Fouling is a challenge because the metals in the residue deactivate the catalysts' active sites. Also, large molecules do not have proper access to the catalytic sites to work efficiently in narrow pores. And the heteroatoms in molecules are positioned in such a way that the molecules cannot have direct access to catalytic surface and hence cannot be converted by catalysts. For these reasons catalytic upgrading is not a suitable application.

1.1.4   Thermal upgrading challenges

There are some challenges that face the upgrading technologies. For example, supplying hydrogen as an additive gas in the residue hydroconversion method is expensive. Free radical addition reaections during thermal cracking also cause problem in thermal upgrading techniques. When the residue molecules are heated, free radicals start to form. Although free radicals allow the light fractions such as naphtha and olefins to be produced, they may also combine with each other and cause unwanted reactions. The unwanted reactions produce heavy

products which are neither desirable nor valuable. The key challenge in thermal upgrading is to stabilize free radicals, thus limiting the additional reactions.

1.1.5   Objectives and challenges for low temperature upgrading

In the literature, it has been observed that the liquid yield obtained during thermal conversion can be improved by performing thermal upgrading at lower temperatures (Dutta, *et al.* 2000). However, some challenges exist for low temperature processes operating at below 400 °C. If the challenges can be overcome, obviously it is logical to perform upgrading technologies at lower temperatures to obtain higher liquid yields. The challenge behind the thermal upgrading at a low temperature is that as the temperature decreases, the conversion rate also decreases. If no solution is found to compensate for the low conversion rate at low temperature conditions, the capital cost will increase for the same production rate. Therefore, it is significant to find a solution to this challenge.

To achieve low temperature thermal upgrading in practice and develop a process that can be industrially applied, the kinetics must be improved to compensate for the decrease in rates. It has been shown in literature that the kinetics of bitumen pyrolysis at lower temperatures can be increased by copyrolysis with more reactive oxygenate rich materials (Pyrolysis is a thermal cracking process without the presence of oxygen).

Oxygenate rich materials have a special feature: carbon-oxygen bonds. These bonds require less bond dissociation energy than the Carbon-Carbon and Carbon-Hydrogen bonds. Adding the named materials enables free radical decomposition to occur at lower temperatures. Setting the initiation step at lower temperatures does not mean that the propagation step and, in general, the total

5

conversion rate would be accelerated; however, it is the first step toward enabling low-temperature bitumen upgrading. Bitumen has some C-O bonds, and when an additive with a larger number of these bonds is combined with bitumen, the free radical decomposition rate is increased, and thereby the conversion rate at low temperature will also increase.

1.2   Objectives

Low temperature (380-390 °C) pyrolysis of oil-sands-derived bitumen was studied as a strategy to increase liquid yield and decrease coke yield during thermal upgrading. In support of this objective, we studied the copyrolysis of oxygenate-containing materials with bitumen. The idea behind copyrolysis of oxygenate-containing materials is to increase the rate of thermal conversion to compensate for the decrease in conversion rate caused by lowering the pyrolysis temperature. Also, the quality of the products has been studied by observing what percentages of the products are light or heavy fractions. Moreover, the elemental analysis of the samples was studied to see if the additives would lower the unwanted heteroatoms as well.

1.3   Scope of work

In this study, bitumen was used as the main feed. It was pyrolysed for one hour at 380 °C. After that, the liquid and the gas products were collected for further analysis. The oxygenate-containing materials used included some coal and biomass samples, and partially oxidized bitumen. The coal samples included subbituminous coal, bituminous coal and lignite. The biomass samples include lignin and cellulose. All of these additives were added separately to bitumen at a

ratio of 1 to 9. In this study, both the raw mixtures and the pyrolysed mixture samples were studied.

Chapter 2 contains more detailed descriptions of the literature dealing with the different feed materials considered for pyrolysis. The chapter also includes an overview of pyrolysis, products from pyrolysis and the free radical chemistry related to pyrolysis.

The experimental investigation was organized by the nature of the techniques employed. The bulk of the experimental detail was reported first (see Chapter 3) and contains a description of the materials that were used, the equipment, experimental and analytical procedures, and calculations and definitions. The experimental investigations were categorized as below:

i.   Thermal analysis (Chapter 4)
ii.   Gas analysis (Chapter 5)
iii. Simulated distillation analysis (Chapter 6)
iv.   Elemental analysis (Chapter 7)

1.4   References:

Carrera, V.; Garcia-Morales, M.; Navarro, F.; Partal, P. L; Gallegos, C. Bitumen Chemical Foaming for Asphalt Paving Applications. *Ind. Eng. Chem*. **2010**, *49*, 8538- 8543

Dutta, R. P.; McCaffrey, W. C.; Gray, M. R.; Muehlenbachs, K. Thermal Cracking of Athabsca Bitumen: Influence of Steam on Reaction Chemistry. *Energy Fuels.* **2000**, *14*, 671-676.

Hein, J. F. Heavy Oil and Oil (Tar) Sands in North America: An Overview & Summary of Contributions. *Natural Resources Research.* **2006**, *15*, 67 -84

Hein, J. F.; Cotterill, K. D. The Athabasca Oil Sands-A regional Geological Perspective, Fort McMurray Area, Alberta, Canada. *Natural Resources Research*. **2006**, *15*, 85-102

Speight, J. G. *Petroleum chemistry and refining*. Taylor & Francis. 1st ed; CRC Press, 1998.

Strausz, O.P.; Lown, E. M. The chemistry of Alberta Oil Sands Bitumens and Heavy Oils. Alberta Energy Research Institute. 2003

Wauquier, J. P. Evaluation of crude oils. In *Petroleum Refining Vol. 1*; BBS. Ed.; Editions Technip: Paris, 1995, p .315-317.

2.   CHAPTER 2: LITERATURE REVIEW

2.1   Introduction

In this study, copyrolysis of bitumen and oxygenate-containing materials have been studied with the objectives of increasing the liquid yield and light fractions, decreasing the coke yield, accelerating the conversion rates and lowering the products' heteroatoms. The pyrolysis reactions were done in micro reactors at 380 ℃ for one hour and the products were collected and analyzed in order to obtain the coke and liquid yields. The liquid products were analyzed to study the amounts obtained in the simulated distillation cuts and also to study the hetero atom percentages in the liquid products.

In its raw state, bitumen is a source of energy but it cannot be used directly as an energy carrier fuel. Some changes must be applied to change it to useful products such as different kinds of fuels. The changes that transform bitumen from an energy source to energy carrier fuels are part of a process called refining. To understand the refining process, the raw materials characterization must be clear.

In the following sections, bitumen (as the main feed) and its characterization are discussed. This discussion will be followed by a section about the other raw materials (which were used as additives). Section four describes pyrolysis (the reaction that changes bitumen to the final products). Section four also contains literature about the free radical mechanism that happens during the pyrolysis reaction. The last section describes investigations of thermal analysis techniques that have been used in the literature, as well as the parameters affecting the pyrolysis, and a review of the kinetics.

2.2 Oil-sands-derived bitumen

2.2.1 Bitumen extraction from oil sands

Because there are many large deposits of oilsand around the world, this energy source is highly attractive compared to other energy sources. Oil sand, also known as tar sand and/or bitumen sand, consists of organic matter, water and mineral water. Specifically, it contains 85% mineral solids, 5% connate water and 10% bitumen. The minerals exist in a wide range of sizes; from 1 mm to smaller than a micrometer. Canada, Russia, Venezuela, America and China have the world's largest oil sand reserves. Canada has the second largest crude oil reserves (after Saudi Arabia), accounting for 15% of the total world reserves. Only about one-fifth of the 170 billion barrels of bitumen in the reserves is recoverable using surface mining. Among all bitumen recovery methods, surface mining provides more than half of the recovered bitumen (Srinivasa, et al. 2012).

Bitumen is recovered from oil sand by extraction technologies. One of the extraction techniques is a physical separation, in which the high viscosity bitumen is separated from the oil sand by size reduction and froth flotation. Twenty percent of the oil sand is bitumen. Using this method, almost 90% of that bitumen can be recovered. The amount of the recovered bitumen depends on the extent of the size reduction and the dispersant addition (Miller, et al. 1982).

In general, extraction methods differ depending on the type of oil sand and the structure of the bitumen. From a commercial point of view, hot water bitumen extraction is a practical method for extracting Athabasca oil sand; this method is also applicable for Utah tar sand, even though the Utah tar sand bitumen is more viscous. Other technologies used to extract bitumen include solvent extraction and thermal recovery (Cottrel, 1963).

The nature of the sand is the key point in extracting bitumen from sand grains; the more hydrophilic the sand, the more easily the bitumen can be extracted (Miller, 1982). According to an estimation from the Alberta Energy and Utilities Board, the Northern Alberta oil sand contains about 2.5×10^{12} barrel (400×10^9 m^3) bitumen, which is enough to meet Canada's domestic demand for 250 years (Yue Ma, et al. 2012).

Smith et al. showed that by mixing the raw oil sand with an appropriate aqueous medium, the mixture disperses. Using this method, the coarse sand can be separated from bitumen because the dispersal method decreases bitumen's viscosity, facilitating the separation (Smith, et al. 1984). In Smith's work, grinding the mineral grains in oil sand slurry made the separation process more efficient. Also, according to his work, adding hydrated lime and flocculent to the tailings improved filtration and enhanced settling (Smith, et al. 1984). Another principle of bitumen separation was proposed by Miller *et al.* Their process relied on phase disengagement of the mixture of the bitumen and the oil sand. Mechanical size reduction made it possible to extract bitumen from oil sand. (Miller et al, 1982).

Basically, the hot water process has not been applied in the same way for both Athabasca and Utah tar sand because of the difference in their structures. Utah tar sand does not contain indigenous water and the bitumen is directly bonded to the sand grains, also the bitumen in Utah tar sand has a much higher viscosity than the Athabasca bitumen (Bukka, *et al.* 1991).

2.2.2 Bitumen characterization

Bitumen consists of various groups of hydrocarbons and some organic portions that are combined with oxygen, nitrogen, sulphur and metallic atoms. The

hydrocarbons are divided into three main chemical groups of parrafins, naphtenes and aromatics. Generally, oil sand contains two main groups: asphaltenes and maltenes. Ashphaltene is insoluble in heptane, and maltene is soluble in heptane. Bitumen is also expressed in terms of chromatography divisions: saturates, aromatics, resins and asphaltenes (SARAs) (Speight, 2006). In this category, the molecular weight, complexity, aromaticity and number of the heteroatoms increase in the order of saturates, aromatics, resins and asphaltenes (Speight, 2006).

The separation of the products according to their boiling points and by means of distillation is the method that has been used for a long time; however, sometimes there is a need to recognize what structures are in the compound. The boiling point can be a proper way to help categorize the compounds according to their core structures. McKenna et al. have grouped the core structures in the crude oil according to their boiling points (McKenna, *et al.* 2010).

Boduszynski has shown that neither a narrow boiling point cut shows that the molar mass of the molecules are almost in the same range, nor a wide boiling point cut represents a wide molar mass range. In other words, they showed that the boiling points of a wide molar mass range of paraffin groups could be very close. In the paraffin groups, as the carbon number increases, the weak Van der Waals forces between the molecules increase. Although the molar masses of the molecules could be very different, their boiling points could be close. However, in some aromatic compounds, the intermolecular forces result in a high boiling point. Although some aromatic molecules have close molecular masses, their boiling points could be different. It can also be concluded that a high boiling point does not always indicate heavy compounds (Boduszynski, 1987).

2.3 Oxygenate containing raw materials

2.3.1 Cellulose characterization

The skeletal component in plants is cellulose; the polysaccharide cellulose has a structure with repeating D-glucose building blocks. By elemental analysis, $C_6H_{10}O_5$ was determined as the formula for cellulose (Klemm, 2005). Annually, 1.5×10^{12} tons of cellulose is produced, making it among the most common organic compounds. The most important source of cellulose is wood pulp, which is usually used to produce paper. According to Klemm et al. the molar mass of cellulose is high, and the intermolecular interactions, cross-linking reactions, and distribution of functional groups in the cellulose molecules determine the properties and the reaction in which cellulose is engaged. Cellulose is basically generated from ß-D-glucopyranose molecules, which are covalently connected by acetal functions. The length of cellulose molecules depends on the number of the anhydroglucose (AGU), which is considered as the degree of polymerization. The basic unit of the chain (AGU) includes a C_4-OH group (the non-reducing end) at one end and a C_1-OH group (the reducing end) at the other. The multitude of the AGUs makes cellulose highly reactive, since it can donate hydrogen from the hydroxide bonds available in each unit's reducing end (Klemm, 2005).

There is less information about cellulose reactions in the liquid phase, as most of the cellulose products are commercially produced in the solid phase. It is always difficult to figure out exactly what is happening in the solid phase. As a result, there is not enough information concerning the organic reactions that take place with cellulose. However, it is known that cellulose reactions are initiated for two main reasons; the accessibility of the O-H groups and their tendency in hydrogen-oxygen bond breaking; and the interaction among the other reactants

or the media present in the reaction conditions (Klemm, 2005). According to the structure of the cellulose that was described, cellulose can be considered as a proper option to accelerate the reaction rate when added to another substitute.

2.3.2 Lignin characterization

Lignin is of the world's most common biomass products. It is distributed in the plant cell walls of various bio products such as a straw of rice, wheat or corn; sugarcane bagasse; tea residue; and bamboo culm (Li, 2012). Unlike single unit polymers, lignin is an amorphous macromolecule consisting of three main monolignols. Depending on the contribution of the monolignols, lignins are categorized in three types: guaiacyl (HSC), syringyl-guauacyl (SG), and p-hydroxyphenyl-syringyl-guaiacyl (HSC) lignin, from softwood, hardwood and grass respectively. The monoligands, which are the constituents of lignin, are p-coumaryl alcohol, coniferyl alcohol, and sinapyl alcohol and, in some cases, other monolignols present in lignin such as coniferyl aldehyde, acetalyted coniferyl alcohol, and ferulic acid. (Li, 2012). The three monoligands that constitute lignin and, as a result, form a three-dimensional copolymer of phenylproponoid, are linked with carbon-carbon bonds and ether groups (Shi *et al.* 2012). According to its non-toxic and natural phenolic structure, lignin is frequently used in food products (Walton *et al.* 2003) and (Bjorsvik, 1999).

Lignin is made up of various phenolic groups. There are aromatic groups with one or more hydroxyl groups all over the lignin macromolecule. Lignin's phenolic structure is what enables it to produce so many free radicals (Balasundram *et al.* 2006). The ability of the phenolic groups to produce free radicals and hydrogen-donating atoms or electrons determines the specific properties of the compound, such as its antioxidant activity (Afanasev *et al.* 1989) and (Amarowicz *et al.* 2004). It is also hypothesized that due to lignin's ability to produce a lot of free radicals, it can be consumed as a reaction accelerator.

2.3.3 Coal characterization

Coal is a carbonaceous hard material that contains carbon, oxygen, hydrogen, sulfur and nitrogen. It is mainly categorized in four groups of lignite, bituminous, subbituminous and anthracite. The hardness and the compositions of each are different. Generally, coal molecule structures are very complicated; it is hard to illustrate their structures with an exact sample model. In 1976, Wender represented some structures for lignite which makes the reactions of various ranks to be understandable and help to predict what happens to the lignite coal (Wender, 1976).

Wender proposed a model in which there are some aromatic rings which are linked by aliphatic side chains and oxygen groups including carboxylic acid, ketone, phenol, alcohol, ether and furan (Wender, 1978). Wender's suggested formula for lignite is $C_{42}H_{40}O_{10}$. In 1984, Philip suggested the molecule of lignite as $C_{115}H_{125}O_{17}NS$, which also has benzofuran units, and aliphatic and aromatic chains as shown in (Philip, et al. 1984). Tromp and Moulijn (Tromp, *et al.* 1987), Huttinger et al (Huttinger, *et al.* 1987) and Patrakov et al. (Patrakov, 2005) introduced their model as $C_{161}H_{185}O_{48}N_2S_1M_4$, $C_{270}H_{240}O_{90}N_3S_3M_{10}$ and $C_{258}H_{256}N_2 O_{78}S$ respectively. Obviously, in all the proposed models, there are some aromatics, aliphatic chains, phenol groups, hydroxyls and aryl groups.

Hatcher *et al.* have studied xylem samples (Xylem is a type of plant tissue) to see what chemical changes are happening when xylem evolves into coal. Xylem was first degraded microbiologically, leading to a selective cellulose removal of about 50% of xylem. As the main part of xylem was degraded, the remaining component was lignin, which remained selectively as a result of its high resistance to microbial degradation. Therefore, after selective enrichment, the major component as a result of xylem coalification is lignin. In the second stage of xylem's evolution to coal, aromatic cross linking increases. The primarily

phenol-like structure is the base of the large macromolecules which consist of the the structures of lignite and subbituminous coal (Hatcher, et al. 1990).

Carlson found that Van der Waals and hydrogen bonding interactions, which are non-bonding interactions, are the forces responsible for forming the three-dimensional structures of the coal models (Carlson, 1992).

The models developed for subbituminous coal have been presented by Shinn et al. (Shinn, 1996) and Hatcher et al. (Hatcher et al. 1990). In these models it is observed that there are small ring structures and the limited amount of hydroaromatics.

The first model represented for coal was the bituminous coal model, proposed by Fuchs (Fuchs, 1942). Mathews et al. introduced a model for subbituminous coal that has 24 attached aromatic systems and three different parts which are linked with "hydroaromatic, cyoclopentane ethers, and diphenylene ketone oxide" (Mathews, et al. 2012). Some other models were proposed for bituminous coal; for example, in 1959, another model was presented, yet the model was changed in the hydroaromatic structures' orientation (Given, 1959). The model, which has been widely cited, was developed by Given, and   includes small aromatic systems with aliphatic groups' linkages but there are no methyl groups at the end of the molecule (Given, 1959).

2.4   Pyrolysis

Pyrolysis is a process in which organic material decomposes with the help of thermal energy. The difference between pyrolysis and other thermal cracking reactions is that it is done in the absence of oxygen. When the feed is heated, the molecules gain energy and start to break the weak bonds and generate free radicals. Free radicals are highly active components and can react with other free

radicals to generate new products or cause other molecules to become free radicals as well. These mechanisms produce new products. Literature on heavy oil pyrolysis has usually been studied in the context of bitumen, conventional crude oil and oil shale pyrolysis. Because the hydrocarbon groups of crude oils are similar, so are their pyrolysis products. Therefore, the mechanisms and compound classes found in the literature for bitumen, oil shale and other forms of crude oils can be discussed as a general topic.

2.4.1 Mechanism of decomposition reactions

When the thermal energy provided to a molecule is sufficient to break the weakest bonds in the molecule, hemolytic bond dissociation can occur. When the thermal energy exceeds the bond dissociation energy, free radicals can be formed. The formation of free radicals is so energy intensive that few free radicals can be produced; therefore, their concentration is very low. Specifically, at lower temperatures, where the thermal energy is only sufficient to break the weakest bonds, the concentrations of free radicals will be very low. The goal in thermal cracking processes is to break the bonds and produce reactive intermediates or radicals. The free radicals undergo some chain processes that convert the feed to the products. This means that the radicals which are produced in one cracking step can combine and produce other components and radicals. The bonds which are of more interest for petroleum upgrading purposes are carbon-carbon, carbon-hydrogen and carbon-oxygen. The bond dissociation energy is a factor which determines the amount of energy needed to break a bond. Table 2.1 shows the bond dissociation energies for carbon-cabon, cabon-hydrogen and carbon-oxygen bonds (Parsons, 2000).

Table 2.1. Bond dissociation energies (Parson, 2000)

Chemical bond	Energy, kJ/mol
C-C	356
C-H (aliphatic)	410
C-H (aromatic)	463
C-O	343

Cold Lake bitumen is made up of 85% Carbon, 10% Hydrogen and 5% Sulfur. The carbon-carbon bonds in aromatics have higher bond dissociation energy than the C-C (carbon-carbon) bond in saturates because of the existence of resonance stabilization in the aromatic rings. At relatively low temperatures, the aromatic rings are very hard to break down. The major break downs happen in the aliphatic bonds.

As shown in Table 2.1, the bond dissociation energy for the C-O (carbon-oxygen) bond is relatively lower than the bond dissociation energy for C-C (carbon-carbon) and C-H (carbon-hydrogen) bonds. Parson suggested using the molecules with low bond energies as radical precursors since they can break down at lower temperatures than the temperature at which the major breakdowns happen. Parson stated that the bonds of heteroatom-heteroatom and heteroatom-carbon break down at lower temperatures than the carbon-carbon and carbon-oxygen bonds, which are too strong to be broken (Parson, 2000). The idea of using molecules with bonds which have lower bond dissociation energies was applied in our study.

As will be explained more in section 4.5, Zhao et al. showed that increasing the temperature increased the reaction rate and the coke yield, but decreased the liquid yield (Zhao, *et al.* 2010). Dutta et al. also showed that increasing the temperature decreased the liquid yield (Dutta, *et al.* 2000). The reason the reaction rate is lower at low temperatures is that the molecules are not provided with sufficient energy to break down the bonds; therefore, few radicals are produced. Because of the low concentration of radicals, the reactions proceed slowly.

The first step in the chain reactions is initiation. In this step, free radicals are generated from the feed. As this stage is energy intensive, radicals are present in low concentrations but they cause a conversion of the feed mixture.

When radicals are generated from the main feed, they can undergo further reactions and produce new and/or more stable radicals (i.e., the propagation step). This is the second step in the chain reaction and can be categorized into four main steps (Parsons, 2000):

a. Abstraction: Radical formed from a non-radical molecule
b. Addition: Radical addition to a non-radical molecule
c. Fragmentation: Radical fragmentation to a new radical
d. Rearrangement: Radical rearrangement

In the abstraction category, the radical removes an atom from a non-radical precursor, which means that a radical attacks the σ bond of an atom and produces a more stable radical. This mechanism needs a weak σ bond in the precursor atom; the weaker this bond is, the more stable the product radical is. Therefore, adding atoms with weak bonds speed up the stage of propagation.

In type "b" reactions (i.e., addition reactions), a carbon radical is usually added to alkenes to form a new σ bond which replaces the previous π bond. In the fragmentation step, however, a radical forms an unsaturated molecule and a new radical. The alkene double bond is weak and its production is not well favored due to its weak bonds. As such, the driving force for the fragmentation reactions should be associated with the presence of a highly weak radical, which can lead to alkene production (Parsons, 2000). There is not a considerable quantity of these radicals in bitumen-containing materials.

The third and the last step in the pyrolysis chain reactions is the "termination" step. In this step the radicals form the products. This step includes two reactions:

a. Radical combination
b. Radical disproportionation

The first reaction is a combination in which two radicals combine and make a covalent bond. The overall rate for this reaction is low because most radicals have a short life. Therefore, to increase the yield there should be more stabilized radicals among the produced radicals and/or there should be a significant amount of radical production in the initiation step or propagation step.

The other form of the termination step is disproportionation. In this reaction type, a β hydrogen of one radical is transferred to another radical, forming one unsaturated and one saturated product. The rates of both termination reactions are the same, so these two reactions compete with each other. For disproportionation reactions, the greater the number of β hydrogen, the faster the disproportionation reactions.

2.4.2   Effect of adding the oxygenate containing materials

The idea used in this study is that adding some precursor atoms with weak bonds benefits all the steps. For this purpose, some oxygenate-containing materials which have weaker bonds than the usual C-H and C-C bonds were chosen. In the initiation step, there are two benefits to use the selected oxygenate-containing materials. First, because the oxygenate-containing materials have bonds with low bond dissociation energy (C-O bonds), the initiation step can start with providing lower enough energy to break down the weak bonds at low temperatures. Second, because the bitumen structure also has weak bonds, adding molecules with mostly weak bonds increases the concentration of total weak bonds which

can be broken; the increase in the concentration of weak bonds helps the initiation step proceed faster.

In the propagation step, the produced radicals which are less stable can break the σ bond between the carbon and the oxygen atoms and, as such, more stable radicals are formed. As discussed previously, in the termination step, the higher the concentration of radicals, the faster the termination step. As the amount of free radicals increases, the termination step is also accelerated. Therefore, by considering all three reaction steps, obviously the addition of the materials which contain weak bonds is beneficial in accelerating the overall reaction rate theoretically. The following sections will discuss how adding oxygenate-containing materials affects kinetics and enthalpy.

2.4.3   Decomposition reaction kinetics

It is not clear exactly what reactions occur during thermal cracking. However, the chain reactions can be simplified in some general categories. As described previously, it takes a lot of energy to break aromatic rings because they have so much resonance stability. Particularly at the studied pyrolysis temperature of 380 °C, there is not much chance to break the aromatic molecules. It could be hypothesized that the main cracking that occurs at this relatively low temperature is aliphatic breaking. The following is a brief decomposition of an aliphatic molecule:

"M" is considered herein as a sample n-alkane.

According to Rice, et al. (Rice, *et al.*1934), the thermal cracking reactions for n-alkane are:

Initiation:

$$M \xrightarrow{k_1} 2R^\bullet \qquad\qquad \text{Reaction (2.1)}$$

Propagation:

$$R^\bullet + M \xrightarrow{k_2} RH + M^\bullet \qquad\qquad \text{Reaction (2.2)}$$

$$M^\bullet \xrightarrow{k_3} N^\bullet + Olefin \qquad\qquad \text{Reaction (2.3)}$$

Termination:

$$2\,R^\bullet \xrightarrow{k_4} Products \qquad\qquad \text{Reaction (2.4)}$$

Equation 2.1 shows the decomposition rate of the feed (M):

$$\frac{d[M]}{dt} = -k_1[M] - k_2[R^\bullet][M] \qquad\qquad \text{Equation (2.1)}$$

Although other reactions may also take place in the termination step, in the present study the aim is to derive the kinetics for the stated termination reaction. The following equations can be written for the rates of the radicals:

$$\frac{d[R^\bullet]}{dt} = 2k_1[M] - k_2[M][R^\bullet] - 2\,k_4[R^\bullet]^2 \qquad\qquad \text{Equation (2.2)}$$

$$\frac{d[M^\bullet]}{dt} = k_2[M][R^\bullet] - k_3[M^\bullet] \qquad\qquad \text{Equation (2.3)}$$

It is important to mention that the changes in the concentrations of the radicals are much lower than the changes in the concentrations of the reactants. Hence, the system is at a pseudo-steady state and it can be considered that the rates of the changes for the radicals are equal to zero (Rice, *et al.*1934).

$$\frac{d[R^\bullet]}{dt} = \frac{d[M^\bullet]}{dt} = 0 \qquad\qquad \text{Equation (2.4)}$$

Therefore, Equations 2.2 and 2.3 are equal, and the concentration of M can be determined based on the concentrations of $R^{\bullet}$ and $M^{\bullet}$ (Equation 2.5)

$$[M] = \frac{2k_4[R^{\bullet}]^2 + k_3[M^{\bullet}]}{2k_1}$$
Equation (2.5)

As discussed earlier, the life of free radicals is very short, which means that free radicals react with each other very quickly. The rate of the propagation step is much quicker than the rate of the initiation step, so in Equation 2.1 the rate of the initiation step is negligible in comparison to the rate of the propagation step. Equation 2.1 can be summarized as Equation 2.6

$$\frac{d[M]}{dt} = -k_2[R^{\bullet}][M]$$
Equation (2.6)

The relationship between $[M]$ and $[R^{\bullet}]$ which is mentioned in Equation 2.5 and Equation (2.1) can be written herein as a function of $[R^{\bullet}]$ and $[M^{\bullet}]$ in Equation 2.7.

$$\frac{d[M]}{dt} = -\frac{k_2 \times [\, k_3[R^{\bullet}][M] + 2\, k_4\, [R^{\bullet}]^3]}{2k_1}$$
Equation (2.7)

Equation 2.7 shows that the order of the reactant decomposition with respect to $R^{\bullet}$ is 3. This equation shows that even a small increase in the free radical concentration highly influences the reactant's decomposition rate.

2.4.4   Enthalpy of the decomposition reactions:

As was discussed previously, propagation is the fastest step in the chain reaction. A variety of reactions occur in the propagation step. The reactions that produce non-radical products in the termination step have almost similar rates. Nevertheless, the ranges of reactions in which radicals are converted to other

radicals differ greatly. It was observed that in the propagation step, some propagation reactions can vary by a factor of 10,000 (Parsons, 2000).

The kinetic equations in the previous section proved that adding the oxygenate-containing materials increases the decomposition reaction rate. One of the most important factors influencing the rates is enthalpy. In this section, the bond dissociation energies and their relationship to the rate will be discussed.

It is known that the rate of the reaction depends on the activation energy (E_{act}). E_{act} is obtained by Equation 2.8 (Parsons, 2000).

$$E_{act} = \Delta H^* + RT \hspace{4cm} \text{Equation (2.8)}$$

The enthalpy of the activation (ΔH^*) shows the difference between the enthalpy of the transition state and the reactant. In this study, at a reaction temperature (i.e., 380 °C), RT is approximately equal to 5.5 kJ. mol^{-1} and this value is constant for all other samples reacted at the same temperature. According to Equation 2.8, the smaller the enthalpy of the activation, the smaller the activation energy and the faster the reaction.

In this part, two groups are compared:

1. Bitumen pyrolysis
2. Bitumen and oxygenate-containing material copyrolysis

For both groups, the products are almost the same in case of the structure, and it can be assumed that the enthalpies of the products are almost in the same range. As shown in Figure 2.1, it can be assumed that the enthalpies of the reactant are almost the same because the ratio of the additive to bitumen is only 1 to 9.
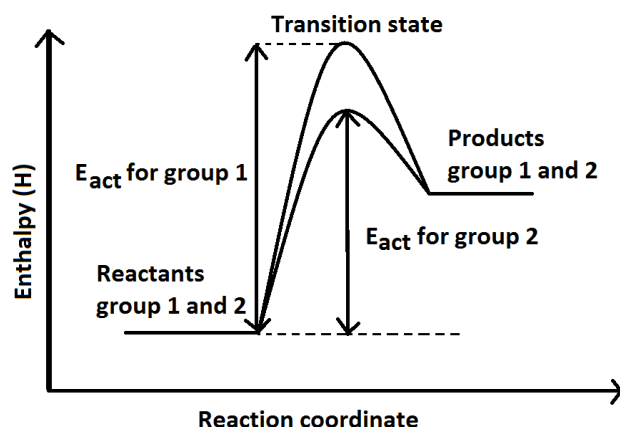
Figure 2.1. Enthalpy versus reaction coordinate for bitumen (group1) and for mixtures (group2)

The main reactions that convert the reactants to the transition state for group one and two are represented in Figure 2.1.
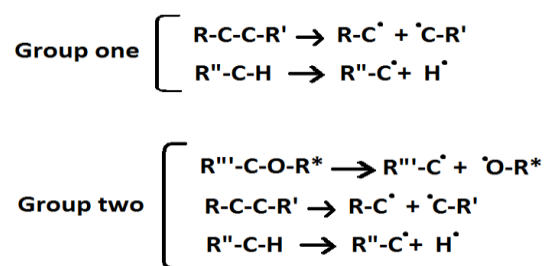
Figure 2.2. Conversion of the reactants to the transition state. Group one represents the reactions for bitumen pyrolysis and group two represents the reactions for the mixture pyrolysis. Each of the R, R', R" and R* represent a group of hydrocarbon.

The enthalpy of the activation for the reactions in Figure 2.2 was achieved by Equation 2.9

$$\Delta H^* = total\ energy\ of\ the\ bonds\ broken \qquad\qquad Equation\ (2.9)$$

The amount of the bond dissociation energy for the O-C (343 kJ. mol^{-1}) is less than that of C-C (356 kJ. mol^{-1}) and C-H (410 kJ. mol^{-1} for n-alkanes and 463 kJ. mol^{-1} for aromatics). Because of the less bond dissociation energy of the carbon-oxygen bonds, the enthalpy of the activation for group two is lower than that for group one. According to Equation 2.9, the activation energy for group two is therefore lower than that for group one (Figure 2.1). To this end, the comparison between the enthalpies of activation (ΔH^*) for the two groups implies

that the mixture of the additive and bitumen decomposes at a faster rate than the bitumen itself.

2.4.5   Bitumen pyrolysis

George *et al.* has studied the way temperature affects the pyrolysis of Athabasca bitumen. They have reported three main regions in bitumen pyrolysis: the gas production region with a retention time up to 2.5 minute; the n-alkane homologous series region with a retention time of 2.5 to 14 minutes; and the third region with a retention time of 14 to 30 minutes (They did not give a special name for this region). Yet, they have not described in detail what happens in each region. George et al. also studied the pyrolysis of maltene and asphaltene . They concluded that maltene does not undergo a pyrolysis reaction until 500 °C and that what really happened to maltene was distillation. Asphaltene played the most important role in pyrolysis. They showed that as the pyrolysis temperature was higher, the emphasis of the pyrolysis reaction was more dominant than the distillation effect. Yet, the exact point at which the physical change is transformed to the chemical change was not clear. According to the results, the residence time is an important factor which determines whether distillation, isomerization or cracking take place (George, *et al.* 1978). Ali et al. reported that asphaltene begins to decompose at about 400 °C. They also reported that the maximum rate for the asphaltene decomposition happens at 500 °C and that asphaltene cracking is almost finished at 600 °C (Ali, *et al.* 1991).

Ali et al. showed that the gases and oil yields of the asphaltene pyrolysis vary for different types of asphaltenes as a function of temperature. For instance, for Arabic light crude oil asphaltene (AL), the gas and oil yield is higher than for the Arabic heavy crude oil asphaltens (AH) at a low temperature (350 °C) ; however, it was observed that AH displayed higher gas and oil yields than AL at higher temperatures (520℃). Ali et al. have compared the pyrolysis products of AH and AL at two operating temperatures of 350 °C and 520 °C. They found

that at the lower temperature (350 °C), almost 85% of the asphaltene remained after the pyrolysis. At 350 °C, the amounts of gases, maltene and coke products were approximately 2%, 2% and 11% respectively. At 520 °C, most of the asphaltene was consumed. The approximate yields of the products at 520 °C were 17%, 22%, 1% and 60% for gases, maltene, asphaltene and coke respectively (Ali, *et al.* 1991).

The most produced gases in the asphaltene pyrolysis are methane and some ordinary alkanes. The discrepancy between the amount of CO and CO_2 production in various asphaltene was due to the difference in the amount of carboxylic acid linkages (Ali, *et al.* 1991).

Unlike the three regions which George et al. introduced for bitumen pyrolysis, Earnest et al. believed that there is one major decomposition which occurs in bitumen pyrolysis. They studied the thermogravimetric (TG) analysis for some selected oil shales in nitrogen atmosphere. According to their results, the first decomposition, of organic components such as kerogen and bitumen, starts in the range of 300-550 °C. At higher temperatures, the changes in TG are due to the production of carbon dioxide from the decomposition of mineral components. They found that the mass loss in TG results varies with the level of the organic and carbonate minerals in the feed. In their study, the mass loss profile continued to almost 500 °C which they attributed to two possible reasons; the continued pyrolysis of hydrocarbons; and the reaction of char with CO_2, which produces CO (C (char) $+CO_2$ (g) -> 2CO(g)), which causes the continuous mass loss of the remaining carbon amount (Earnest, 1982).

The products of bitumen pyrolysis are gases, oil, and coke. Basily *et al.* have studied the bitumen products by separating bitumen into six fractions (saturates, monoaromatics, biaromatic, polyaromatic, resin and asphaltene). They pyrolysed each fraction in two stages to obtain a maximum ethylene and propylene yield because these two products are valuable in chemical synthesis and for

oligomerization. They stated that pyrolysis in two stages showed more advantages in comparison to one pyrolysis process at a high temperature. (Basily, *et al.* 1990).

2.4.6   Oil shale and crude oil pyrolysis

The pyrolysis of oil shale and crude oils showed some fundamental similarities with bitumen pyrolysis. This makes sense, as bitumen can be extracted from oil shale and crude oils. Thakur et al. studied Moroccan oil shale thermogravimetry using isothermal and non-isothermal TG. Non isothermal TG curves have been investigated under various heating rates but the mass loss in all was almost in the same range. A range of 0.5-0.75% of the mass loss was observed in Moroccan oil shale below 200 °C, which is due to moisture loss. The decomposition related to a carbonate compound happened at 525 °C or above, which was about 25-26 wt%. Thakur et al. suggested that there are two consecutive reactions which happen at the temperature range of 300-600 °C: Kerogen is converted to gas, bitumen and carbon; and these products undergo changes which produce gas, oil and coke as well (Thakur, 1987). Dogan et al. have also proved that Kerogen decomposition happens in two first-order reactions similar to those presented by Thakur et al.

Paul et al. pyrolyzed four oil shale samples. Although each showed different thermogravimetry results, there are some common results which can be understood from the TGA diagrams; they all showed a lower temperature range peak that contributed to the moisture loss or loss of water from the mineral clay. This region ends at about 200 °C for all. The second region is related to the loss of volatile components and some types of light hydrocarbons. Three out of the four oil shale samples had one-step decomposition in this stage, which happens at about 200-620 °C. The other oil had two steps in this stage which also has been observed by Haddadin et al. (Haddadin, *et al.* 1974) and Dogan *et al.* (Dogan, *et al.* 1996) works. In addition to the two main oil shale pyrolysis

reactions that have been cited in the literature, Ahmed et al. proposed the third stage in TG results for oil shale decomposition, which is considered to be anything above 600 °C and is caused by carbonate decompositions such as calcite and ankerite decomposition (Williams, *et al.* 1999). Chishti et al. have also studied an oil shale pyrolysis and found that bitumen is converted to oil at temperatures up to 500 °C. At higher temperatures, secondary reactions occur on char, leading to higher methane and ethane production (Chishti, Williams, 1999). Gersten *et al.* also studied the thermal decomposition of polypropylene, oil shale and their mixture at temperature ranges of 30-900 °C. The activation energies which have been obtained and reported are 250, 63 and 242 kJ/kg for polypropylene, oil shale and the mixture respectively. Gersten et al. used the mixture as a feed for thermal decomposition in order to improve the effectiveness of the process and to reduce the waste problem. They reported two stages in polypropylene and three stages in oil shale pyrolysis. Propylene begins to melt at 156.85 °C (430 K) and starts to decompose at 208.85 °C (482 K). The first stage of weight reduction for oil shale continues up to 181.85 °C (455 K) and is 10%. The second stage is due to the decomposition of the organic matter, which is 11% and is in the range of 289.85-554.85 °C (563-828 K). The last stage occurs at 665.85-684.85 °C (939-958 K), which is related to the decomposition of the minerals. Gersten et al. also stated that the temperature range varies depending on the heat range. For instance, at heating rates of 5, 10 and 15 K/min, the temperature of the initial pyrolysis is 550, 554 and 560 °C (Gersten, *et al.* 1999).

Ranjbar *et al.* have studied the pyrolysis of crude oil, asphaletene and resin. According to their results, at the range of 350-450 °C, there is a high fuel concentration reduction, especially for resin-rich oils. According to the thermal analysis results, it was confirmed that resin is thermally unstable in the same range. It was found that the maximum pyrolysis rate would be 420 °C for resin pyrolysis and 480 °C for asphaltene pyrolysis. Moreover, Ranjbar et al. stated that coke is not produced in all thermal cracking processes. If the feed is parrafin

hydrocarbons, coke production only happens when all the paraffins decompose. When the feed is polyolefins, if the reacted polyolefins are removed after the reaction, the cracking does not produce coke,. The products of paraffins, olefins and naphtenes react with each other and coke is produced in this stage. Therefore, the coke produced from the paraffins and olefins and naphtenes has a naturally long induction time which decreases when the temperature increases. However studies about asphaltene cracking showed that it produces coke without any induction time (Ranjbar, *et al.* 1990). Huttinger *et al.* showed that molecular weight of asphaltens remained constant after the pyrolysis, which shows that there is no induction time in asphaltene pyrolysis (Huttinger, *et al.* 1989).

The particle sizes seem to have no effect on the pyrolysis results. Dogan et al have investigated the thermogravimetric results of three types of oil shales with different particle sizes and at various temperatures (400, 550 and 700 °C). They concluded that the particle sizes do not affect the reaction conversion, and that the higher the final temperature, the higher the conversion. Unlike the size of the oil shales, the type of the oil shale affects the pyrolysis kinetics of the oil shale pyrolysis. Dogan's study showed that for one of the oil samples, a single kinetic expression worked for the whole heating period; however, for the other two samples, two kinetic expressions were valid during the pyrolysis. This shows that the type of oil demands different rate expressions. It also shows that decomposition rates vary in some critical temperature ranges, although this is independent of the reaction order (Dogan, *et al.* 1974).

In addition to studying pyrolysis for crude oil, shale oil and bitumen, Coll et al. investigated TG studies on coal pyrolysis and found that there are three main decomposition regions which take place up to 950 °C (1223 K): the decomposition of light molecules which are physically linked to coal; the breaking of higher molecular weight hydrocarbons; and the coking of coal (Coll, *et al.* 1992).

2.4.7   Thermal behavior of biomass and biomass/coal copyrolysis

Vuthaluru studied the thermal behavior of biomass and coal copyrolysis (Vuthaluru, 2003). Vuthalaru et al. prepared mixtures of coal and biomass. They used Collie subbituminous coal (CSC), While wood waste (WW) and wheat straw (WS). They observed three main regions. The first two regions were because of the biomass pyrolysis and the last was because of the coal pyrolysis. They observed that the residual yield increased when the ratio of coal to biomass increased. They attributed this to the difference in the strength of the molecular structures. They claimed that the macromolecules of cellulose and lignin are linked with weak ether bonds with a bond dissociation energy of approximately 400 kJ/mol. They stated that these bonds are less resistant at low temperatures (400-500 °C). However, coal containing high aromatic macromolecules is mostly linked with aromatic C=C bonds with a bond dissociation energy of 1000 kJ/mol and is more resistant to heat. Therefore, the mass loss caused by the coal polycyclic aromatic defragmentation is less than that caused by the biomass molecules. Moreover, Vuthaluru did not find much interaction between the coal and biomass samples during the pyrolysis. The blends followed the same characteristics that each individual coal or biomass presented. Vuthalaru studied the pyrolysis of each of the char, coal and biomass separately. A linear relationship was obtained for the amount of the biomass in the blend and the char yield (Vuthaluru, 2003).

Thermal characteristics of cellulose and lignin have been studied at low temperature pyrolysis (Yang, *et al.* 2007). Cellulose was found to have greater thermal stability than lignin. In the TGA run, Yang et al. have used approximately 10 mg of the sample under nitrogen flow from room temperature to 600 °C with a heating rate of 10 °C/min. The main pyrolysis temperature range for cellulose is 310-390 °C and the mass loss amount is 88%. For lignin the main pyrolysis temperature range is 200-550 °C and the mass loss is 35%. The maximum heating rate for cellulose pyrolysis is 360 °C and the rate is 25%/min. The maximum heating rate for lignin is 352 °C and the rate is 2%/min.

Basically, the thermal behavior of the components depends on their structures (Varhegyi, *et al.* 1996). Varhegyi et al. showed that at a low reaction rate, cellulose is converted in two main reactions: it converts to char and gases, and it converts to volatile tars. They also stated that at a low temperature, these two sets of reactions are equally important, yet when the temperature goes up, the conversion of cellulose to volatile tars dominates. Varhegyi et al. compared lignin pyrolysis to cellulose pyrolysis and resulted that DTG (Derivative Thermogravimetric Analysis) results of lignin showed wider and flatter peaks. Cellulose contains D-glucose groups, which are bonded with glycosidic linkages. When cellulose is pyrolysed, these bonds are broken easily because of their simple chain structure; however, cellulose macromolecules are generally thermally resistant because of the high energy demanded for breaking the bonds between two pyrans (Yi-min, *et al.* 2009). Yi-min et al. also state that lignin has three dimensional macromolecules which consist of phenylpropane, which has C-C and C-O-C bonds and is complicated to disintegrate; therefore, the temperature range of lignin pyrolysis is very wide.

2.4.8 Pyrolysis products

The general correlation between the temperature and pyrolysis reactions is that as the temperature goes higher, more reactions happen. Liquid and gas production will be higher at high temperatures. This general idea has been proved in some temperature regions. For example, Ma *et al.* probed the pyrolysis and extraction of Buton oil sand bitumen. They proved that the higher the temperature, the more gas and oil are produced in the range of 380-480 °C. The oil and gas yields increase a lot; however, at the temperature range of 480-500℃, the yields are mainly constant (Ma, *et al.* 2012). However, there are some traces which show that as the temperature increases, the gas and liquid production decreases and more coking takes place instead.

Zhao et al. (Zhao, *et al.* 2010) have studied the pyrolysis of one of the heaviest bitumen fractions, asphaltene, at temperature ranges between 430 ° to 550 ℃ and they have observed the products yields of this pyrolysis. According to their results, there was an induction time of 3-4 minutes before coke formed at 430 ℃. As the pyrolysis temperature increased, the induction time increased as well, up to a temperature of 480 ℃, at which the induction time disappeared. The required time to reach to the ultimate coke yield decreased from 60 minute at 430 ℃ to 20 minutes at 550 ℃. The coke yield increased as the temperature increased. The gas yield also increased as both the temperature and the reaction time increased. What is interesting about Zhao's work is that the ending liquid yield was same for all the temperature ranges, but the reaction time was shorter at higher temperatures. This means that the reaction rate was faster at higher temperatures. At the same reaction time, the higher liquid yields belong to lower temperatures. For instance, at the reaction time of 20 minutes, the liquid yields are 85 wt%, 72 wt%, 58 wt%, 54 wt%, 53 wt% and 52 wt% for pyrolysis at 430 ℃, 450 ℃, 480 ℃, 500 ℃, 520 ℃ and 550 ℃ respectively (Figure 2.5).

Zhao also studied the the H/C ratio, and found that it showed the same trend for gas and coke products; it decreased when the temperature and reaction time increased. However, a different ratio was observed for the liquid product. At lower temperatures, the H/C ratio decreased with reaction time and then increased; conversely, at higher temperatures, the H/C ratio increased and then decreased. This change can be explained by the amount of gas and coke production. It was observed that at low temperatures, the gas production was more favored; however, at higher temperatures the coke production was more dominant. Also, as the pyrolysis proceeded and as the reaction time increased, more coke was produced at lower temperatures. At higher temperatures, as the reaction time increased, more gases were produced. It can be concluded that the reaction time and temperature have opposite effects on H/C ratio for liquid product (Zhao, *et al.* 2010).

Dutta et el. studied the effect of steam on thermal cracking of Athabasca bitumen. The effect of adding steam was observed by adding doped water with D_2O. The products were then analyzed using NMR and stable isotope mass spectrometry. The results showed that the steamed pyrolysis decreased the coke yield, sulfur concentration and H/C ratio of the liquid products. According to the results, the liquid yield decreased when the temperature increased (Dutta, *et al.* 2000).

2.5   Pyrolysis investigations using thermal analysis techniques

Thermal energy changes the petroleum component molecules depending on the amount of thermal energy provided to the molecules. The behavior of the component molecules during the temperature change indicates what physical and chemical changes have taken place in the substance. The main methods that have been used to study the behavior of the petroleum substances are Thermogravimetry (TGA) and Differential Scanning Calorimetry (DSC). TGA shows the stages that the substance go through, including dehydration, hydrogenation, and thermal cracking reactions. A more detailed discussion on TGA is included in Chapter 4. Also, information about the energy needed for physical and chemical changes to petroleum substances can be calculated analyzing DSC results. The following provides information about the petroleum DSC results in the literature. Finally, in order to have clear insight of the relativity of the time and the concentrations, the kinetics are discussed briefly in the final sections of this chapter.

2.5.1   Effect of heating rate on pyrolysis

Different experiments have been conducted on the influence of the heating rate on thermal decomposition. These experiments showed that the apparent activation energy is increased by increasing the heating rate. Collett et al. studied four pitch samples over different linear ranges. They found that the activation energy was increased by increasing the temperature so that the importance of the

different reactions leading to weight reduction varied by the temperature rise (Collet, *et al.* 1980). Thakur *et al*. also had results that agreed with the idea that the heating rate affects the pyrolysis results. They studied the thermal decomposition of Kerogen and reported that with a heating rate of 10 °C/min, only half of the Kerogen was decomposed at 500 °C, while the total Kerogen was decomposed at the same temperature but with a different heating rate of 50 °C/min. The reason for this is a shorter exposure time to a specific temperature at higher heating rates. On the other hand, other studies showed that the heating rate does not affect the activation energies. Rajeshwar studied thermogravimetric kinetics from the thermal decomposition of Green River oil shale Kerogen and showed that the kinetic parameters are not dependent on the heating rate in non-isothermal thermogravimetry conditions (Rajeshwar, 1981).

2.5.2   Endothermic and exothermic events during pyrolysis

DSC results show the endothermic and exothermic properties of the samples. From these properties, it is possible to obtain the apparent energy needed for the physical and chemical changes that occur in the sample. Mahajan *et al.* analyzed 12 coal samples of various ranks using DSC, and reported that coal types ranging from Anthracite to bituminous coals were endothermic and that lignite and subbituminous coals were exothermic and the thermal effects depend on the rank of the coal (Mahajan, *et al.* 1977). These results were also proved by Haykiri-Acma *et al.* Haykiri-Acma et al. also used DTA and GTA to investigate the behavior of fossil fuels such as peat, lignite, bituminous coal, anthracite, oil shale and asphaltene samples under nitrogen. They specified the endothermic and exhothermic regions for each fossil fuel and showed that lignite has two main endothermic regions. The first endothermic region is due to mass loss, which appears at temperatures below 400 °C, and the other endothermic region is related to the mineral decomposition which was shown at temperatures higher than 400 °C. Haykiri-Acma observed that the maximum weight reduction rate in lignite decomposition occurred at a temperature of 380 °C (Haykiri-Acma,

1993). A DSC data analysis showed that oil sand bitumen had three endothermic ranges of (25-150 °C), (400-500 °C) and above 550 °C. These ranges are related, respectively, to the loss of moisture, devolatilization of organic compounds, and pyrolysis cracking (Rosenvold, *et al.* 1982).

2.5.3 Pyrolysis kinetics

Determining kinetic parameters of reactions has been an interesting subject to study. Thermogravimetric analysis (TGA) has been used in samples to investigate physical changes such as devolatilization and kinetic parameters. Thermal analysis has been used to measure a substance's physical properties as a function of temperature. The equipment most often used for thermal analysis includes DSC, TG/DTG and differential thermal analysis (DTA). A controlled temperature program has been applied to all three. DSC measures the difference in energy input between the sample and the reference. TG measures the mass loss during any physical change or mainly in the reactions, and DTA measures the temperature difference between a sample and a reference (Kok, *et al.* 1995).

TGA was widely used to observe the effects of heating rates and the pyrolysis temperature on reaction kinetics. Rajeshwar *et al.* have studied the kinetics of thermal decomposition of Green River oil shale Kerogen by non-isothermal thermogravimetry. The activation energy needed for Kerogen to decompose to bitumen and for bitumen to decompose to oil, gas and carbonaceous residue have been estimated at 62 and 152 kJ/mol respectively, with frequency factors of 10^6 1/min and 10^{14} 1/min respectively. It was observed that the first order reaction was adequate for thermal behavior of Green River oil shale (Rajeshwar, 1981). The three main kinetic equations which are applied to thermal analysis data are the Arrhenius method, the Freeman-Carroll method and the Coats-Redfern method. They are described in the following sections.

The Arrhenius method

In the Arrhenius method, decomposition can be shown as a function of temperature:

$$\frac{d\alpha}{dt} = kf(\alpha) \qquad \text{(Equation 2.2)}$$

Where $\frac{d\alpha}{dt}$ is the weight change in time, k is the rate constant and $f(\alpha)$ is the decomposition function. The rate constant is also a function of temperature as:

$$k = A\exp(-\frac{E}{RT}) \qquad \text{(Equation 2.3)}$$

Where E is the activation energy, R is the gas constant and A is the frequency factor. E and A are different for different decomposition mechanisms. The general Arrhenius equation is in the form of Equation 2.4.

$$\frac{d\alpha}{dt} = Af(\alpha)\exp(-\frac{E}{RT}) \qquad \text{(Equation 2.4)}$$

By applying the heating rate ß, (ß $= \frac{dT}{dt}$), the Arrhenius equation is in the form of Equation 2.5.

$$\frac{d\alpha}{dT} = A/ßf(\alpha)\exp(-\frac{E}{RT}) \qquad \text{(Equation 2.5)}$$

Assuming that the reaction function is presented as $f(\alpha) = (1-\alpha)^n$ (n is the reaction order and was suggested by Coats et al to be in values of 0, 1/2, 2/3 and 1 for solid state kinetics) (Coats, et al. 1964), the Arrhenius function would be expressed as:

$$\frac{d\alpha}{dT} = A/ß\exp(-\frac{E}{RT})\,(1-\alpha)^n \qquad \text{(Equation 2.6)}$$

or

$$\ln\left[\frac{\frac{d\alpha}{dT}}{(1-\alpha)^n}\right] = -\frac{E}{RT} + \ln(\frac{A}{ß}) \qquad \text{(Equation 2.7)}$$

By linear regression of plotted $\ln\left[\frac{\frac{d\alpha}{dT}}{(1-\alpha)^n}\right]$ vs. *1/T*, parameters of E and A can be obtained (Rajeshwar, 1981).

Coats and Redform method (Coats, et al. 1964)

The integral method represented by Coats and Redform is in Equation 2.8.

$$\ln\left[\frac{1-(1-\alpha)^{1-n}}{T^2(1-n)}\right] = \ln\left(\frac{AR}{\text{ß}E}\right)\left[1 - \frac{2RT}{E}\right] - E/RT \qquad \text{(Equation 2.8)}$$

Equation 2.8 is applied for n values more than one. For n=1, the equation is summarized as Equation 2.9:

$$\ln\left[-\frac{\ln(1-\alpha)}{T^2}\right] = \ln\left(\frac{AR}{\text{ß}E}\right)\left[1 - \frac{2RT}{E}\right] - E/RT \qquad \text{(Equation 2.9)}$$

It has been shown that the first term in (Equations 2.8 and 2.9) is almost constant for all values of E (Coats, Redfern, 1964), so if $\ln\left[-\frac{\ln(1-\alpha)}{T^2}\right]$ is plotted versus *1/T*, the slope would be E/R (Rajeshwar, 1981).

Freeman and Carroll method (Freeman, Carroll, 1958)

In the method developed by Freeman and Carroll, *n* can be obtained directly from the plot. This difference-differential method has the base use of (Equation 2.6), which is changed to form Equation 2.10.

$$\ln A/\text{ß} - E/RT = \ln\left(\frac{d\alpha}{dT}\right) - n\,ln(1-\alpha) \qquad \text{(Equation 2.10)}$$

By differentiating equation (9) and integrating, and dividing the equation by $\Delta ln(1-\alpha)$, (Equation 2.11) is derived.

$$-\left[\frac{-\frac{E}{R}\Delta(\frac{1}{T})}{\Delta\ln(1-\alpha)}\right] = \left[\frac{\Delta\ln(\frac{d\alpha}{dT})}{\Delta\ln(1-\alpha)}\right] - n \qquad \text{(Equation 2.11)}$$

By plotting $\left[\frac{-\frac{E}{R}\Delta(\frac{1}{T})}{\Delta\ln(1-\alpha)}\right]$ versus $\left[\frac{\Delta\ln(\frac{d\alpha}{dT})}{\Delta\ln(1-\alpha)}\right]$, values of *n* and *E* can be obtained (Rajeshwar, 1980).

2.5.4 Mechanisms of oil sand decomposition

Rajeshwar *et al.* have applied the three stated equations and calculated the average for the amounts obtained from the stated methods. They have investigated the overall thermal decomposition rate constants for decomposing Kerogen to bitumen (k_1) and bitumen to oil and residues (k_2) (Rajeshwar, 1981).

$$k_1 = 3.3 \times 10^6 \exp\left(-\frac{7445}{T}\right) (min^{-1}) \qquad \text{(Equation 2.12)}$$

$$k_2 = 9.8 \times 10^{13} \exp\left(-\frac{18175}{T}\right) (min^{-1}) \qquad \text{(Equation 2.13)}$$

Thakur *et al.* studied the pyrolysis of Moroccan oil shale by thermogravimetry by both isothermal and nonisothermal thermogravimetry (TG). The isothermal study was analyzed with three models — the Chen and Nuttall model, Coats and Redfern model and Anthony and Howard model — while the isothermal study used the integral method. In Chen-Nuttal and Coats-Redfern models, the reactions were assumed to be first order reactions; however, the Anthony-Howard model was for various parallel first-order reactions which were taking place during the decomposition. Experiments performed by Thakur et al. also proved what Rajeshwar *et al.* found: that oil shale was decomposed in two main reactions. First, oil shale was decomposed to bitumen, gas and carbon and then the products were converted to gas, oil and coke. In the non-isothermal study, two mechanisms were assumed. In the first mechanism, Kerogen was converted to products directly in the temperature range of 300-500℃. In the second assumed mechanism, Kerogen was converted to gas, bitumen and residue in the temperature range of 300-375°C and the products were then converted to gas, oil and coke in the temperature range of 375-500℃. For the two-step reactions, Thakur et al. applied the Coats-Redfern and Chen-Nuttall methods and plotted the graphs. Two slope lines stood out in their results. The frequency factors and activation energies were obtained from the plots. The average activation energy and frequency factor for the first step were 40 kJ/mol and 0.14×10^3 1/min. For the second step the identical data were 58.1 kJ/mol and 0.19×10^4 1/min. (Thakur and Nuttall, 1987)

Coll *et al.* studied the thermogravimetric analysis of coal pyrolysis. They reported that the heating rate definitely affects TG results. They used lignite from Figols (Catalonia, Spain) in their work. They showed that pyroloysis of lignite can be considered in three parallel decomposition reactions, all of which are first order reactions. They used the Arrhenius law to analyze the TG data and

obtained the activation energies and the frequency factors as 24750, 82485 and 291270 $J\,mol^{-1}$ and 2.9, 1230 and 7.56$\times 10^{10}\ s^{-1}$ respectively (Coll, Perales, Arnaldos, and Casal, 1991).

Skala *et al.* studied the kinetic expressions of the pyrolysis of oil shale. Oil shale pyrolysis was commonly showed in the form of first order (Equation 2.14).

$$K \rightarrow f_1 P + f_2 R \qquad \text{(Equation 2.14)}$$

Kerogen concentration *is K*, *P* denotes the volatile products (gas and oil) and *R* shows the residue. It is apparent that $f_1 + f_2 = 1$. In the Skala et al. study, the non-isothermal pyrolysis was done at a temperature range of 303-873 K in nitrogen flow and in the isothermal analysis; sample was heated till it reaches to the temperature range of 673-794 K. The integral method was applied to both methods. The average value obtained for *f₁* was 0.74. Skala et al. showed that *f₁*, which showed the extent of gas and oil drops to lower than 0.5 when temperature increased to higher than 550 °C. They suggested that the reason for the decrease in the amount of *f₁* is that the main processes that occur in oil shale pyrolysis at higher temperatures are coking and cracking so less oil and gas is produced. This means that coke production will increase, and oil and gas production will decrease at high temperature reactions (Skala, *et al.*1992).

Lozano *et al.* have studied the thermal degradation of bitumen from Faja, in the Orinoco and have monitored the amount of the bitumen that is converted to gas. Equation 2.15 was applied to the gas changes.

$$\frac{d(a_n - X_n)}{dt} = -K_n (a_n - X_n)^n \qquad \text{(Equation 2.15)}$$

Lozano et al. divided the thermal degradation temperature regions into three distinct parts. The first region includes temperatures below 325 °C, for which the zero-order reaction has been consumed. The second region is in temperature range of 325-420 °C, for which the sum of reactions in the order of zero and *n*

was considered. The third region is the temperature range above 420 °C. In this range, the reaction order is one (Lozano, et al. 1978).

George *et al.* have studied Athabasca pyrolysis. They stated that below 500 °C, more evolutions occurred due to distillation. They also found that in the temperature range of 500-950 °C, fraction crackings and degradation to gases were more dominant. At temperatures of about 440 °C, the activation energies obtained for bitumen and asphaltene were 45.98 kJ/mol and 188.10 kJ/mol respectively. The low bitumen activation energy in this range was attributed more to the latent heat of volatilization than to hemolytic degradations, the latter of which caused the high asphaltene activation energy (George *et al.* 1978).

2.6   Copyrolysis of bitumen and oxygenate-containing materials and its attribution to industry

The goal of the refining processes is to convert crude oil to useful products such as fuel gas, kerosene, gasoline, diesel fuel and fuel oil. There are numerous refining processes. As discussed before, these include visbreaking, coking and residue hydroconversion. Other processes common in refineries are naphtha hydrotreating, distillate hydrotreating, fluid catalytic cracking, residue hydroconversion and deasphalting. The process used depends on the type of feed and the type of product.

In this study, bitumen was copyrolysed with oxygenate-containing materials. The main feed was bitumen and the reaction was pyrolysis. Neither hydrogen nor a catalyst was added. The feed was pyrolysed at 380 °C in a micro batch reactor and the gas and the residue products were collected for further analysis. Comparing the pyrolysis system studied to the primary upgrading processes used in industry revealed many similarities between the two processes.

Delayed coking is a semi-batch process in which the feed is first heated to about 480 °C in a furnace and the free radicals start to be produced. After that, the feed is directed to a large vessel, in which the free radicals react to each other and finally the coke is produced. At the end of the process, the coke is removed. The products of delayed coking are gas, naphtha, distillate, gas oil and coke (Wauquier, 1995).

In this study, a batch micro reactor was heated to 380 °C and during the heating process, it produced free radicals. The produced coke was collected after the reaction. The products in this study were naphtha, kerosene, distillate oil, gas oil and coke. There are many similarities between the studied process and the delayed coking process in terms of free radical production (cracking bitumen to free radicals without the presence of oxygen, hydrogen and catalyst) and types of products.

One difference between the two processes is the reaction time. In the delayed coking process, the total cycle takes about 48 hours. Most of this cycle time is consumed with filling the coke drum with coke and cooling, and for other uses. The total warm-up time for the delayed coking process is seven hours (Gary, *et al.* 2007).

In industry, the approach to upgrading is to produce light fractions. Depending on the crude oil substitute, the upgrading operations vary. In Suncor, for example, there are number of upgraders that produce different materials. One of these is the Millennium upgrader, which produces gas oil. A delayed coking process in the Millenium upgrader sequence converts bitumen to coke and coke distillates.

The Voyageur upgrader is another Suncor operating refinery. Similar to the Millennium upgrader, the Voyageur upgrader uses the delayed coking technology. One of the main differences between the Millenium and the Voyageur is that in the latter, there is a gasification unit for hydrogen production.

In the Suncor upgrading technologies, the delayed coking process is among the primary upgrading units and its products undergo additional secondary upgrading technologies in order to obtain diesel and gas fuel. In the Husky Bi-Provincial upgrading process sequence, a delayed coking process is among the secondary upgrading technologies. The Husky product (mainly coke) is collected as one of the Husky Bi-Provincial process final products and not much further secondary upgrading processes are operated on its product.

One aspect that has always been interesting in industry is the mass yield of the liquid products per mass of the initial feed. This study will show that the mixtures of some oxygenate-containing materials and bitumen increased the total liquid yield in comparison to the plain bitumen pyrolysed at a higher temperature. Also, some additives in this study increased the amount of the light fractions and decreased the coke yield. The other advantage of using the additives in this study is that the reaction time decreased when the oxygenate containing materials were copyrolysed with bitumen. This technology can be used for delayed coking processes in industry to obtain more light fractions, less coke yield, and a faster reaction rate.

2.7 References

Afanasev, I. B.; Dorozhko, A. L; Brodskii, A. V. Chelating and free –radical scavenging mechanisms of inhibitory-action of Rutin and Quercetin in lipid-peroxidation. *Biochemical pharmacology.* **1989**, *38 (11),* 1763-1769

Ali, M. F.; Saleem, M. Thermal decomposition of Saudi crude oil asphaltenes. *Fuel Science and Technology International.* **1991**, *9(4),* 461-484

Amarowicz, R.; Pegg, R. B.; Rahimi-Moghaddam, p. Free-radical scavenging capacity and antioxidant activity of selected plant species from the Canadian prairies. *Food Chemistry.* **2004**, *84(4),* 551-562

Balasundram, N; Sundram, K.; Samman, S. Phenolic compounds in plants and agri-industrial by-products: Antioxidant activity, occurrence, and potential uses. *Food Chemistry.* **2006**, *99(1), 191-203*

Basily, I. K.; Ahmed, E.; Nashed, N.; Factors affecting the yields produced from the 2-stage pyrolysis of Egyptian bitumen. *Analytical and Applied pyrolysis.* **1990**, *17(2),* 153-167

Bjorsvik, H. R. Fine chemicals from lignosulfonates. 1. Synthesis of vanillin by oxidation of lignosulfonates. *Organic Process Research Development.* **1999**, *3(5),* 330-340.

Boduszynski, M. M. Composition of heavy petroleums .1. Molecular-weight, Hydrogen deficiency, and heteroatom concentration as a function of atmospheric equivalent boiling point up to 1400 degree Fahrenheit (760-degrees-C). *Energy Fuels.* **1987**, *1(1)*, 2-11.

Bukka, K.; Miler, J. D; Oblad, A. G. Fractionation and characterization of Utah tar sand bitumens-Influence of chemical composition on bitumen viscosity. *Energy Fuels.* **1991**, *5*, 333-340

Carlson, G. A. Computer simulation of the molecular structure of bituminous coal. *Energy Fuels.* **1992**, *6(6)*, 771-778.

Coats, A. W.; Redfern, J. P. Kinetic parameters from thermogravimetric data. *Nature.* **1964**, *201(491),* 68-69.

Coll, T.; Perales, J. F.; Arnaldos, J. Coal pyrolysis – Thermogravimetric study and kinetic modeling. *Thermochimica Acta.* **1992**, *196(1),* 53-62.

Collett, G. W.; Rand, B. Thermogravimetric investigation of the pyrolysis of pitch materials – A compensation effect and variation in kinetic- parameters with heating rate. *Thermochimica Acta.* **1980**, *41(2),* 153-165.

Cottrel, J. H. *Development of anhydrous process for oil-sand extraction.* Research Counsil of Alberta. **1963**, 193-206

Dogan, O. M.; Uysal, B. Z. Non-isothermal pyrolysis kinetics of three Turkish oil shales. *Fuel.* **1974**, *75(12),* 1424-1428.

Dutta, R. P.; McCaffrey, W. C.; Gray, M. R. Thermal cracking of Athabasca bitumen: Influence of steam on reaction chemistry. *Energy Fuels.* **2000**, *14(3)*, 671-676.

Earnest, C. M. Thermogravimetry of selected American and Australian oil shales in inert dynamic atmospheres. *Thermochimica Acta.* **1982**, *58(3)*, 271-288.

Fuchs, W.; Sandhoff, A. G. Theory of coal pyrolysis. *Industrial and Engineering Chemistry.* **1942**, *34,* 567-571.

Gersten, J.; Fainberg, V.; Hetsroni, G. Kinetic study of the thermal decomposition of polypropylene, oil shale, and their mixture. *Fuel.* **2000**, *79(13)*, 1679-1686.

George, R.; Ritchie, S.; Roche, R. S.; Steedman, W. A pyrolysis-gas chromatographic analysis of Athabasca bitumen. *Industrial and Engineering chemistry product research and development.* **1978**, *17,* 370-372

Given, P. H. Structure of bituminous coals- Evidence from distribution of hydrogen. *Nature.* **1959**, *184(4691),* 980-981.

Haddadin, R. A.; Mizyed F. A. Thermogravimetric analysis kinetics of Jordan oil shale. *Industrial Engineering Chemistry Process Design and Development.* **1974**, *13(4),* 332-336.

Hatcher, P. G.; Lerch, H. E.; Verheyen, T. V. Organic geochemical studies of the transformation of Gymnospermous Xylem during peatifiction and coalification to subbituminous coal. *International Journal of Coal Geology.* **1990**, *16(1-3),* 193-196.

Haykiri-Acma, H.; Ukbayrak, S. K.; Gunduz, O. Thermal analysis of different fossil fuels. *Fuel Science and Technology International.* **1993**, *11(11),* 1611-1627.

Huttinger, K. J.; Michenfelder, A. W. Molecular structure of a brown coal. *Fuel.* **1987**, 66(8), 1164-1165.

Huttinger, K. J.; Lietzke, G. A. Steam gasification mechanisms and kinetics - The role of hydrogen inhibition. *Erdo Kohle Erdgas Petrochemie.* **1989**, *42(6),* 241-245.

Klemm, D.; Heublein. Cellulose, B.: Fascinating biopolymer and sustainable raw material. *Angewandte Chemie-International Edition.* **2005**, *44*(22): 3358-3393.

Kok, M. V.; Pamir, M. R. Pyrolysis and combustion studies of fossil fuels by thermal analysis methods. *Analytical and Applied Pyrolysis.* **1995***, 35(2)*, 145-156.

Lazano, J. A. F.; Gonzalez, R. Z.; Fernandez, M. C. Thermal degradation of bitumen from the Faja of the Orinoco Ind. *Eng. Chem. Prod.* **1978**, *17(1),* 71-79

Li, M. F.; Sun, S. N. Microwave-assisted organic acid extraction of lignin from bamboo: Structure and antioxidant activity investigation. *Food Chemistry.* **2012**, 134(3), 1392-1398.

Ma, Y.; Li, S. The pyrolysis, extraction and kinetics of Buton oil sand bitumen. *Fuel Processing Technology.* **2012**, *100*, 11-15.

Mahajan, O. P.; Tomita, A.; Nelson, JR. differential scanning calorimetry studies on coal. 2. Hydrogenation of coals. *Fuel.* **1977**, *56(1),* 33-39.

Mathews, J. P.; Chaffee, A. L. The molecular representations of coal - A review. *Fuel.* **2012**, *96(1)*, 1-14.

McKenna, A. M.; Purcell, J. M. Heavy Petroleum Composition. 1. Exhaustive Compositional Analysis of Athabasca Bitumen HVGO Distillates by Fourier Transform Ion Cyclotron Resonance Mass Spectrometry: A Definitive Test of the Boduszynski Model. *Energy Fuels.* **2010**, *24*, 2929-2938.

Mcmillen, D. F.; Lewis, K. E.; Smith, G. P. Laser-powered homogenous pyrolysis- Thermal studies under homogeneous conditions, validation of the technique, and application to the mechanism of Azo compound decomposition. *Physical Chemistry.* **1982**, *86(5),* 709-718

Miller, J. D.; Misra, M. Hot water process-development for Utah tar sands. *Fuel Processing Technology.* **1982**, *1*, 27-59.

Patrakov, Y. F.; Kamyanov, V. F. et al. A structural model of the organic matter of Barzas liptobiolith coal. *Fuel.* **2005***, 84(2-3)*, 189-199.

Parsons, A. F.; *An introduction to free radical chemistry,* Blackwell Science: York, 2000

Philip, C. V.; Anthony, RG.; Cui, Z. D. Structure and reactivity of Texas lignite. *A. C. S.* **1983**, *186(AUG),* 66-74

Rajeshwar, K. The kinetics of the thermal decomposition of Green River oil shale kerogen by non-isothermal thermogravimetry. *Thermochimica Acta*. **1981**, *45(3),* 253-263.

Ranjbar, M.; Pusch G. Pyrolysis and combustion kinetics of crude oils, asphaltenes and resins in relation to thermal recovery processes. *Analytical and Applied Pyrolysis*. **1990**, 20, 185-196.

Rosenvold, R. J.; Dubow, J. B.;Rajeshwar, K. Thermo-physical characterization of oil sands. 4. Thermal analysis. *Thermochimica Acta*. **1982**, *58(3)*, 325-331.

Savage, P. E.; Klein, MT. Asphaltene reaction pathways 2. Pyrolysis of N-pentadecylbenzene. *Industrial Engineering Chemistry Research.* **1987**, *26(3),* 488- 494

Schramm, L. L; Smith, R. G; Stone, J. Interfacial chemistry of the hot water process for recovering bitumen from the athabasca oil sands. *A.C. S.* **1984**, *187,* 209-216.

Shi, Z. J.; Xiao, L. P.; Deng, J. Physicochemical characterization of lignin fractions sequentially isolated from bamboo (Dendrocalamus brandisii) with hot water and alkaline ethanol solution. *Applied Polymer Science.* **2012***, 125(4),* 3290-3301.

Shinn, J. H. Visualization of complex hydrocarbon reaction systems. *A.C.S. 1996, 211,* 510-515.

Skala, D.; Sokic, M. The determination of a complex kinetic expression of oil shale pyrolysis using combined nonisothemal and isothermal TG. *Thermal Analysis.* **1992**, *38(4),* 729-738.

Speight, J. G. *The Chemistry and Technology of Petroleum*, 3ed; CRC Press: New York, 2006

Srinivasa, S.; Flury, C.; Afacan, A.; Masliyah, J.; Xu, Z. Study of Bitumen Liberation from Oil Sands Ores by Online Visualization. *Energy Fuels.* **2012**, *25*, 2883-2890

Thakur, D. S.; Nuttall, H. E. Kinetics of pyrolysis of Moroccan oil shale by thermogravimetry. *Industrial Engineering Chemistry Research.* **1987**, *26(7)*, 1351-1356

Tromp, P. J. J.; Kapteijn, F.; Moulijn, JA. Characterization of coal pyrolysis by means of Differential Scanning Calorimetry. 1. Quantitative heat-effects in an inert atmosphere. *Fuel processing technology.* **1987**, *15,* 45-57

Tye, C. T.; Smith, K. J. Cold Lake bitumen upgrading using exfoliated MoS2. *Catalysis Letters***. 2004***, 95(3-4)*, 203-209.

Varhegyi, G.; Antal, M. J.; Jakab, E.; Szabo, P. Kinetic modeling of biomass pyrolysis, *Analytical and Applied Pyrolysis.* **1997**, *42,* 73-87.

Vuthaluru, H. B. Thermal behavior of coal/biomass blends during co-pyrolysis. *Fuel Processing Technology.* **2004**, *85,* 141-155

Walton, N. J.; Mayer, M. J.; Narbad, A. Molecules of interest - Vanillin. *Phytochemistry.* **2003**, *63(5)*, 505-515.

Wender, I. Catalytic synthesis of chemicals from coal. *Catalysis Reviews-Science and Engineering.* **1976**, *14(1)*, 97-129.

Williams, P. T.; Ahmad, N. Investigation of oil-shale pyrolysis processing conditions using thermogravimetric analysis. *Applied Energy*. **2000**, *66(2)*, 113-133.

Yang, H.; Yan, R.; Chen, H.; Lee, D. H.; Zheng, C. Characteristics of hemicellulose, cellulose and lignin pyrolysis. *Fuel.* **2007**, *86(12-13)*, 1781-1788

Yi-min, w.; Zhao, Z. l.; Hai-bin, L. I.; HE, F. Low temperature pyrolysis characteristics of major components of biomass. *Fuel Chemistry and Technology.* **2009**, *37(4),* 427-432

Zhao, Y.; Wei, F.; Ying, Y. Effects of reaction time and temperature on carbonization in asphaltene pyrolysis. *Petroleum Science and Engineering.* **2010**, *74(1-2)*, 20-25

3. CHAPTER 3: EXPERIMENTAL

3.1 Materials

3.1.1 Oil sands derived bitumen

Bitumen:

Bitumen used in this work was from Cold Lake, Alberta, provided by Imperial Oil Limited. The bitumen properties are presented in Table 3.1.

Table 3.1. Properties of Cold Lake bitumen used in the current study

Elemental analysis (wt %)	
C	84.13
H	9.95
N	0.60
S	5.32
Asphaltene content	19.34
Ash Content	0.68
Raw Bitumen fractions at atmospheric pressure (wt %)	
Light naphtha (40-79 °C)	<1%
Medium naphtha (79-121 °C)	<1%
Heavy naphtha (121-191 °C)	<1%
Kerosene (191-277 °C)	<1%
Distillate fuel oil (277-343 °C)	6%
Gas oil or lube stock (343-566 °C)	42%
Residuum (>566 °C)	~50%

3.1.2 Oxygenate containing raw materials

Biomass additives:

Celullose:	Lignin:
Sigma-Aldrich	Lignin, kraft
Cotton linters Cellulose powder	Low sulfonate content
Fibers (medium)	Provided by Sigma-Aldrich
Product of United Kingdom	Product of USA
C6288-100G	471003-100G
Lot# 120M01837	Lot# 04414PEV
Product code: 1000998367	Product code: 1000958047
CAS: 9004-34-6	CAS: 8068-05-01
Calculated ash percentage: < 1% ± < 1%	

Coal additives:

Table 3.2. Characterization of the Canadian Lignite (Zhao, 2012), subbituminous coal and bituminous coal (Rivolta, 2012)

Description	Lignite	Subbituminous	Bituminous
Origin	Boundary Dam	Coal Valley	Teck
Proximate analysis (wt %)			
moisture	23.5	5.5	1.9
ash[*]	13.1	12.4	10.5
volatile matter	43.2	31.4	24.6
fixed carbon	20.2	50.7	63.0
Ultimate analysis (wt %)			
carbon	58.7	65.4	84.3
hydrogen	4.4	4.2	4.6
nitrogen	0.9	0.8	1.4
sulfur	0.8	0.4	0.7

*Additional ash analyses were performed for lignite, subbituminous coal, bituminous coal and the other samples. The method that was used to analyze the ash content is brought in section (3.4.6) and the results are followed in Table 3.4.

3.1.3 Solvents, chemicals and materials

Table 3.3. List of solvents, chemicals and materials

Toluene Sigma- Aldrich CHROMASOLV®, for HPLC, 99.9% CAS: 108-88-3 Pcode: 1001209108	**ASTM** ASTM D5307 Crude Oil Internal Std., SUPELCO Analytical 4-8479
Carbon disulfide (CS2) Sigma- Aldrcih Carbon disulfide Lot# MKBG 3797V Pcode: 4100434063	**Sulfanilic acid** Sigma Aldrich Lot# MKAA0502V Pcode: 1001323936 251917- 25G
Cupric Nitrate Hemipentahydrate Fisher Scientific Lot# 108217 CAS 19004-19-4	**Vial** Fisherbrand Vial, SCREW THREAD With Teflon Lined Cap 25 ml glass vial with
Spatula Fisher Scientific Fisherbrand Semimicro Spatula with One Tapered End, One Rounded End Stainless-steel Tip thickness: 0.035in. (0.89mm) One end tapered to 0.14in. (3.5mm) rounded tip for use in conical-bottom tubes Rounded end has 0.25in. (6.6mm) rounded	**Spoonula** Fisher Scientific Fisherbrand Spoonula Lab Spoons Polished stainless-steel Snag-free Spoon end: 1.25L x 0.56in. W (32 x 14mm) Spatula end: 2L x 0.31in. W (51 x 7.9mm)

tip for regular tubes	
Balance (used for TGA samples) METTLER TOLEDO Inc. Excellence XS105 DualRange	**Bacti- Cinerator** OXFORD RECORDER HRI 8889- 001007 135 WATS
TGA crucible METTLER TOLEDO Inc. ME-00024123 (70ul)	**Hood** LABORATORY Fume Hood, model: 115/230 Vac 15 A:111- 6OPP
Sealant Swagelok PTFE Tape Part No.: MS-STR-8 Describtion: PTFE Tape Thread Sealant, 1/2 $\times$ 288 in. (12.7 $\times$ 732 cm)	**Temperature controller for sand bath** Omron Controller E5CK-AA1 100-240 VAC
Heater and Mixer Fisher Scientific Thermix® STIRRING HOT PLATE MODEL 210 T	**Purging apparatus** Elementar 0.05 ml-Sn
Lubricant Swagelok Part No.: MS-TL-SGT Description: Silver Goop® Thread Lubricant, Oil-Based, 1 oz. (29.5 cm3) Tube	**Balance (used for Sim-Dist samples)** METTLER TOLEDO AB 265-S/FACT Max 61g, 220 g d= 0.01 mg/0.1 mg
Vial (used for Sim-Dist samples) Chromatographic specialties INC. C779100 VIAL, CHROMSPEC, SCREW Thread 2ML, 12×32 MM Lot# 22991106V31	**Micro pipet** Fisher Scientific Fisher brand 9" Disposable Pasteur Pipets Borosilicate Glass/Non- Sterile Cat. N. 13-678-20C
Polywax 655 SUPELCO Analytical 4-8477	**Micro Balance (used for CHNS samples)** METTLER TOLEDO 1128281345 MX5 Max 5 g, d=1 ug
Pan for CHNS (tin boat) Pan for solid powder samples: Elementar Analysensysteme GmbH 22 137 418 Tin boats 4 $\times$ 4 $\times$ 11 mm Pan for liquid samples: Art-No.: 03951619 Tin capsules, volume 0.05 ml 3.5 $\times$ 9 $\times$ 0.1 mm	**Liquid Leak Detector** Swagelok Part No.: MS-SNOOP-8OZ Description: Snoop® Liquid Detector, 236 mL Bottle Specification summary: eClass (4.1) 30040101 eClass (6.0) 30-04-01-01 UNSPSC (4.03) 40141616 UNSPSC (SWG01) 40141616
XRF Brand: Bruker AXS	**XRF Cup** isoSPEC

Model Designation: S2 RANGER Part Number: A20-X10-1A2D2B	P/N: 2143 XRF sample cup, 40.00 mm, PK100 Lot#: 011876M
XRF Sample Support Carrier Frame Spectromembrane Chemplex	**Balance** METTLER TOLEDO EXCELLENCE PLUS XP1203S
Weighing paper Fisher Scientific Fisherbrand 3"×3" Cat. No. 09-898-12A	**Gas Bag** Sigma-Aldrich Tedler Gas Sampling Bag Tedler® Maximum volume × W × L: 1L × 7in. × 9in

3.2 Equipment and procedure

3.2.1 Preparation of reactor feed

About 1g of bitumen was added to a micro reactor. A measured amount of an additive was added in a way that the additive percentage would be 10% of the mixture. The amount of the additive which was added to the reactor was calculated by Equation 3.1(W_a is the additive weight and W_b presents the bitumen weight).

$$\left[\begin{array}{l} \dfrac{w_a}{w_b + w_a} = 0.1 \\[2em] w_a = w_b/9 \end{array} \right. \qquad \text{(Equation 3.1)}$$

Besides using the mixtures in the experiments, the raw materials were also used separately as the reactor feed. Two of the feeds which were neither mixtures nor raw materials, were prepared experimentally. One of them is POB (partially oxidized bitumen) and the other is asphaltene, the preparation methods for both are further described.

3.2.2 Reactor description and loading

After the addition of the additive to bitumen, a small amount of lubricant was added to the reactor lid to ensure that the later opening of the reactor lid after

high temperature reaction could be done easily and then the reactor lid was closed by holding it on a bench vice and using a wrench for tightening. Then, system was tightened by hand loosely just to measure the initial weight of the whole system before purging the nitrogen gas (W1). The system was then attached to a nitrogen cylinder to fill the reactor with nitrogen gas. After that the system was checked for any leakage. It was connected to the cylinder and was checked at 4 MPa using a liquid leak detector (LLD). The LLD was poured on every connection in the system and the system was carefully checked to see whether there is any bubble coming out or not. Some bubbles were found on some connection parts for instance around the reactor lid. Any bubble resulted in disconnecting the system from the cylinder, purge the gas out under the hood by opening the valve loosely and then the reactor lid and any other connections were tightened again and finally the same procedure to check for any leakage was done again until there was no further leakage. The pressure in the micro reactor was set to exactly 4 MPa, the valve was closed so the system was able to be disconnected from the Nitrogen cylinder and then the entire system was disconnected and it was left idle (vertically on floor) for 20 minutes just to make sure if the pressure that the gauge showed before remains the same. If no, the stated steps were redone, if yes, the reactor system outer layers were dried by use of lab napkins to ensure no LLD is remained on the outer walls. After that, the reactor system's weight was measured precisely on the balance and the measured weight was recorded (W2).

By subtracting W2 from W1, the weight of the purged nitrogen gas is calculated (Wg= weight of the Nitrogen gas purged in the system).

$$W1 - W2 = Wg$$ (Equation 3. 2)
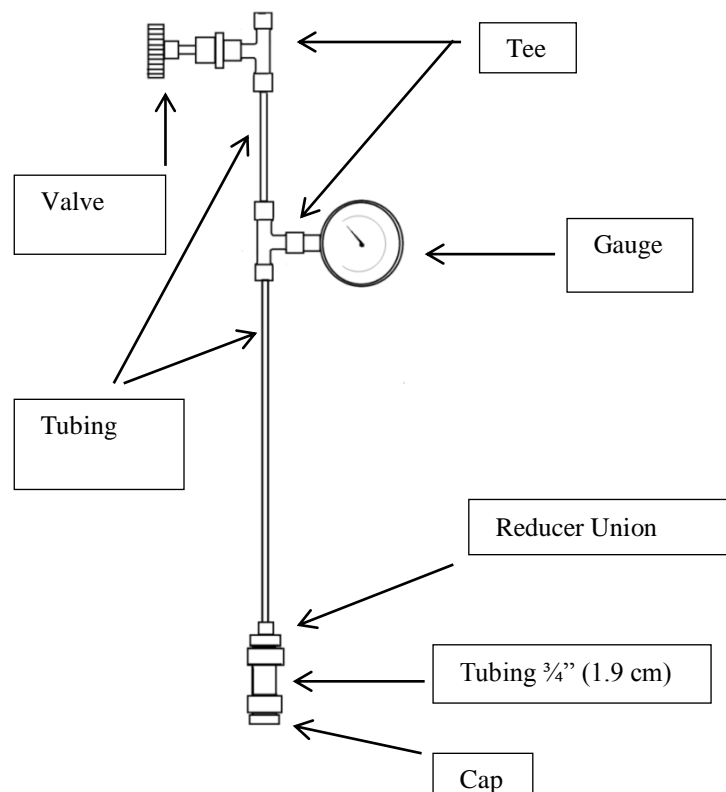
Figure 3.1. The system used in the current study for pyrolysis

All the fittings and the material shown in Figure 3.1 were purchased from Swagelok and their specified numbers are followed:

Reducer: SS-100-R-4BT
Tee: SS-400-3
Tubing: SS-1RS4
Tee for gauge: SS-400-3-4TTF
Gauge: PGI-63C-0G1000-LA07
Reducing union: SS-1210-6-4
Tubing 3/4 ": SS-T12-S-049-20
Cap: SS-1210-C
Clear tubing: PFA- T4- 062

The micro reactor is shown in Figure 3.2. Its capacity is 15 mL and the Diameter Nominal is 10 mm.

Figure 3.2. Micro reactor provided by Swagelok

3.2.3 Sand bath preparation:

The reactor set up was then carried out in a fluidized sand bath for one hour at 380 °C. A TECHNE fluidized Sand Bath (Model No: SBS-4) was used in this work. The sand bath is filled with silica sand which is fluidized by an increase in temperature and provides a homogenous heat transfer media. The air flow was kept constant by setting the flow at a constant range. The temperature was initially set as 380 °C. There was a thermocouple designed in the sand bath which measured the temperature and the temperature controller showed that the temperature after reaching the set point remains constant. It took about 30 minutes for the sand bath to reach 380 °C and in further 10 minutes it was observed just to make sure that the sand temperature does not fluctuate and no fluctuation was observed.
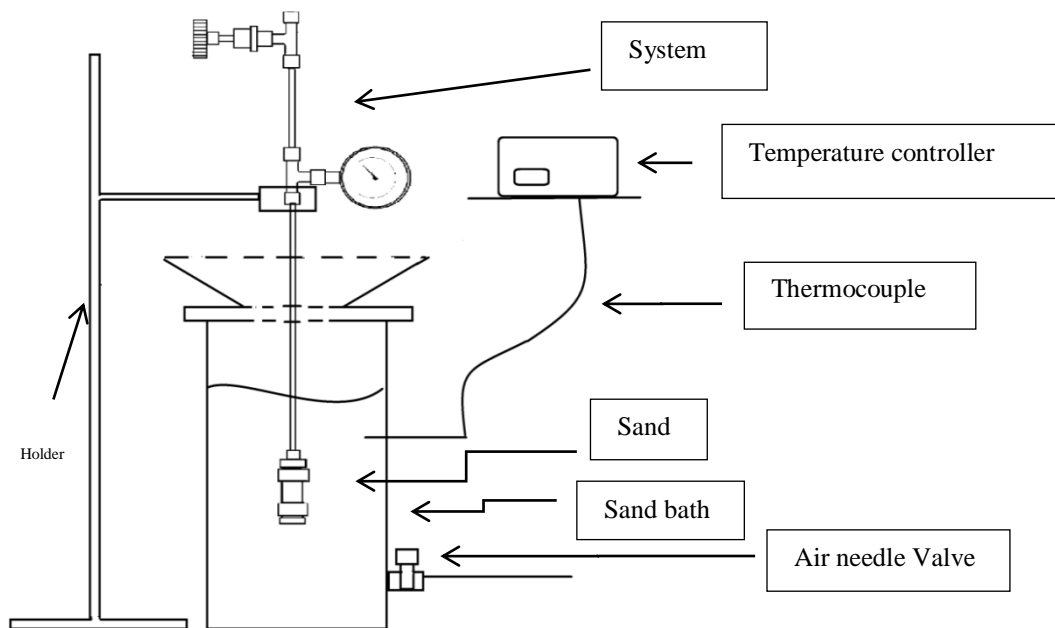
Figure 3.3. The system and the sand bath

The micro reactor which was attached to a clamp and a holder was put inside the sand bath for one hour. After one hour, it was taken out and put on a bench idle for one hour to be cooled down to the room temperature. When it is completely cooled, the system was cleaned from the contaminated sand and the weight of the system was measured (W3) with the same balance that was previously used for the weight measurement before heating. The difference in the weight was less than 1% of the total input nitrogen, therefore there is a negligible amount of mass loss during the process.

$$\frac{(W3-W2)}{Wg} < 1\%$$ (Equation 3.3)

3.2.4 Gas sampling procedure

A gas bag was then attached to the system to collect the produced gases as well as the initial nitrogen gas. The gas bag was connected to the system by clear tubing and to avoid gas leakage during the collection, some Teflon tape (PTFE tape) was used to tighten the part of the attachment of the tube to the gas bag. For the other end of the tube which is connected to the system, a nut and ferrule was used and the tube was completely connected to the system top part. After that, the valve was opened. The pressure gauge showed a drop off in pressure immediately and the gas bag become full. The gas bag and the valve were then closed and the gas bag and the plastic tube were detached from the system.
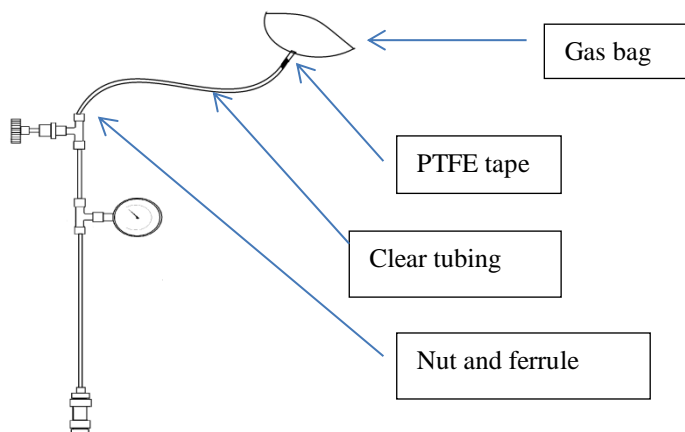
Figure 3.4. Collection of gas from the system

The gas was then analyzed by means of GC. The gas bag was connected to the inlet of the GC by use of clear tubing. The GC results give the area of the peaks which demonstrate presence of different gases which were produced. Based on the initial mass of the purged nitrogen and because the percentages of the produced gases can be calculated from the GC data, the amounts of the gases produced by pyrolysis were obtained.

3.2.5 Liquid sampling procedure

After the gas product was collected, the liquid residue was also collected using a spatula and was stored in a Teflon lined vial. It should be protected in the Teflon lined vials because the other types of the vial lids were not appropriate for chemical storage and the lid material would react with the chemical while it was stored. After removing the samples from the reactors, the reactors were washed thoroughly with toluene and napkins three times to make sure that they were clean for further uses.

3.3 Feed preparation procedures

3.3.1 Preparation of partially oxidized bitumen (POB)

One gram of Cold Lake bitumen was added to a micro reactor; the micro reactor was sealed by a lid and attached to a tube. The tubing and the end part of the tube was left under the fume hood. The whole system was held using a clamp. The reactor and a small part of the tube were put inside the sand bath and remained for three hours at 380 °C. The system was not purged with the nitrogen gas. It was also not supplied by a constant air supply but just exposed to air while it was heated. The prepared partially oxidized bitumen is considered as one of the raw materials which were later added as an additive to the plain bitumen. More details are shown in Figure 3.5. After three hours, the system was taken out and remained idle to cool down to the room temperature. After one hour, the lid was removed and the partially oxidized bitumen was taken out

using a spatula and was put into a 25 mL glass vial with a Teflon lined lid. The lid was checked to be properly closed.
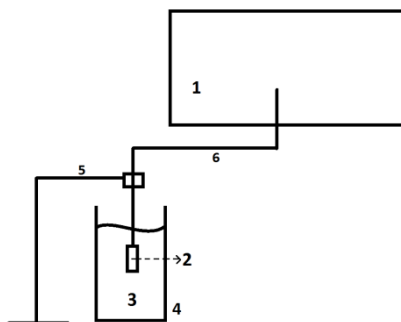
Figure 3.5. Preparation of the partially oxidized bitumen. (1- Fume hood, 2- Micro reactor, 3- Sand, 4- Sand bath, 5- Clamp, 6- Tubing)

3.3.2 Preparation of bitumen and oxygenate containing co-feed mixtures

In order to compare the results of the pyrolyzed mixtures with the same type raw samples, there was a need to prepare the raw mixtures. Since bitumen is highly viscous, the mixture would not be homogenous at room temperature; however, mixing the mixture by a spatula and providing some heating to the mixture would make it as a homogenous mixture. For preparing the raw mixtures, the same compositions of the samples which were put into the micro reactors were prepared (90% bitumen and 10% of the additive). First, about one gram of bitumen was added to the vial and then the amount of the additive was added to the mixture according to Equation 3.1. Temperature of the heater was measured using a thermocouple inside the beaker filled by water and the heating rate was controlled in such a manner in which the thermocouple shows constant 70°C. Then, the vials were put on the heater with open lids. A spatula was used for mixing the samples manually. The spatula was cleaned by a napkin and toluene after mixing each sample. The total time that the samples were on the heater was 30 minutes and they have been mixed each for 3 minutes in three series of one minute each. When the mixing process was done, the vials were closed and stored.

3.3.3 Preparation of bitumen and Cupric Nitrate Hemipentahydrate co-feed mixtures

A solution of Cupric Nitrate Hemipentahydrate ($Cu(NO_3)_2.2.5H_2O$) and Mili-Q water (ultra-distilled water) was made in such a way that the concentration of the Cupric Nitrate in water would be 200 ppm. In order to make this solution, 0.1 g of $Cu(NO_3)_2.2.5H_2O$ was added to 500 mL purified water.

After that, as it was described in the previous sections, about 1g of bitumen was added to the micro reactor. Later, about 0.1 g of the solution (the mixture of metal and water) was added to the micro reactor. So, basically the additive in this section is the solution of 200ppm $Cu(NO_3)_2.2.5H_2O$ in water. When the feed was ready, the reactor was loaded according to section 3.2.2.

3.4 Analyses

3.4.1 Thermogravimetric analysis (TGA)

Thermal degradation analysis were performed using a TGA/DSC1 LF FRS2 MX5 with a sample robot manufactured by METTLER TOLEDO Inc. and 70 µL aluminum oxide pans provided from the same company. The measurements were operated under nitrogen gas at a flow rate of 20 mL/min. The heating rate was 20 °C/min and the temperature ranges was programmed from 20 °C to 900 °C and the nitrogen flow was 20 mL/min. STARe software for TGA/DSC 1 system was used for the analysis of TGA results. Many features of the software such as; first derivative, second derivative, single value, step horizontal and sample size were already provided in the software.

First the crucibles were put into the furnace (Bacti- Cinerator) for 30 minutes so that if there is any tiny particle inside would burn with oxygen. Then, it was cleaned with toluene and napkins thoroughly. Then, the crucible was put on the balance and the balance number was set to zero with the crucible on it. After that, the crucible was taken out of the balance and about 5 mg of the sample was added to the crucible and the exact mass of the sample read from the balance was

put as the initial sample mass data into the TGA. After the TGA procedure, the crucibles should to be put into the furnace and washed with toluene with the same method.

3.4.2 Gas chromatography for the off-gas

Gas chromatography analyses of the gas samples were performed using an Agilent 7890A Gas Chromatograph with flame-ionization detector (FID) and thermal conductivity detector (TCD). The FID heater temperature was set at 250 °C, the hydrogen flow was 60 mL/min and its air flow was 400 mL/min. The TCD heater temperature was set at 200 °C and its reference flow was 35 mL/min. A 243.84 cm × 0.32 cm (8 feet × 1/8 inch) HayeSep R stainless steel column was used for TCD and a 304.80 cm × 0.32 cm (10 feet × 0.125 inch) Molecular Sieve was used for FID. The injector gas was Helium with the flow rate of 25 mL/min at 200 °C. The inlet flow is 28 mL/min, inlet set point was 200 °C and the septum purge flow was 3 mL/min. The temperature program started at 70 °C and remained at that temperature for 7 minutes.   The temperature was then increased to 250 °C by 10 °C/min with a hold time of 2 minutes and then cooled down to 70 °C at 30 °C/min. The column temperature was maintained at 70 °C for 8 minutes. The GC calibration was checked with a standard gas sample (provided by Specialty Gases and Equipments). It was injected to the GC with the same method that the other sample gases were injected.

3.4.3 Simulated Distillation analysis (Sim-Dist)

For processing the Sim-Dist (Simulated Distillation Anayalysis) procedure, two 2 mL vials should be prepared for each sample. One is the internal standard vial. About 20-25 mg of sample was weighed and poured into the vial. Then, the internal standard (ASTM D5307 Crude Oil Internal Std.) was added with a micropipette for amount of 0.004-0.006g. After that, 1.8-2.0 g of carbon

disulfide was the last adding substance. By adding the stated components, the concentration of the sample was supposed to be almost 1%. The second sample was prepared by adding 20-25 mg of the sample and diluting it with 1.802.0 g of carbon disulfide and closing the cap.

The Varian 450-GC Gas Chromatograph with a 1093 Septum-Equipment Programmable Injector and a CP-8410 autosampler was used. The injection volume was 0.2 µl. The 5m × 0.53mm × 0.09 µm, Ultimetal Agilent J&W Column was used, the P/N number of the column is CP7569. Column flow was helium with flow rate of 15 mL/min. The flame ionization detector (FID) at 400 °C was used with the helium flow of 5ml/min, combustion (H_2) flow of 30 mL/min, and the combustion air flow of 300 ml/min. All runs were 45 min in length. The injector starts at 100 °C and increases to 400 °C with heating rate of 150 °C/min, then stays at 400 °C for 43 minutes. The initial temperature of the oven is 35 °C, it stays at this temperature for 1 minute, then increases to 400 °C with heating rate of 20 °C/min.

The column used in the Varian gas chromatograph was calibrated before using by ASTM D-5307 method which provides the calibration for the hydrocarbon mixture from C5 or C10 to C100. The calibration mixture was polywax 655 and ASTM D5307. Polywax provides the retention time of C10 to C100, different cuts with different boiling points were identified by polywax calibration. Using the known amount of ASTM D5307 that was injected for calibration, amount of C14, C15, C16 and C17 were specified; therefore, the other hydrocarbons injected after calibration should be analyzed according to the retention time that was achieved by the calibration method. This mixture helped identify the hydrocarbons with different carbon numbers to the instrument according to their retention times.

After the hydrocarbons were identified for the instrument, the samples were prepared with the method that was described in the previous section and then

were introduced to the instrument. Galaxie Chromatography data system software was used to integrate the amount of cuts in different temperatures. The samples used in this study were Raw Bitumen(RB), Pyrolysed Bitumen (PB), Pyrolysed Bitumen at 380 °C (PB), Pyrolysed Bitumen at 390 °C (PBat390), Raw partially oxidized bitumen at 380 °C (RPOB), pyrolysed mixture of bitumen and partially oxidized bitumen at 380 °C (P(B+POB)), Raw mixture of Bitumen and partially oxidized bitumen (R(B+POB), Pyrolysed mixture of bitumen and lignite at 380 °C (P(B+lignite)), Pyrolysed mixture of bitumen and cellulose at 380 °C (P(B+C)), Pyrolysed mixture of Bitumen and Bituminous Coal at 380 °C (P(B+BC)), Pyrolysed mixture of Bitumen and Lignin at 380 °C (P(B+lignin)), Pyrolysed mixture of Bitumen and Subituminous Coal at 380 °C (P(B+SC)).

3.4.4   Elemental analysis (Carbon, Hydrogen, Nitrogen and Sulfur analysis)

Elemental CHNS VARIO MICRO Cube was used for measurement of the amounts of carbon, hydrogen, nitrogen and sulfur. The furnace worked with a combustion tube working at 1150 °C and a reduction tube working at 850 °C. There is an Elemental adsorption column working at 40 °C at the time of running the instrument. The detector was TCD with the reference flow of 42 mL/min. The carrier gas was helium with the flow rate of 200 mL/min.

According to the sample phase, the samples used for CHNS (Elemental micro analysis) should be prepared in different crucibles. For liquid phase samples, tin capsules were used and for the solid phase samples tin boats were used.

- Powder sample preparation:

  2 mg of the powder sample was added to the tin boat and was completely pressed by the bottom of a spatula and should be folded to be completely flat that no sample could come out of the tin boat crucible.

Figure 3.6. Sample preparation method for CHNS

For both solid and liquid samples, 2 mg of sulfanilic acid samples were prepared for five times in the tin boat crucibles with the same method that the powder samples were prepared.

- Liquid sample preparation:

2 mg of the liquid sample was added to the tin capsules, then the air presenting in the capsules was purged out by use of the purging gas apparatus and at the same time, the top part of the capsule was then pressed by the pressing apparatus.

3.4.5   Further analysis (Asphaltene precipitation)

More experiments were done for various reasons which are summarized in this section. Asphaltene was precipitated and separated from bitumen in order to compare its results with the TGA results of bitumen and its mixtures. The ash contents were analyzed in order to get the complete information of the raw materials. Also, the X-Ray Flurosence was used to measure the sulfur amount of the mixture but this method was not successful and after that the elemental analysis equipment which is described in section 3.4.4 was used for analyzing the sulfur content as well as other element contents.

Asphaltene was recovered from the Cold Lake bitumen. About 10 g of bitumen was added to a flask and forty volume of n-pentane was added. Also, two magnetic stirrers were added to the mixture. The flask was covered by an aluminum foil on the top and was put inside the ultrasonic dispersion for thirty minutes, later it was put on the heater (with no heating, just the mixing property was used) for twelve hours. Then, the vacuum pump and filter papers were used

to collect the solvent. One flask which was attached to the vacuum pump was used, a filter paper was placed on its top and another upside down flask which has an opening top was used on top. The vacuum pump is turned on and the mixture was poured from the topper flask. Because the pressure in the collecting flask is almost vacuum, the solvent was absorbed from the filter paper and the solid parts would remain on the filter paper. After that, the pump was turned off and separated from the flask. Then, the filter paper was taken out carefully. For increasing the precision, more than one filter paper were used since the filter paper would be stocked with the solid particles and would not be able to transfer much amount of the solvent to the lower flask. Each time, the filter paper was collected and placed on an aluminum pan. Then, all the aluminum pans were placed into the vacuum oven for three hours. The weight of all the aluminum pans and the filter papers were measured right before their usage and right after they were taken out from the vacuum oven. Also, the remaining content on the filter papers were collected as the asphaltene, the amount of asphaltene was 19.34% of the initial weight of the raw bitumen.
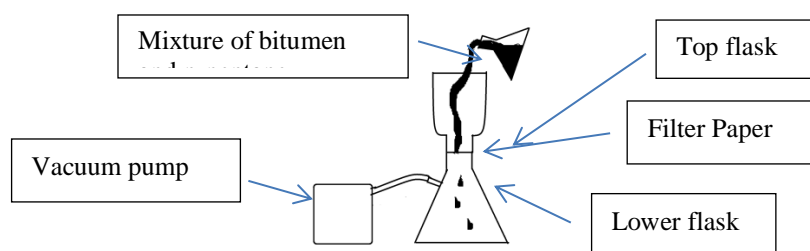
Figure 3.7. Asphaltene precipitation

3.4.6   Further analysis (Ash content analysis)

For analyzing the ash content of raw samples, Barnstead Thermolyne was used following towards the ASTM D3174 method. In this method, the particle size was suggested not to be more than 250 μm and the initial sample weight should be 1 g ± 0.1 mg. The ceramic capsules were completely washed with toluene and nitric acid to be uncontained of any inorganic and organic substances. Toluene could be poured a little bit on a clean napkin and used for cleaning the capsules

and for cleaning by nitric acid, for each capsule, about 20 mL of the acid was first added to an empty bicker, then water is added for amount of approximately 200 mL and the capsule is then carefully put inside the solution for about one day. After the capsules were cleaned thoroughly, the initial weight of the capsule was measured. Then, about 1 g of the sample was added to the capsule and the exact weight was saved. The capsules were put inside the furnace. The ASTM D3174 method suggests that the samples should first be heated to 450 °C in the first hour with the heating rate of 7 °C/min. In the next hour, the sample is heated to 750 °C with the heating rate of 5 °C/min. Then, furnace keeps the temperature at 750 °C for two hours and this is the end of the method. After that, the furnace is cooled down to the room temperature. And the ash content equals to the difference of the total weight of the capsule and the sample before and after the heating process, divided by the weight of the sample which was added to the capsule initially. Table 3.3 shows the ash content of the raw samples.

Table 3.4. Ash content of the samples (wt%)

Sample	Ash content (%)
bitumen	0.68
cellulose	<1
lignin	18.23
lignite	15.25
subbituminous coal	10.58
Bituminous coal	10.22

4.5.3. Further analysis (X-Ray Fluorescence Analysis):

Bruker AXS XRF (S2 Ranger) was used for bitumen mixtures to analyze the concentration of the sulfur in the samples, however, the XRF samples should completely cover the XRF cup surface and the bitumen sample does only cover a small part of the surface. As such, toluene was used for making a bitumen mixture solution and then covering the cup surface. However, it was noticed that toluene solves the plastic cover of the cup as well. Therefore, XRF could not be used for bitumen mixture analysis. As time passed, acetone was also tested and

observed. The bottom cover would also be affected by acetone as well. Also, bitumen could not be dissolved in acetone properly.

4.5.4. Further analysis (Separation of mixtures using Rota vapor)

The Gas Chromatography mainly shows the hydrocarbons with less than seven carbons in their molecular chain. For the hydrocarbons with higher number of carbons in their molecular chain, there is a need to separate the cuts. In order to have a clearer view of the sample cuts, Rota vapour was considered to be used to distillate different groups of hydrocarbons in various temperature ranges by means of increasing the temperature. The brand of Rota vapor used is Heidolph and its type is Heizbad Heiz-Vap (No: 517-61000-01-1). According to ASTM Manual on Hydrocarbon Analysis (ASTM, 1916), the hydrocarbons can be grouped on the basis of their distillation points (Table 3.5). Rotavapour was connected to the vacuum pressure so the temperatures given in the second column of Table 3.5 have been converted to the same range temperature points at almost vacuum pressure. The other reason of temperature conversion is that the maximum temperature for the rotavapour bath was 180 °C so the procedure had to be processed at low pressure (close to vacuum) to fulfill the equal distillation temperature ranges. Accordingly, the temperatures at the atmosphere pressure were converted to the temperatures at 50 mmHg.

Table 3.5. Bitumen cuts according to their distillation points

Hydrocarbon range	Distillation point at 760 mmHg, (° C) (ASTM, 1916)	Distillation point at 50 mmHg, (° C)
Gas	<40	<30
Light naphtha	40-79	<30
Medium naphtha	79-121	30-45
Heavy naphtha	121-191	45-105
Kerosene	191-277	105-175
Distillate fuel oil	277-343	175-235
Gas oil or lube stock	343-566	235-450
Residuum	>566	450

First, bitumen samples were diluted 4 times in toluene and were added to a flask and the flask was put into the rotavapour bath with the initial temperature of 30

°C and the pressure of 50 mmHg which was controlled by a vacuum pump. Heidolph pump (Rota Vac Vario Pumping Unit, No: 591-00142-00) was used for this study. Initially, not much distillate was observed; however, still the system was remained at the stated temperature for 10 minutes to ensure that there would be no further distilled drops. Then, the temperature was increased to 45 °C with the same procedure. As temperature was increased, more droplets were collected in the distilled flask. The procedure was continued to the maximum temperature that the instrument could provide. Then, the vacuum pump was turned off and the total distilled product was collected in to a vial for further analysis by GC-FID.

However, it was very unsatisfactory that the GC-FID could not recognize the peaks and it was only able to recognize the toluene. It showed 100% of toluene in the solution and the other components in the solution were not recognizable. Also, collecting the distilled amounts from Rota vapor flasks in different cut points separately was not a precise work. Therefore, using Rota vapour was not helpful at this stage to separate the samples into its main cuts. At this step, working with Simulatied Distillation analysis was useful.

3.5   References

ASTM. D3174 - 12 Standard Test Method for Ash in the Analysis Sample of Coal and Coke from Coal; ASTM: West Conshohocken, PA, 1973.

Manual on hydrocarbon analysis, 4th ed; Drews, A. W. Ed.; ASTM publication: Philadelphia, 1989.

Rivolta, M. *Solvent Extraction of Coal: Influence of solvent chemical structure on extraction yield and product composition*; Master thesis, University of Alberta, Edmonton, Alberta, Canada, 2012

Zhao, J. Effect of Hydrothermal Treatment on the Low Rank Coal Flotation. *Preprnits of American Chemical Society.* Div. Fuel Chem. **2012**, *57(1)*, 205-206

4. CHAPTER 4: THERMAL ANALYSIS OF THE COPYROLYSED BITUMEN WITH OXYGENATE CONTAINING MATERIAL

4.1 Introduction

Oxygenate containing materials contain C-O bonds. The C-O bonds have lower homolytic bond dissociation energy than C-C and C-H bonds. Oxygenates need less energy (lower temperature) to break the C-O bonds down to radicals than C-C and C-H bonds.

At lower temperature, although there are some advantages in terms of achieving to higher liquid yield, there is an important disadvantage which is the low reaction rate of thermal cracking reactions at low temperatures. However, if by some means, the initiation rate of the reactions could be increased, the conversion rate of the mixture could potentially increase as well. Although the propagation rate is not a function of the initiation rate, increasing the initiation rate would improve the chance of increasing the total reaction rate. The co-feeding of oxygenate rich material is a way to increase the rate of free radical production at lower temperatures.

Thermogravimetric Analysis (TGA) employs an instrument by which the change in the mass of a sample can be monitored as the temperature is changed. Also, the derivative of the mass change can be obtained by TGA, which shows the rate of mass change. Sample mass does not change with a constant rate and usually some peaks are observed in the Derivative Thermogravimetry (DTG). The maximum points of the peaks show exactly at what point, maximum mass losses occur in the sample. The second derivative shows the changes of the mass loss rates in time.

Co-processing of the coal and bitumen has long been studied. A literature study on bitumen, biomass and coal pyrolysis is provided in Chapter 2. Bitumen and in

general heavy bottom residue has been considered as an alternative to the recycling liquid in coal liquefaction technology. Medina *et al.* showed that when bitumen and coal are co-processed, the yield of light fractions increased and the heteroatoms in the light fraction decreased (Medina, et al. 1989). Some studies were done on copyrolysis of biomass and coal, both being oxygenate rich materials, but not many synergistic interactions were found (Pan, et al., 1996). A systematic study of the characteristics and potential benefits of the copyrolysis of oxygenate rich feed materials with Canadian oil sands derived bitumen is not available.

TGA study was done to understand the temperature dependent behavior of biomass and coal types and the blends with bitumen. The following was of interest:

(a) TGA of the raw materials provided information on the onset temperature of pyrolysis (initiation of decomposition), the relationship between temperature and pyrolysis related mass loss, as well as the micro carbon residue (MCR) of each feed material. The onset value of pyrolysis provided some indication of the minimum temperature at which the raw material on its own would start to thermally decompose. The relationship between temperature and pyrolysis provided a measure of the relative reactivity of the material for thermal cracking. Of specific importance to this study was the fraction of mass loss below 400 °C, because it indicated the pyrolysis reactivity in the low temperature regime. The MCR can be related to the Conradson carbon residue and is a measure of the coking propensity of the feed. It also provided the baseline for the maximum yield of volatile pyrolysis products that can be obtained by simple pyrolysis of the raw material in a thermal upgrading process.

(b) TGA data was obtained for both the raw and the pyrolysed materials. The pyrolysed materials were the materials that had been pyrolysed in a micro reactor for one hour at 380 °C previously. TGA data shows the relationship

between the temperature and the mass loss of the samples. The relationship between temperature and pyrolysis related mass loss and the MCR were provided.

MCR can be related to the coking propensity of the mixture. TGA also provides the information on the starting points of decomposition. By comparing these temperatures between the raw mixtures and the pyrolysed mixtures, the roles of the oxygenate containing materials are highlighted.

4.2. TGA samples

Before analyzing the results, we introduce the sample names and the abbreviations that were used for them in this study. We categorized the samples in to four groups; the individual raw samples, the individual pyrolysed samples, the raw mixed samples and the pyrolysed mixed samples. For each group, the figures of mass loss and the derivative thermogravimetric analysis will be presented.

4.2.1. Individual raw samples

The raw samples include lignin, cellulose, bituminous coal, subituminous coal, lignite, bitumen, asphaltene and partially oxidized bitumen. The first six samples have been existed in the raw format, yet the latest two samples have been prepared by doing experiments. The preparation method is described in the following sections. The abbreviations of the raw materials are followed:

Raw bitumen: RB
Raw partially oxidized bitumen: RPOB

Raw cellulose: RC

Raw lignin: Rlignin

Raw lignite: Rlignite

Raw bituminous coal: RBC

Raw subbituminous coal: RSC

Raw asphaltene: RA

Figures 4.1 and 4.2 show the mass loss and the derivative thermogravimetric analysis for the raw materials.
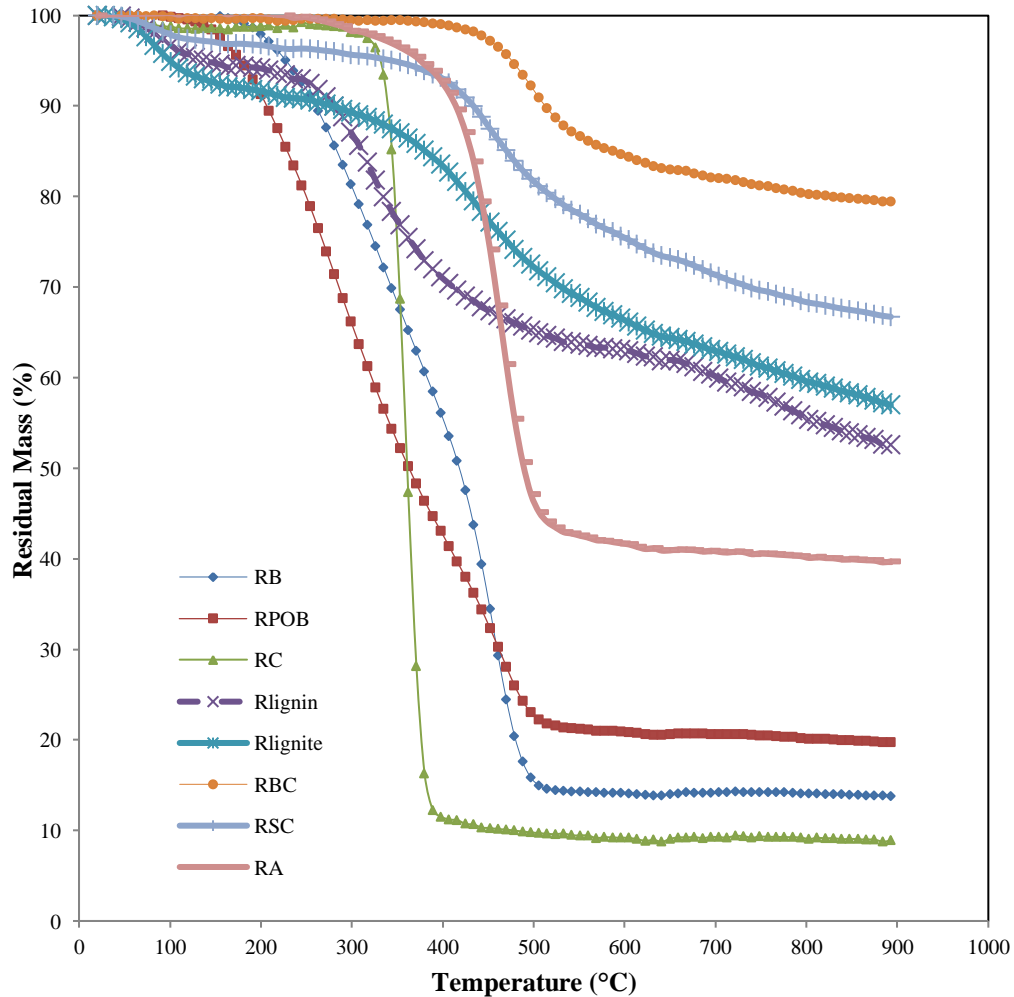
Figure 4.1. Mass losses for individual raw materials under nitrogen flow rate of 20mL/min and heating rate of 20 °C/min in temperature range of 20 °C to 900 °C. (RB: raw bitumen, RPOB: raw partially oxidized bitumen, RC: raw cellulose, Rlignin: raw lignin, Rlignite: raw lignite, RBC: raw bituminous coal, RSC: raw subbituminous coal, RA: raw asphaltene)
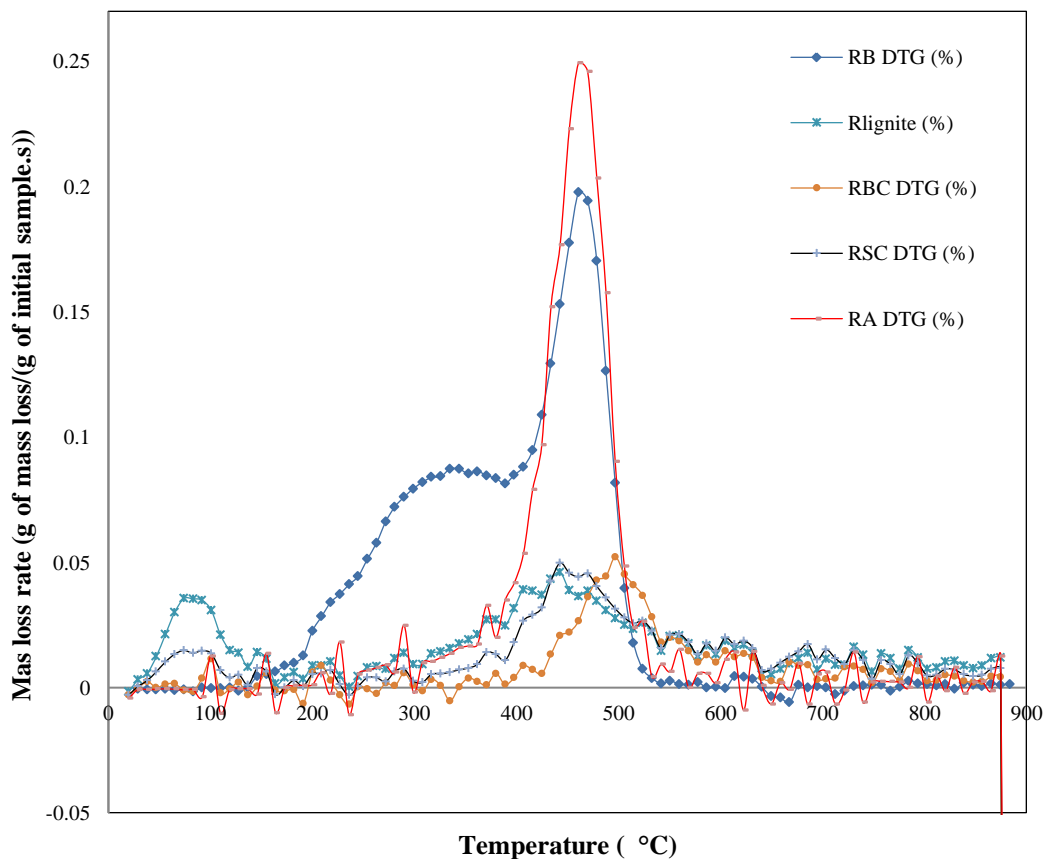
Figure 4.2. derivative thermogravimetric analysis for individual raw materials under nitrogen flow rate of 20ml/min and heating rate of 20 ℃/min in temperature range of 20 ℃ to 900 ℃
(RB: Raw bitumen, RPOB: Raw partially oxidized bitumen, RC: Raw cellulose, Rlignin: Raw lignin, Rlignite: Raw lignite, RBC: Raw bituminous coal, RSC: Raw subbituminous coal, RA: Raw asphaltene)

4.2.1.   Individual pyrolysed samples:

These samples have been pyrolysed in a micro reactor for one hour at 380 ℃ and 4MPa. The procedure of the reactor and sand bath preparation was described in Chapter three. The pyrolysed samples were then collected in the vials and have been used as the samples for the TGA runs. The sample names and abbreviations are as below:

bitumen pyrolysed at 380 °C for one hour: PB
bitumen pyrolysed at 390 °C for one hour: PBat390
partially oxidized bitumen pyrolysed at 380 °C for three hours: PPOB

cellulose pyrolysed at 380 °C for one hour: PC

lignin pyrolysed at 380 °C for one hour: Plignin

lignite pyrolysed at 380 °C for one hour: Plignite

bituminous coal pyrolysed at 380 °C for one hour: PBC

subituminous coal pyrolysed at 380 °C for one hour: PSC

asphaltene pyrolysed at 380 °C for one hour:PA

Figures 4.3 and 4.4 show the mass loss and the derivative thermogravimetric analysis for the individual pyrolysed samples.
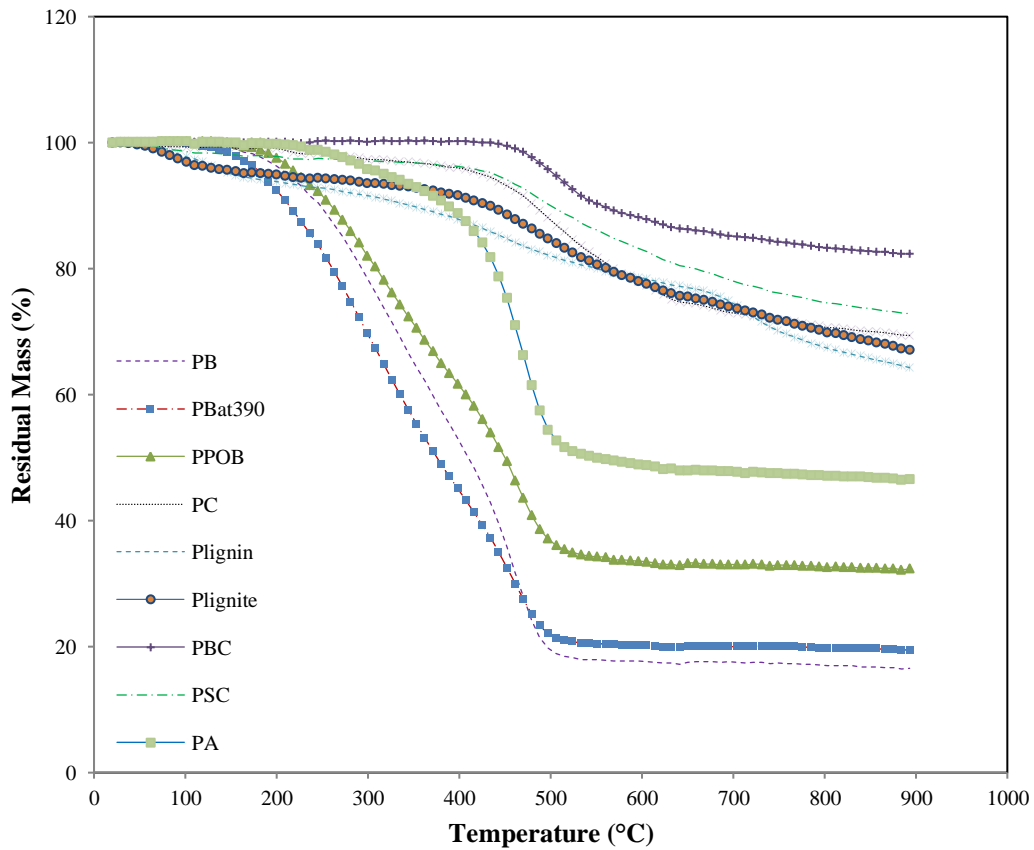
Figure 4.3. Comparison of residual mass for individual pyrolysed materials under nitrogen flow rate of 20mL/min and heating rate of 20 °C/min in temperature range of 20 °C to 900 °C
(PB: Pyrolysed bitumen at 380 °C, PBat390: Pyrolysed bitumen at 390 °C, PPOB: pyrolysed partially oxidized bitumen at 380 °C, PC: Pyrolysed cellulose at 380 °C, Plignin: Pyrolysed lignin at 380 °C, Plignite: Pyrolysed lignite at 380 °C, PBC: Pyrolysed bituminous coal at 380 °C, PSC: Pyrolysed subbituminous coal at 380 °C, PA: Pyrolysed asphaltene at 380 °C)
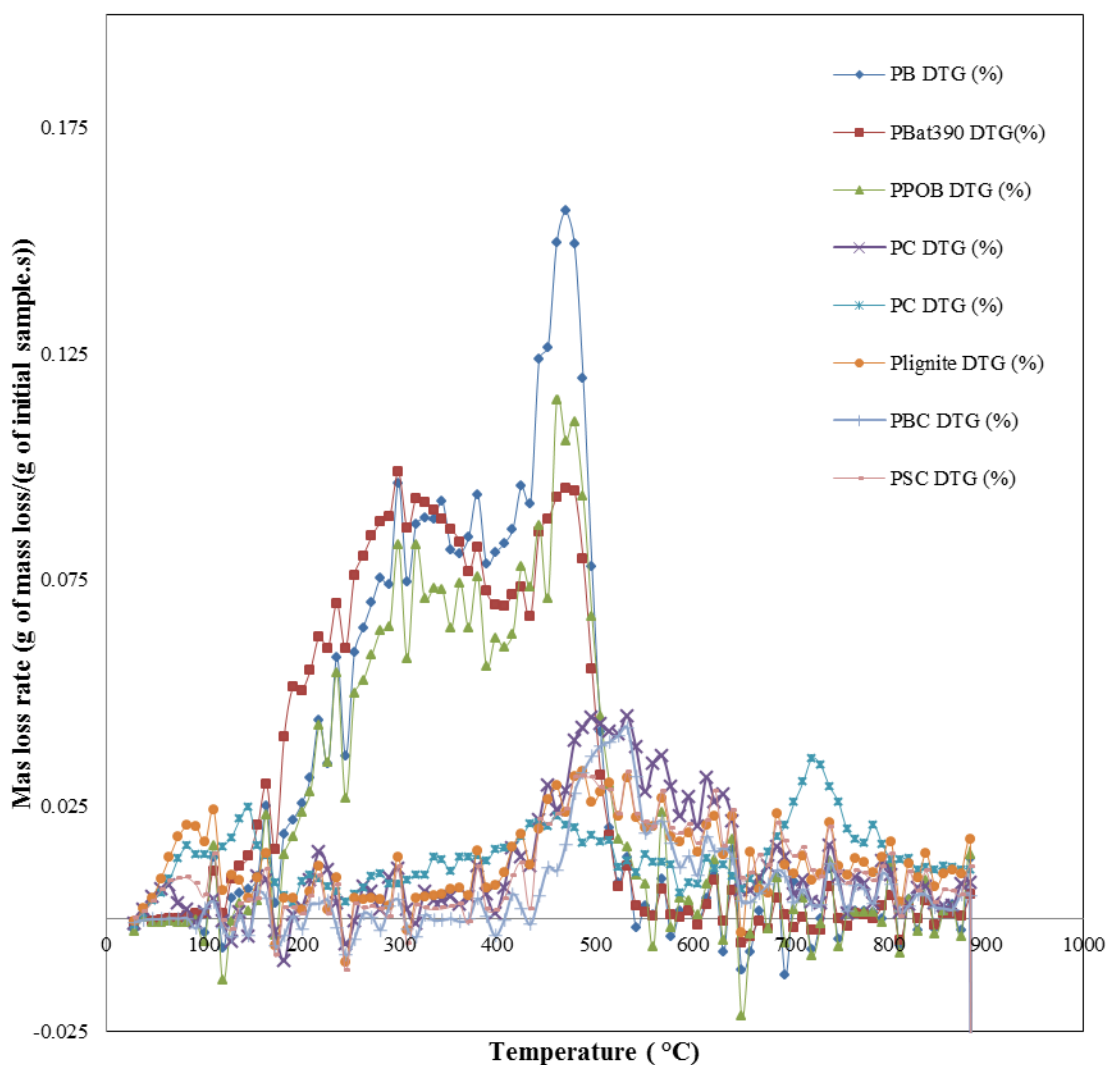
Figure 4.4. Comparison of derivative thermogravimetric analysis for individual pyrolysed materials under nitrogen flow rate of 20 mL/min and heating rate of 20 ℃/min in temperature range of 20 ℃ to 900 ℃ (PB: Pyrolysed bitumen at 380 ℃, PBat390: Pyrolysed bitumen at 390 ℃, PPOB: pyrolysed partially oxidized bitumen at 380 ℃, PC: Pyrolysed cellulose at 380 ℃, Plignin: Pyrolysed lignin at 380 ℃, Plignite: Pyrolysed lignite at 380 ℃, PBC: Pyrolysed bituminous coal at 380 ℃, PSC: Pyrolysed subbituminous coal at 380 ℃, PA: Pyrolysed asphaltene at 380 ℃)

4.2.2. Raw mixed samples:

The preparation method of the raw mixed samples was described in Chapter three, section 3.3.2.

Raw mixture of bitumen and partially oxidized bitumen: R(B+POB)

Raw mixture of bitumen and cellulose: R(B+C)

Raw mixture of bitumen and lignin: R(B+lignin)

Raw mixture of bitumen and lignite: R(B+lignite)

Raw mixture of bitumen and bituminous: R(B+BC)

Raw mixture of bitumen and subbituminous coal: R(B+SC)

Figures 4.5 and 4.6 show the mass loss and the derivative thermogravimetric analysis of the raw mixed compounds respectively.
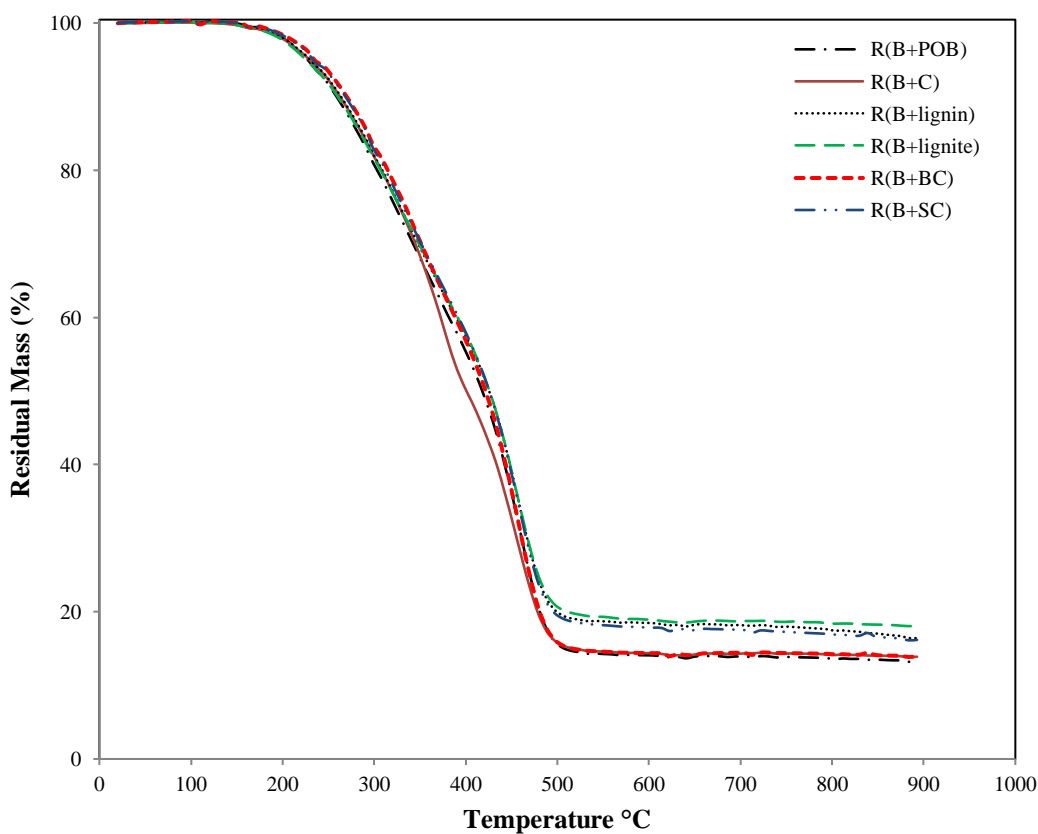
Figure 4.5. Comparison of residual mass for raw mixed compounds under nitrogen flow rate of 20 mL/min and heating rate of 20 °C/min in temperature range of 20 °C to 900 °C. The mixtures have not been previously pyrolysed in a micro reactor. (R(B+POB): Raw mixture of (90% bitumen and 10% partially oxidized bitumen), R(B+C): Raw mixture of (90% bitumen and 10% cellulose), R(B+lignin): Raw mixture of (90% bitumen and 10% lignin), R(B+lignite): Raw mixture of(90% bitumen and 10% lignite), R(B+BC): Raw mixture of (90% bitumen and 10% bituminous coal), R(B+SC): Raw mixture of (90% bitumen and 10% subbituminous coal). The preparation method of the mixtures is described in section 2.2.1 to 2.2.4.
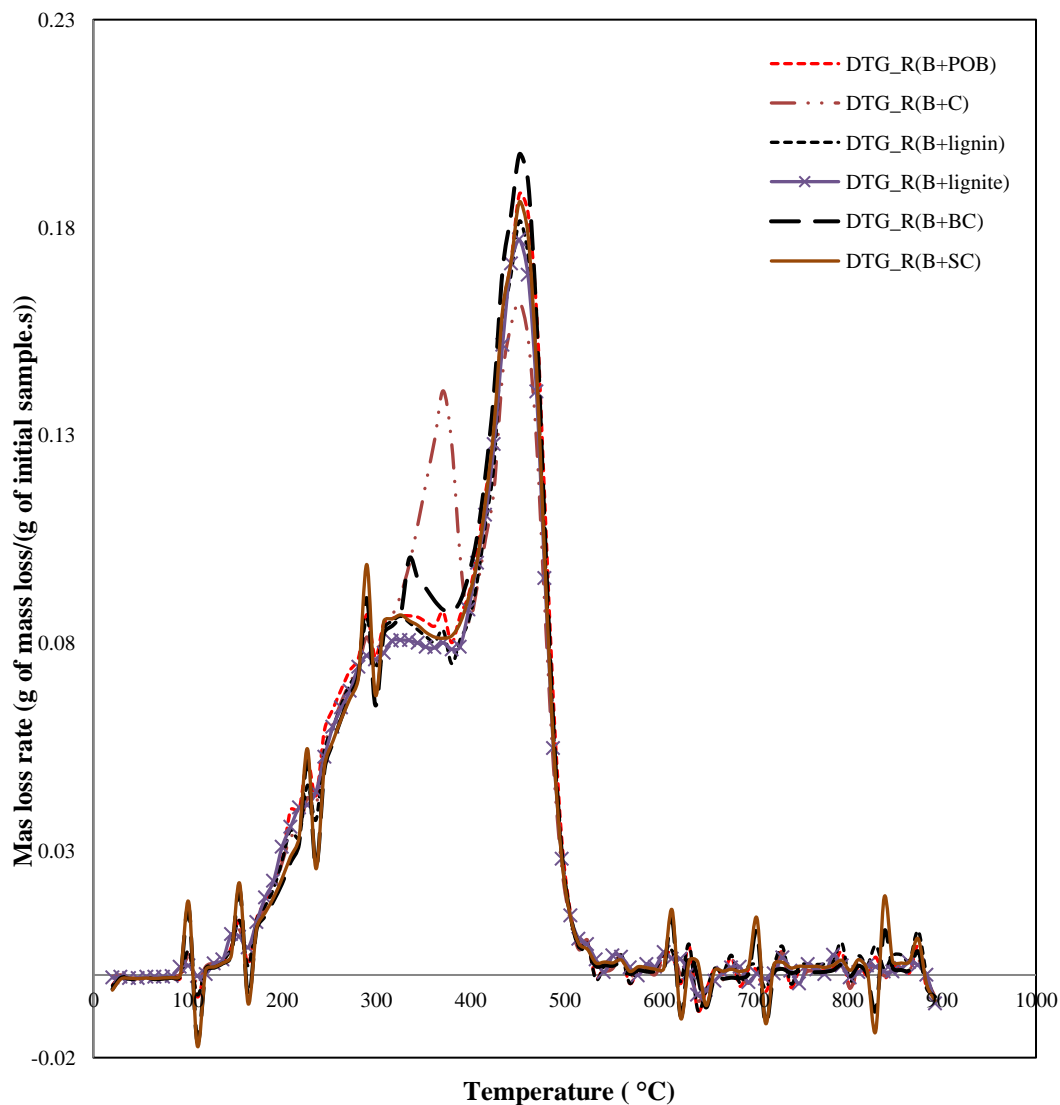
Figure 4.6. Comparison of derivative thermogravimetric analysis for raw mixed compounds under nitrogen flow rate of 20 mL/min and heating rate of 20 °C/min in temperature range of 20 °C to 900 °C. The mixtures have not been previously pyrolysed in a micro reactor. (R(B+POB): Raw mixture of (90% bitumen and 10% partially oxidized bitumen), R(B+C): Raw mixture of (90% bitumen and 10% cellulose), R(B+lignin): Raw mixture of (90% bitumen and 10% lignin), R(B+lignite): Raw mixture of(90% bitumen and 10% lignite), R(B+BC): Raw mixture of (90% bitumen and 10% bituminous coal), R(B+SC): Raw mixture of (90% bitumen and 10% subbituminous coal). The preparation method of the mixtures is described in section 2.2.1 to 2.2.4.

4.2.3. Pyrolysed mixed samples:

Raw bitumen and raw partially oxidized bitumen mixture was pyrolysed at 380 °C for one hour: P(B+POB)

Raw bitumen and Cellulose mixture was pyrolysed at 380 °C for one hour: P(B+C)

Raw bitumen and lignin mixture was pyrolysed at 380 °C for one hour: P(B+lignin)

Raw bitumen and lignite mixture was pyrolysed at 380 °C for one hour: P(B+lignite)

Raw bitumen and bituminous coal mixture was pyrolysed at 380 °C for one hour: P(B+BC)

Raw bitumen and subbituminous coal mixture was pyrolysed at 380 °C for one hour: P(B+SC)

Figures 4.7 and 4.8 show the mass loss and the derivative thermogravimetric analysis of the pyrolysed mixed samples.
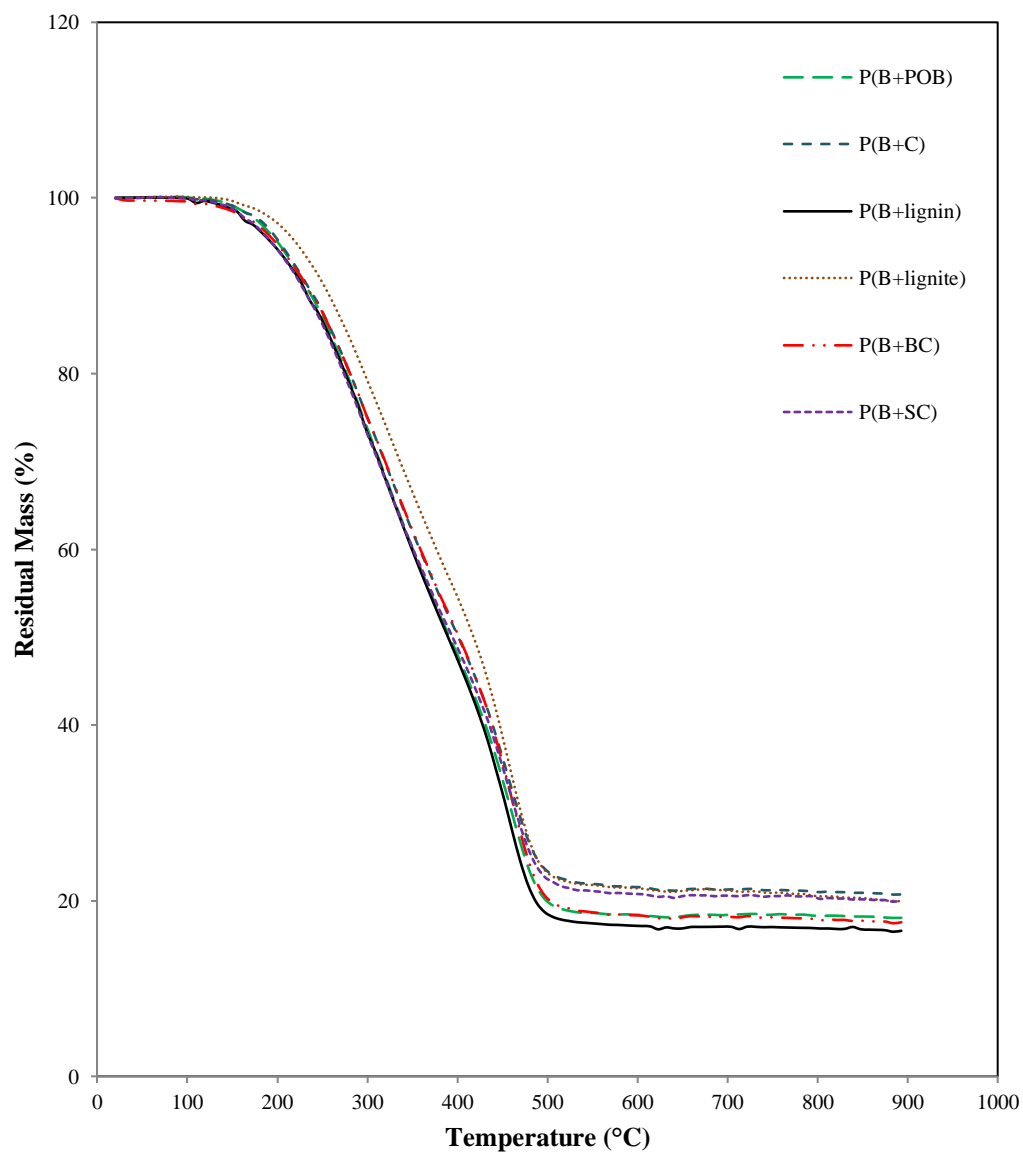
Figure 4.7. Comparison of residual mass for pyrolysed mixed compounds under nitrogen flow rate of 20ml/min and heating rate of 20 °C/min in temperature range of 20 °C to 900 °C. All the mixtures have been previously pyrolysed in a micro reactor for one hour at 380 °C. (P(B+POB): Pyrolysed mixture of (90% bitumen and 10% raw partially oxidized bitumen), P(B+C): Pyrolysed mixture of(90% bitumen and 10% cellulose), P(B+lignin): Pyrolysed mixture of (90% bitumen and 10% lignin), P(B+lignite): Pyrolysed mixture of (90% bitumen and 10% lignite), P(B+BC): Pyrolysed mixture of (90% bitumen and 10% bituminous coal), P(B+SC): Pyrolysed mixture of (90% bitumen and 10% subbituminous coal). The preparation method of the mixtures is described in section 2.2.6.
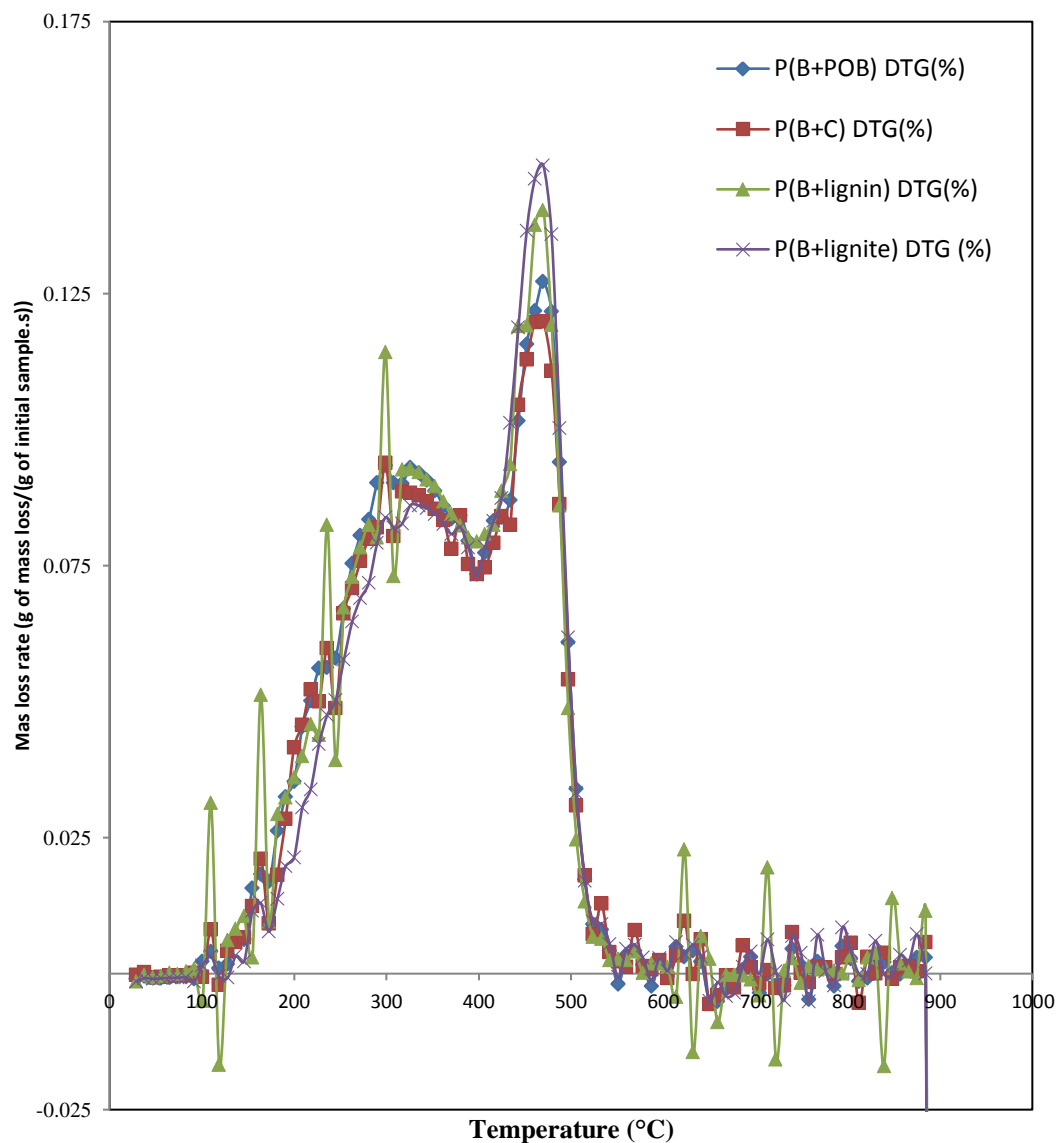
Figure 4.8. Comparison of derivative thermogravimetric analysis for raw mixed compounds under nitrogen flow rate of 20 mL/min and heating rate of 20 °C/min in temperature range of 20 °C to 900 °C. The mixtures have not been previously pyrolysed in a micro reactor. (P(B+POB): Pyrolysed mixture of (90% bitumen and 10% raw partially oxidized bitumen), P(B+C): Pyrolysed mixture of (90% bitumen and 10% cellulose), P(B+lignin): Pyrolysed mixture of (90% bitumen and 10% lignin), P(B+lignite): Pyrolysed mixture of(90% bitumen and 10% lignite), P(B+BC): Pyrolysed mixture of (90% bitumen and 10% bituminous coal), P(B+SC): Pyrolysed mixture of (90% bitumen and 10% subbituminous coal). The preparation method of the mixtures is described in section 2.2.1 to 2.2.4.

4.3. Results and discussions

4.3.1. Onset temperatures of samples pyrolysis

Chu et al. showed that any peak which is below 250 °C was caused by the volatilization of the monomers and they also demonstrated that no monomer was volatile at temperatures higher than 250 °C. They also showed that lignin does not decompose at temperatures below 250 °C. According to their FTIR results, some amount of hydroxyl groups and C-H bonds in the aliphatics still existed at high temperatures (about 550 °C); however, the carbonyl group had a noticeable decrease by temperature increase and almost disappeared at high temperatures. Their results also showed that at higher temperatures, the polyaromatic structures formed. They believed that the major reaction happened in the temperature range of 350-450 °C when the polyaromatic rings started to form and there was a huge mass loss in this range. They also found that in fast pyrolysis, there is more carbon in the heavier species (Chu et al. 2013).

The reactions that occur to cellulose when heated to high temperatures were categorized in three pathways. In the first pathway, below 300 °C, the glycosyl units in the cellulose degraded, some evolution of water, carbon dioxide and carbon monoxide and some char was produced. The second sets of reactions happened at temperatures above 300 °C which include depolymerisation of cellulose molecules, the glycosyl units of the cellulose molecules cleaved and form the 1,6-anhydro-β-D-glucopyranose. And the other type of reactions happened to cellulose at temperatures higher than 500 °C, these later reactions broke down the cellulose molecules to low molecular weight products such as carbon monoxide, carbon dioxide, hydrogen and some hydrocarbons (Cheng et al. 2012). Rosenvold et al. studied twenty one bituminous coals using differential scanning calorimetry (DSC) and thermogravimetry analysis (TGA) and found

that in the temperature range below 150 ˚C, the mass loss was caused because of the moisture loss (Rosenvold et al. *1982).*

The mass loss that happened because of the devolatilization of the monomers and the loss of moisture was not a good indicator of when the real sample molecules started to crack. In this study, it was assumed that all the volatiles and the moisture were taken out into the gas form and the remaining solid did not contain any more volatiles after 250 °C. In order to have a certain parameter to compare the reactivity of the samples, the onset temperature is defined as the temperature at which the sample loses one percent more of its initial mass after 250 °C. For example, according to the TGA results the remaining mass of the raw bitumen in the TGA pan is 91.78% at 250 °C and the temperature at which the remaining mass of this sample in the TGA pan is 90.78% is read and is called as the onset temperature for this sample. Table 4.1 shows the onset temperatures of all the samples. This Table also shows the temperatures at which five and ten percent of the mass losses happen after 250 °C.

Table 4.1. Onset temperature for raw and mixture samples. (RB: raw bitumen, RPOB: raw partially oxidized bitumen, RC: raw cellulose, Rlignin: raw lignin, Rlignite: raw lignite, RBC: raw bituminous coal, RSC: raw subbituminous coal, RA: raw asphaltene. PB: Pyrolysed bitumen at 380 °C, PBat390: Pyrolysed bitumen at 390 °C, PPOB: pyrolysed partially oxidized bitumen at 380 °C, PC: Pyrolysed cellulose at 380 °C, Plignin: Pyrolysed lignin at 380 °C, Plignite: Pyrolysed lignite at 380 °C, PBC: Pyrolysed bituminous coal at 380 °C, PSC: Pyrolysed subbituminous coal at 380 °C, PA: Pyrolysed asphaltene at 380 °C. PB: Pyrolysed bitumen at 380 °C, PBat390: Pyrolysed bitumen at 390 °C, PPOB: pyrolysed partially oxidized bitumen at 380 °C, PC: Pyrolysed cellulose at 380 °C, Plignin: Pyrolysed lignin at 380 °C, Plignite: Pyrolysed lignite at 380 °C, PBC: Pyrolysed bituminous coal at 380 °C, PSC: Pyrolysed subbituminous coal at 380 °C, PA: Pyrolysed asphaltene at 380 °C. R(B+POB): Raw mixture of (90% bitumen and 10% partially oxidized bitumen), R(B+C): Raw mixture of (90% bitumen and 10% cellulose), R(B+lignin): Raw mixture of (90% bitumen and 10% lignin), R(B+lignite): Raw mixture of(90% bitumen and 10% lignite), R(B+BC): Raw mixture of (90% bitumen and 10% bituminous coal), R(B+SC): Raw mixture of (90% bitumen and 10% subbituminous coal. P(B+POB): Pyrolysed mixture of (90% bitumen and 10% raw partially oxidized bitumen), P(B+C): Pyrolysed mixture of(90% bitumen and 10% cellulose), P(B+lignin): Pyrolysed mixture of (90% bitumen and 10% lignin), P(B+lignite): Pyrolysed mixture of (90% bitumen and 10% lignite), P(B+BC): Pyrolysed mixture of (90% bitumen and 10% bituminous coal), P(B+SC): Pyrolysed mixture of (90% bitumen and 10% subbituminous coal)

Sample name	Temperature at which 1% of mass is lost after the wt% at 250 °C (°C)	Temperature at which 5% of mass is lost after the wt% at 250 °C (°C)	Temperature at which 10% of mass is lost after the wt% at 250 °C (°C)
RB	255.42	275.77	297.18
RPOB	253.67	268.44	285.93
RC	303.53	333.07	339.73
Rlignin	262.44	295.92	321.94
Rlignite	288.79	372.22	423.77
RBC	419.17	479.36	516.23
RSC	327.60	421.13	460.58
RA	289.88	367.38	413.69
R(B+POB)	255.21	275.21	296.41
R(B+C)	255.52	276.39	298.29
R(B+lignin)	255.59	276.69	298.21
R(B+lignite)	255.58	276.98	299.42
R(B+BC)	255.96	278.09	299.07
R(B+SC)	255.92	278.07	298.39

In this study, it was assumed that all the devolatalization of the monomers and the moisture loss happened below 250 °C and at temperatures above 250 °C, the mass loss was caused by the reactions that happen among the molecules. As it was mentioned in Chapter two, the cracking reactions include three steps; initiation, propagation and the termination. In each of the three steps, different sets of reactions happen; therefore, there is not a single variable which exactly differentiates the start and end point of each step. Radicals which play important roles in cracking reactions are generated in the initiation step. In order to have a clear idea to compare the temperature ranges of the initiation steps for the samples, the initiation step was analyzed based on the initial mass losses that

occur above 250 ℃. The temperature at which the sample loses one percent of its initial amount of mass (defined as the onset temperature) was thought to be very close to the temperature at which the radicals are formed i.e. the initiation step.

In Chapter one (section 1.1.5), it is stated that the low temperatures at which the initiation steps happen do not indicate that the total reaction rate is low. In other words, the fact that the initiation step happens in a short time does not prove the idea that the total reaction happens in a short time. However, the low temperature of in the initiation step shows that the bitumen upgrading is possible to proceed at low temperatures. As discussed, it was hypothesized that the additives cause the free radical decomposition to happen at low temperatures.

Table (4.1) shows the temperatures at which one, five and ten percent of the mass is lost above 250 ℃. According to this table, the addition of the oxygenate containing materials to bitumen did not lower the onset temperature. The comparison of the onset temperature for the raw bitumen to the same temperatures for the raw mixtures show that after the addition of the oxygenate containing materials, the changes in the onset temperatures are negligible (less than 1 ℃) and are less than the changes that happened to the temperatures at which five and ten percent mass losses happened.

According to Table (4.1), the only raw mixture which has a lower onset temperature than the onset temperature of the raw bitumen is the mixture of bitumen and POB (partially oxidized bitumen). The onset temperatures for the individual raw materials also show that POB has a lower onset temperature than the other plain samples.

4.3.2. Mass loss rates of samples

Previously in Chapter two, section 2.4.3; in terms of the equations it was discussed the fact that an increase in the amount of the radical concentrations caused an increase in the reaction rate. In the same chapter, section 2.4.4, it was explained that the activation energy for the mixture samples is less than the activation energy for the plain bitumen. Therefore the mixtures' pyrolysis reactions proceed with higher rates in comparison to the plain individual bitumen pyrolysis.

In this study it was hypothesized that the addition of the additives with weak bonds can accelerate the pyrolysis reaction rates. Although there are some rate laws existing in the open literature with which the pyrolysis kinetics have been explained (White, et al. 2011) (Yu, et al. 2011) and (Sonobe, et al. 2008), the aim of this study is not to calculate the precise reaction rates by use of the kinetics. According to Cheng, et al. it is very complicated to describe the entire pyrolysis reactions because there is a sequence of concurrent reactions with their individual kinetics and activation energies (Cheng, et al. 2012). In this section the aim is not trying to present the kinetics of the pyrolysis but to give an idea of the mass loss changes that happen during sample pyrolysis at low temperature ranges.

To study the mass loss rates (MLRs) of different types of samples, the average MLRs at five different relatively low temperature ranges starting from 200 ˚C to 400 ˚C were compared in Table (4.2).

Table 4.2. Mass loss rates for raw and mixture samples at low temperatures. (RB: raw bitumen, RPOB: raw partially oxidized bitumen, RC: raw cellulose, Rlignin: raw lignin, Rlignite: raw lignite, RBC: raw bituminous coal, RSC: raw subbituminous coal, RA: raw asphaltene. PB: Pyrolysed bitumen at 380 °C, PBat390: Pyrolysed bitumen at 390 °C, PPOB: pyrolysed partially oxidized bitumen at 380 °C, PC: Pyrolysed cellulose at 380 °C, Plignin: Pyrolysed lignin at 380 °C, Plignite: Pyrolysed lignite at 380 °C, PBC: Pyrolysed bituminous coal at 380 °C, PSC: Pyrolysed subbituminous coal at 380 °C, PA: Pyrolysed asphaltene at 380 °C. PB: Pyrolysed bitumen at 380 °C, PBat390: Pyrolysed bitumen at 390 °C, PPOB: pyrolysed partially oxidized bitumen at 380 °C, PC: Pyrolysed cellulose at 380 °C, Plignin: Pyrolysed lignin at 380 °C, Plignite: Pyrolysed lignite at 380 °C, PBC: Pyrolysed bituminous coal at 380 °C, PSC: Pyrolysed subbituminous coal at 380 °C, PA: Pyrolysed asphaltene at 380 °C. R(B+POB): Raw mixture of (90% bitumen and 10% raw partially oxidized bitumen), R(B+C): Raw mixture of (90% bitumen and 10% cellulose), R(B+lignin): Raw mixture of (90% bitumen and 10% lignin), R(B+lignite): Raw mixture of(90% bitumen and 10% lignite), R(B+BC): Raw mixture of (90% bitumen and 10% bituminous coal), R(B+SC): Raw mixture of (90% bitumen and 10% subbituminous coal. P(B+POB): Pyrolysed mixture of (90% bitumen and 10% raw partially oxidized bitumen), P(B+C): Pyrolysed mixture of(90% bitumen and 10% cellulose), P(B+lignin): Pyrolysed mixture of (90% bitumen and 10% lignin), P(B+lignite): Pyrolysed mixture of (90% bitumen and 10% lignite), P(B+BC): Pyrolysed mixture of (90% bitumen and 10% bituminous coal), P(B+SC): Pyrolysed mixture of (90% bitumen and 10% subbituminous coal)

Sample name	Average MLR in 175-225 °C (%/s)	Ave MLR in 225-275 °C (%/s)	Ave MLR in 275-325 °C (%/s)	Ave MLR in 325-375 °C (%/s)	Ave MLR in 375-425 °C (%/s)
RB	0.019	0.046	0.077	0.086	0.089
RPOB	0.053	0.080	0.094	0.084	0.065
RC	-0.001	-0.004	0.006	0.304	0.244
Rlignin	0.003	0.010	0.046	0.064	0.037
Rlignite	0.005	0.005	0.010	0.016	0.030
RBC	<0.001	-0.001	<0.001	<0.001	0.004
RSC	0.002	0.002	0.004	0.006	0.017
RA	-3E-04	0.003	0.009	0.014	0.040
PB	0.024	0.050	0.080	0.086	0.086
PBat390	0.046	0.069	0.090	0.088	0.073
PPOB	0.020	0.044	0.068	0.071	0.065
PC	0.002	0.003	0.005	0.004	0.008
Plignin	0.007	0.006	0.009	0.012	0.015
Plignite	0.004	0.002	0.005	0.006	0.011
PBC	-7.7E-04	<-0.001	-1.5E-04	-2.6E-05	0.001
PSC	0.002	<0.001	0.002	0.002	0.006
PA	<-0.001	0.009	0.019	0.020	0.039
R(B+POB)	0.017	0.048	0.076	0.086	0.089
R(B+C)	0.016	0.044	0.073	0.096	0.112
R(B+lignin)	0.017	0.043	0.073	0.085	0.084
R(B+lignite)	0.018	0.045	0.071	0.080	0.084
R(B+BC)	0.011	0.040	0.071	0.091	0.093
R(B+SC)	0.011	0.041	0.073	0.085	0.087
P(B+POB)	0.034	0.062	0.088	0.090	0.081
P(B+C)	0.032	0.059	0.083	0.086	0.078
P(B+lignin)	0.032	0.061	0.087	0.090	0.083
P(B+lignite)	0.021	0.052	0.078	0.085	0.080
P(B+BC)	0.030	0.057	0.082	0.086	0.079
P(B+SC)	0.035	0.063	0.086	0.084	0.076

According to Table (4.2), the MLRs for the raw bitumen are almost less than the MLRs for the pyrolysed bitumen in all the ranges except in 375-425 °C. According to Zhao et al. at about 380 °C, most of the inorganic compounds were produced. So the raw bitumen still had some inorganic compounds to lose and

the mass loss rate in temperature range close to 380 °C was higher than the pyrolysed bitumen.

According to Table (4.2), at lower temperatures (less than 325 °C), the mass loss rates for the raw mixtures are less than for the raw bitumen. However, at temperature ranges of 325-375 °C and 375-425 °C, the mass loss rates for the raw mixed samples are almost higher or about the same as the mass loss rates for the raw bitumen pyrolysis.

Zhao et al. studied the thermal characteristics of bitumen pyrolysis. They showed that different products evolved in different temperature ranges (Zhao, *et al. 2012*). According to their results, alkane and alkene production happened mainly in the temperature range of 130-480 °C, Benzene, toluene, and styrene were produced in the temperature range of 100-420 °C and the inorganic compounds were released at about 380 °C (including H_2O, CO_2 and SO_2). They demonstrated that the major products of bitumen pyrolysis are alkanes, alkenes, aromatic compounds and inorganic compounds. The FTIR results in their study showed much intensity for stretching and bending of different bonds including alkane bonds, alkene bonds, nitro group bonds and carbon sulfur bonds. As the temperature increased, the intensity of these bonds decreased. The FTIR results for the bitumen pyrolysis at 110 °C showed many bond stretches and bending, including many alkene and alkane bond stretching and bending. The amount of these bonds decreased when bitumen was pyrolysed at higher temperatures (380 °C and 600 °C). It shows that the breaking of the weak links were approximately complete at 380 °C. According to their Gas Chromatography/ Mass Spectrometry (GC/MS) results, the bitumen that was pyrolysed at lower temperature (100 °C) contained low molecular weight compounds (C6-C10) and mid molecular weight compounds (C11-C15), and the bitumen pyrolysed at

higher temperature (380 °C) had high molecular weight compounds (>C15) (Zhao, et al. *2012*).

According to the results obtained from Table (4.2), because the mass loss rate is almost higher for the raw mixed samples than the raw bitumen at temperature range of 325-425 °C, the raw mixed samples seem to have more intensity of molecules to react at those temperature ranges than the raw bitumen. According to Zhao et al. the pyrolysis products in this temperature range are alkanes, alkenes, benzene, toluene, styrene and some inorganic compounds. It can be concluded that the raw mixed samples produced more of the named products than the raw bitumen at temperature range of 325-425 °C.

In this study, the raw samples were pyrolysed at 380 °C in a batch micro reactor for one hour. The reaction temperature (380 °C) is almost in the middle of the temperature range of 325-425 °C. According to the Gas Chromatography (GC) results, which are more explained in Chapter five, the total gases that were produced from the mixtures were almost higher than the gas yield of the raw bitumen pyrolysis. The gas phase consisted of inorganic compounds such as CO_2, alkanes and alkenes. These results show that more inorganic, alkanes and alkenes were produced from the pyrolysis of the mixtures than the raw bitumen in the same time or, the mass loss rates were higher for mixtures at this temperature and this is why the mass loss rates for the pyrolysed bitumen is higher than the mass loss rates for the pyrolysed mixtures in temperature range of 375-4 (table 4.2).

According to Zhao et al. work, the bitumen which was pyrolysed at 380 °C had high molecular weight compounds (>C15) than the bitumen pyrolysed at lower temperatures and probably than plain bitumen. They also showed that most of the inorganic compounds were released at approximately 380 °C (Zhao, *et al*. 2012). In our study, the PB already lost some inorganic compounds during one hour pyrolysis at 380 °C and the compounds were collected in the form of gas;

therefore, the MLRs for the PB were lower than the MLRs for the plain bitumen at temperatures about 380 ℃. This means that the plain bitumen had more inorganic compounds to lose at temperatures close to 380 ℃ in the same time length than the PB so it presented higher MLRs at this range.

The MLRs for the PBat390 (bitumen pyrolysed at 390 ℃) were higher than the MLRs for the PB, this may be because of the higher productions of alkane, alkene, benzene, toluene, styrene at a higher temperature (According to Zhao et al. these products were produced in a temperature range of 100-420 ℃ (Zhao, *et al.* 2012)). Because there was a higher amount of the products in the same length of time, the mass loss rates were also higher for the PBat390 than for the PB.

It is interesting that the MLRs for the pyrolysed mixed samples were higher than the MLRs for the PB. The higher amounts of rates show that more mass was lost for the pyrolysed mixed samples than the pyrolysed bitumen. The more amount of mass loss shows that more products were able to go under reactions in the pyrolysed mixed samples than in the pyrolysed plain bitumen. The components that could go under reactions at low temperature range were the light products because at low temperatures not much energy is provided to molecules to break the strong bonds. For example the C-C bonds in the high molecular weight aromatic molecules require higher energy to break down than the C-C bonds in the light molecular weight molecules such as alkanes and alkenes (Chapter 2, Section 2,4,1). The fact that we obtained higher MLRs for the pyrolysed mixtures showed that we have achieved one of our goals which is to have more light products by mixing the additives to bitumen. In the other words, the higher MLRs for the pyrolysed mixed samples than for the pyrolysed plain bitumen demonstrated that the addition of those materials to bitumen helped to produce light fractions.

Also, the high MLRs for the pyrolysed mixed samples at relatively low temperatures show that after pyrolysis of the mixture for one hour, the additives

helped bitumen to release the products which have more weak bonds that can break at relatively low temperatures with high rates.

According to chapter two (section 2.4.4), the fastest step among the decomposition reactions is the propagation step. The higher mass loss rates for the pyrolysed mixed samples than the pyrolysed bitumen was related to the faster propagation steps for the pyrolysed mixed one. In all the four categories of the propagation step, which were explained in chapter two (section 2.4.1.), the radicals are the initial reactants. As it was stated previously, the additives have many bonds with low amounts of bond dissociation energies; therefore, the radicals that were produced from sample pyrolysis still have some links which can break easily to form other radicals and products. The higher rate of the propagation step shows that there was a more intensity of radicals produced during one hour pyrolysis of the bitumen and the oxygenate containing material. In other words, the addition of the components to bitumen increased the production of free radicals and increased the reaction rate.

According to section 2.4.1 in Chapter 2, one of the steps in the propagation step is the fragmentation step. In this step one radical produces another radical and an alkene. To proceed the fragmentation step efficiently, the initial radical should have weak σ bonds so that they can break easily (Parsons, 2000). As it was hypothesized, the additives added in this study have bonds with less bond dissociation energy so it can be assumed that the produced radicals from pyrolysis of the mixture have weak σ bonds as well. The DTG results in this section approved that the additives have molecules with low bond dissociation enegires that could produce many weak radicals which also resulted to the production of the molecules with weak bonds such as alkenes.

4.3.3. Coke yields

In order to have a clear picture of the residual amounts, the residual coke yields of the samples are brought in Table 4.3. Also, it was important to observe how much mass loss occurred as a result of the pyrolysis reactivity in temperature below 400 °C (low temperature regime). In order to have a more accurate result on the mass loss which happened as a result of pyrolysis reactions, the water loss was deducted from the total mass loss that happened below 400 °C and the results are brought in Table 4.3.

Table 4.3. Mass losses up to 110 °C (ML110) and 400 °C (ML400) and the coke yields of the samples at 900 °C. (CY: Coke yield of the mixture or the residual yield of the sample at 900 °C, SD: Standard Deviation of the resulted coke yield, ML110: Mass loss up to 110 °C, ML400: Mass loss up to 400 °C, LTML: Low temperature mass loss, RB: raw bitumen, PB: bitumen pyrolysed at 380 °C for one hour, PBat390: bitumen pyrolysed at 890 °C for one hour, RPOB: raw partially oxidized bitumen, PPOB: pyrolysed partially oxidized bitumen, RC: Raw Cellulose, Rlignin: raw lignin, Rlignite: raw lignite, RBC: raw bituminous coal, RSC: raw subbituminous coal, PC: cellulose pyrolysed at 380 °C for one hour, Plignin: lignin pyrolysed at 380 °C for one hour, Plignite: lignite pyrolysed at 380 °C for one hour, PBC: bituminous coal pyrolysed at 380 °C for one hour, PSC: subbituminous coal pyrolysed at 380 C for one hour, R(B+POB): mixture of raw bitumen and partially oxidized bitumen, P(B+POB): mixture of (bitumen and partially oxidized bitumen) pyrolysed at 380 °C for one hour. R(B+C): Raw mixture of bitumen and cellulose, P(B+C): mixture of (bitumen and cellulose) pyrolysed at 380 °C for one hour, R(B+lignin): Raw mixture of bitumen and lignin, P(B+lignin): mixture of (bitumen and lignin) pyrolysed at 380 °C for one hour, R(B+lignite): Raw mixture of bitumen and lignite, P(B+lignite): mixture of (bitumen and lignite) pyrolysed at 380 °C for one hour, R(B+BC): Raw mixture of bitumen and bituminous coal, P(B+BC): mixture of (bitumen and bituminous coal) pyrolysed at 380 °C for one hour, R(B+SC): Raw mixture of bitumen and subbituminous coal, P(B+SC): mixture of (bitumen and subbituminous coal) pyrolysed at 380 °C for one hour)

Sample*	ML110 (%)	SD for ML110 (%)	ML400-ML110 (LTML) (%)	SD for (ML400-ML110) (%)	CY (%)	SD CY* (%)
RB	0.15	0.03	43.81	0.86	13.96	0.21
PB	0.31	0.25	46.83	0.18	15.72	0.65
PBat390	0.55	0.29	55.23	0.85	19.73	1.14
RPOB	0.43	0.19	56.43	0.59	20.25	0.62
PPOB	0.08	0.17	38.93	0.48	32.11	0.92
RC	1.68	0.24	86.45	0.58	8.68	0.47
Rlignin	3.18	2.29	26.56	1.63	50.64	1.67
Rlignite	4.91	0.68	10.79	0.15	57.88	0.84
RBC	0.23	0.12	0.44	0.11	79.70	0.21
RSC	2.59	0.31	4.49	0.07	66.73	0.35
PC	0.64	0.15	2.86	0.38	70.52	1.18
Plignin	3.12	0.45	9.41	0.07	63.18	0.75
Plignite	3.28	0.30	4.84	0.01	67.28	0.53
PBC	0.17	0.10	0.14	0.13	82.52	0.92
PSC	1.47	0.24	2.04	0.04	73.24	0.42
R(B+POB)	0.03	0.05	45.25	1.08	13.55	0.45
P(B+POB)	0.16	0.11	51.50	0.03	17.23	0.74
R(B+C)	0.03	0.04	47.77	1.24	13.89	0.21
P(B+C)	0.08	0.06	45.65	0.50	20.52	1.65
R(b+lignin)	0.01	0.05	42.62	0.96	15.99	0.58
P(b+lignin)	0.18	0.13	47.14	4.83	16.26	0.49
R(B+lignite)	0.03	0.06	42.11	0.70	17.91	0.49
P(B+lignite)	0.02	0.09	46.00	1.02	20.21	1.28
R(B+BC)	0.11	0.13	43.64	0.82	13.82	0.09
P(B+ BC)	0.35	0.33	48.33	0.08	17.34	0.85
R(B+ SC)	0.20	0.21	44.38	4.25	16.51	1.21
P(B+ SC)	0.76	0.49	49.17	1.30	19.98	0.97

*This information was not collected for the raw asphaltene, the pyrolysed asphaltene and the mixtures of them with bitumen.

Table 4.3 shows the mass losses at 110 °C, 400°C and 900 °C. The mass loss at 110 °C is attributed to the physical water loss of the sample. The difference in

the mass losses at 110 °C and 400 °C, showed the mass loss that happened because of the decomposition of the sample at low temperature and it is named herein as low temperature mass loss (LTML).

The LTML for the pyrolysed bitumen was higher than the raw bitumen. This shows that PB had more mass to lose at lower temperature than the raw bitumen. In other words, when bitumen was pyrolysed in a micro reactor, it was converted to some components which could go under further decompositions at low temperature. According to the previous chapter, the components which can go under decomposition at low temperatures are alkane, alkene, styrene, benzene, toluene and some inorganic compounds. It is concluded that after one hour pyrolysis of the bitumen, there are more of the name components than the plain raw bitumen.

According to Table (4.3), the LTML for the biomass additives (cellulose and lignin) are much higher than the LTML for the raw coal samples. This shows that the biomass samples can degrade easier than the coal samples at low temperatures. As discussed in section 2.4.7 in chapter two, according to Vuthaluru, the approximate bond dissociation energy for cellulose and lignin macro molecules is low (about 400kJ/mol); therefore these molecules are more able to react at low temperatures (less than 500 °C) than the coal samples. They stated that most of the biomass macromolecules are linked with ether bonds which need much less energy than the coal aromatic macromolecules which are mainly linked with C=C bonds in aromatic structures with bond dissociation energy of about 1000 kJ/mol. They showed that defragmentation of the coal molecules caused less mass loss than the degradation of the biomass samples. Vuthaluru studied pyrolysis of the mixtures of the biomass and coal as well as the pyrolysis of each of the components separately and found that there is not a significant interaction between coal and biomass samples (Vuthaluru, 2003).

Although Vuthaluru showed that there was not much interaction between the coal and biomass samples, the current study shows that there was some interaction between the bitumen and coal samples. According to Table (4.3), the LTML for the pyrolysed bitumen is much higher than the LTML for the

pyrolysed coal samples; however, it was shown that these samples increased the LTML of the mixture when they were copyrolysed with bitumen. The pyrolysed mixtures of bitumen and subbituminous coal (SC), as well as the pyrolysed mixture of bitumen and bituminous coal (BC) presented higher LTML than pyrolysed bitumen. This shows that pyrolysis of the mixtures of bitumen with either of SC or BC at 380 ℃ produced low and medium molecular weight compounds including alkanes, alkenes, some low molecular weight aromatic compounds and inorganic compounds (Zhao, *et al.* 2012). This fact showed that the named coal samples increased the reactivity of the bitumen.

Table 4.4 gives a clear idea whether the addition of the oxygenate containing materials benefit the pyrolysis in terms of lowering the micro carbon residue or not.

Table 4.4. Gas yield, liquid yield and the MCR of the samples at low temperature. (PB: bitumen pyrolysed at 380 ℃ for one hour, PBat390: bitumen pyrolysed at 390 ℃ for one hour, RPOB: raw partially oxidized bitumen, PC: cellulose pyrolysed at 380 ℃ for one hour, Plignin: lignin pyrolysed at 380 ℃ for one hour, Plignite: lignite pyrolysed at 380 ℃ for one hour, PSC: subbituminous coal pyrolysed at 380 C for one hour, P(B+POB): mixture of (bitumen and partially oxidized bitumen) pyrolysed at 380 ℃ for one hour, P(B+C): mixture of (bitumen and cellulose) pyrolysed at 380 ℃ for one hour, P(B+lignin): mixture of (bitumen and lignin) pyrolysed at 380 ℃ for one hour, P(B+lignite): mixture of (bitumen and lignite) pyrolysed at 380 ℃ for one hour, P(B+BC): mixture of (bitumen and bituminous coal) pyrolysed at 380 ℃ for one hour, P(B+SC): mixture of (bitumen and subbituminous coal) pyrolysed at 380 ℃ for one hour)

Sample*	Gas yield from LT pyrolysis (wt %)	MCR of 1h pyrolyzed sample (wt %)	Total liquid & gas produced (wt %)	Effective MCR of LT pyrolyzed sample (wt %)	MCR of raw sample (wt %)	Relative change in MCR
PB	3.00	15.72	81.75	18.25	13.96	0.31
PBat390	4.01	19.73	77.05	22.95	13.96	0.64
PPOB	5.52	32.11	64.14	35.86	20.25	0.77
PC	72.42	70.52	8.13	91.87	8.68	9.58
Plignin	26.36	63.18	27.11	72.88	50.64	0.44
Plignite	22.79	67.28	25.26	74.74	57.88	0.29
PBC	7.63	82.52	16.14	83.85	79.70	0.05
PSC	12.96	73.24	23.29	76.71	66.73	0.15
P(B+POB)	2.78	17.23	80.47	19.53	13.55	0.44
P(B+C)	7.77	20.52	73.30	26.69	13.89	0.92
P(B+lignin)	4.75	16.26	79.76	20.24	15.99	0.26
P(B+lignite)	3.94	20.21	76.65	23.35	17.91	0.30
P(B+ BC)	2.34	17.34	80.72	19.27	13.82	0.39
P(B+ SC)	2.93	19.98	77.67	22.32	16.51	0.35

*This information was not collected for the pyrolysed asphaltene and its mixture with bitumen.

In Table (4.4), the second column from left shows the gas yield of the sample pyrolysis after one hour at 380 ° (More description on the gas yield is provided in Chapter 5). In the third column from left, the MCR after one hour sample pyrolysis in the micro reactor is provided. The next column shows the total liquid and gas that was produced when sample was pyrolysed in the TGA pan and is obtained by Equation 4.1. The Effective MCR of LT pyrolyzed sample is obtained by Equation 4.2.

Total liquid & gas produced (wt%)= (1- (Gas yield from LT pyrolysis/100))×(1- (MCR of 1h pyrolyzed sample /100))× 100   Equation (4.1)

Effective MCR of LT pyrolyzed sample= 100- Total liquid & gas produced (wt%)

Equation (4.2)

MCR of the raw samples show the residue amount of the raw samples that were only pyrolysed by TGA and not in the micro reactor. The relative change in MCR is provided by Equation 4.3.

Relative change in MCR= (Effective MCR of LT pyrolyzed sample- MCR of raw sample)/

MCR of raw sample   Equation (4.3)

According to Table 4.4, it is observed that the gas and liquid productions are higher for pyrolysed bitumen at 380 °C than for the pyrolysed bitumen at 390 °C. Also, the Effective MCR of PB is lower than PBat390. It is also observed that raw partially oxidized bitumen (RPOB), raw bituminous coal (RBC) and raw lignin (Rlignin) also produce high amount of gas and liquid amount and less amount of Effective MCR at low temperature.

By comparison of the total gas and liquid production and the coke yields of the mixtures and the plain bitumen at the same temperature (380 °C), it is observed that none of the additives increased the gas and liquid production, nor they decreased the coke yield amount. However, the total gas and liquid productions from most of the mixtures' pyrolysis at 380 °C were still more than the amount of the gas and liquid products from bitumen pyrolysed at 390 °C. Also, the effective coke yield of most of the pyrolysed mixtures at 380 °C were less than the effective coke yield of the pyrolysed bitumen at 390 °C. This shows that the addition of the studied samples to bitumen was beneficial in case of increasing the total gas and liquid yield and decreasing the coke yield comparing to pyrolysis at a higher temperature (390 °C).

It was noticed that the experimental residual yield was different from the coke yield that was obtained by calculations (the theoretical coke yield, $CY_{theoretical}$). The theoretical coke yield is calculatede by adding the value of the pyrolysed bitumen's coke yield to the value of the individual sample's coke yield in ratio of nine to one (the same ratio of the bitumen to the additive in the micro reactor).

It was calculated based on Equation 4.4 (CY and x show the coke yield and the weight percent) and the amounts are shown in table 4.5. The value of $\frac{CY_{difference}}{CY_{theoretical}}$ (%) shows the ratio of the coke yield difference to the theoretical coke yield. The high amount of $\frac{CY_{difference}}{CY_{theoretical}}$ (%) is an indication of reactions happening among the bitumen and an additive's molecules. These reactions caused the production of the gas and liquid compounds; therefore, the experimental coke yields for the mixed samples are less than the theoretical coke yields according to Table 4.5.

$$\left[\begin{array}{l} CY_{difference} = CY_{theoretical} - CY_{experimental} \\ CY_{theoretical} = [x_{bitumen} \times CY_{bitumen}] + [x_{additive} \times CY_{additive}] \end{array} \right.$$

Equation (4.4)

Table 4.5. Experimental and theoretical coke yields and standard deviations

Sample*	$CY_{experimental}$ (%)	SD* (%)	$CY_{theoretical}$ (%)	$CY_{difference}$ (%)	$\frac{CY_{difference}}{CY_{theoretical}}$ (%)
P(B+POB)	17.23	0.74	17.36	0.13	0.73
P(B+C)	20.52	1.65	21.20	0.68	3.19
P(b+lignin)	16.26	0.49	20.46	4.20	20.55
P(B+lignite)	20.21	1.28	20.87	0.66	3.16
P(B+ BC)	17.34	0.85	22.40	5.06	22.56
P(B+ SC)	19.98	0.97	21.47	1.49	6.93

*This information was not collected for the mixtures of bitumen and asphaltene.

According to Table 4.5, the mixture of pyrolysed bitumen and lignin and the pyrolysed mixture of bitumen and bituminous coal have the highest amounts of $\frac{CY_{difference}}{CY_{theoretical}}$ (%) values. Chu et al. studied the pyrolysis chemistry of a type of lignin (β-O-4 type oligomeric lignin). They believed that lignin is a three dimensional polymer with more than eight types of linkages in its structure, among which the β-O-4 bond is the major type. Chu et al. believed that the cleavage of the β-O-4 bonds is the start point of the free radical production in the lignin molecule. They showed that the formation of much amount of acetic acid and 1,4-butanediol diacetate in the products is because of the easily breaking of the C-O bonds in lignin molecules. It was shown that the β-O-4 bond in the lignin molecule can easily break down (Chu, *et al.* 2013). The ability of the lignin molecules to be

broken easily helps it be a proper option to react with bitumen molecule and increase the liquid and gas products and decrease the coke yield.

Wiser et al. studied the bituminous coal pyrolysis. Their infrared spectra experiments on the subbituminous molecules failed to show the existence of the carbonyl compounds; however, they suggested that the presence of high amount of methane, ethane and propane in the products of the low temperature bituminous coal pyrolysis was because of the presence of the aliphatic linkages in its molecules (Wiser, *et al.* 1967). Depp et al. also stated that at low temperature bituminous coal pyrolysis, the weak carbon-carbon bond was the main linkage that produces the free radicals (Depp, *et al.* 1956). In total, it can be concluded that the bituminous coal has many aliphatic carbon-carbon weak bonds which can break down and produce radicals.

Obviously, the structures of all the materials during their pyrolysis time have not been covered completely in the literature. According to the previous paragraphs it can be concluded that lignin and bituminous coal present variety of linkages which are easy to break down. Therefore, these two additives increased the liquid and gas products and decreased the coke yields consequently.

4.3. References

Burhenne, L.; Messmer, J.; Aicher, T.; Laborie, M. The effect of the biomass components lignin, cellulose and hemicellulose on TGA and fixed bed pyrolysis. *J. Analytical and Applied Pyrolysis.* **2013**, *101,* 177-184

Cheng, K.; Winter, W.; Stipanovic, A. A modulated-TGA approach to the kinetics of lignocellulosic biomass pyrolysis/combustion. *Polymer Degradation and Stability.* **2012**, *97*, 1606-1615

Chu, S.; Subrahmanyam, A.; Hubert, G.; The pyrolysis chemistry of a β-O-4 oligomeric lignin model compound. *Green Chem.* **2013**, *15,* 125-136

Depp, E.; Stevens, C.; Neuworth, M. Pyrolysis of bituminous coal models. *Fuel*, **1956**, *35(4)*, 437-445

Medina, R. J.; Keogh, R.; Davis, B. H. Co-Processing coal and tar-sand resid: a new approach to alternative transportation fuels. Sixth Annual International Pittsburgh Coal Conference, Sept 25-29, 1989, cd 483

Pan, Y. G.; Velo. E.; Puigjaner, L. Pyrolysis of blends of biomass with poor coals. *Fuel.* **1996**, *75:4*, 412-418

Parsons, A. F.; *An introduction to free radical chemistry,* Blackwell Science: York, 2000

Rosenvold, R.; Bubow, J.; Rajeshwar, K. Thermal analysis of Ohio Bituminous Coals. *Thermochimica Acta.* **1982**, *53,* 321-332

Sonobe, T.; Worasuwannarak, N. Kinetic analyses of biomass pyrolysis using the distributed activation energy model. *Fuel.* **2007**, *87,* 414-421

Varhegyi, G.; Antal, M. J.; Jakab, E.; Szabo, P. Kinetic modeling of biomass pyrolysis, *Journal of Analytical and Applied Pyrolysis.* **1997***, 42,* 73-87.

Vuthaluru, H.B. Thermal behavior of coal/biomass blends during co-pyrolysis. *Fuel Processing Technology.* **1987,** *85,* 141-155

White, J.; Catallo, W.; Legendre, B.; Biomass pyrolysis kinetics: A comparative critical review with relevant agricultural residue case studies. *Journal of Analytical and Applied Pyrolysis.* **2011**, *91*, 1-33

Wiser, W.; Hill, G.; Kertamus, N. Kinetic study of the pyrolysis of a high-volatile bituminous coal. *I&EC process design and development,* **1967**, *6(1)*, 133-138.

Yang, H.; Yan, R.; Chen, H.; Zheng, Ch.; Lee, D.; Liang, D. In-Depth Investigation of Biomass Pyrolysis Based on Three Major Components: Hemicellulose, Cellulose and Lignin. *Energy Fuels.* **2006**, *20(1),* 388-393

Yu, J.; Yao, C.; Zeng, X.;Geng, S.; Dong, L.; Wang, Y.; Gao, S.; Xu, G.Biomass pyrolysis in a micro-fluidized bed reactor: Characterization and kinetics. *Chemical Engineering Journal.* **2011**, *168*, 839-849

Zhao, H.; Cao, Y.; Sit, S.; Lineberry, Q.; Pan, W. Thermal characteristics of bitumen pyrolysis. *Journal of Thermal analysis and Calorimetry.* **2012**, *107*, 541-547

5. CHAPTER 5: GAS ANALYSIS OF BITUMEN COPYROLYSIS WITH OXYGENATE CONTAINING MATERIALS

5.1. Introduction

As discussed in chapter two, one group of the pyrolysis products is gases. Gaseous products are not much preferred, but some gases can be used as a source of energy, like methane. The production of some other gases is environmentally hazardous such as carbon dioxide (CO_2) and carbon monoxide (CO). The literature on copyrolysis of the oxygenate containing materials and bitumen and their effect on the coke yield was discussed in Chapter 2. Although, the liquid product of bitumen pyrolysis is more needed, it is important to know what gases are produced by pyrolysis. This can give an idea of the chemistry that happens during the pyrolysis reactions. This chapter focuses on the gas yield that is produced by copyrolysis and studies different gas groups that were produced after pyrolysis. By having the gas yields obtained in this chapter and the coke yields obtained in chapter three, the liquid product yields were calculated. Also, the Carbon to Hydrogen ratio of the produced gases was studied. Diversity in the produced gas compositions reflects the difference in the feed types and the different chemistry that took place during the pyrolysis time. The addition of some of the oxygenate containing materials affected the amounts of the production of some gases.

5.2. Calculations

Gas chromatography (GC) provided the measured retention times for different gases. Different gases produced during copyrolysis were identified according to their retention times. For each gas species, GC provided a peak with some amount of area underneath. The areas that the GC results provided were representatives of the amounts of the gases. The areas that each detector showed had a different unit. The FID showed the area in pico Amper second (pA*s) and

the TCD showed the area in micro Volt second ($\mu V*s$). The molar percentages of the components (Mi) that GC provided for each gas was resulted from Equation 5.1.

$$M_i = \frac{A_i \times R_i}{\sum A_i \times R_i}$$
(Equation 5.1)

Ai= Area of the peak

Ri= Response factor of the component

Mi= Mole percent of the component

Units of Equation (5.1) for FID: Ai[pA*s], Ri[mole/(pA*s)]

Units of Equation (5.1) for TCD: Ai[$\mu V*s$], Ri[mole/($\mu V*s$)]

A standard gas was used to check the calibration. The calibration was performed in such a way that the molar percentages of the fractions were obtained. This also implies that the response factors for both FID and TCD are based on the molar mass of the components.

The FID and TCD response factors of the reference gas are shown in Table 5.1.

Table 5.1. Response factors for FID and TCD detectors

Gas name	FID response factor	Gas name	TCD response factor
methane	1.45E-5	carbon dioxide	3.42E-4
ethylene	8.10E-6	carbon monoxide	4.49 E-4
acetylene	7.32E-6		
ethane	8.25E-6		
propylene	5.96E-6		
propane	5.48 E-6		
i-butane	4.61 E-6		
n-butane	5.21 E-6		
cis 2-butene	6.69 E-6		
i-pentane	9.68 E-6		
n-pentane	2.16 E-5		
i-hexene	1.28 E-5		
n-hexane	7.4 E-6		

For the gas samples, in order to find out the total gas mass in gram and the total C/H molar ratio, the molar amounts (in mol) for each component should be calculated. The calculations are as followed:

The initial nitrogen gas which was purged into the system was known and it was about 1.295 g or 0.046 mol. The system was weighted before and after each

97

nitrogen purge. Moreover, the nitrogen concentration (% mol) was achieved by Equation 5.1. Based on the nitrogen concentration (% mol) and its initial value (in mol), the amount of other produced gases (total molar amount for each component) in mole could be calculated according to Equation 5.2 (K_i, M_i, K_{N2} and M_{N2} represent the molar amount (mol), gas concentration (% mol), initial nitrogen amount and the nitrogen concentration (% mol) respectively).

$$K_i = (M_i \times K_{N2})/M_{N2} \hspace{4cm} \text{(Equation 5.2)}$$

As the molar amount of the component is achieved, the mass amount of each component can also be calculated according to Equation 5.3. (M_i, G_i and MW_i show the molar amount of the gas (mole), mass amount of the gas (g) and the molar weight of the produced gas).

$$G_i = M_i \times MW_i \hspace{4cm} \text{(Equation 5.3)}$$

For calculating the molar fraction of the produced gases, the molar amount of each gas is divided to the total moles of the produced gases except for the Nitrogen and Argon because these two types of gases were not among the produced gases. The nitrogen gas was initially purged and the argon existed because of the presence of some air in the injecting tube which was attached to the GC. The amount of these two gases were subtracted from the total mole of the produced gases according to Equation 5.4 (C_i, M_i, M_t, M_{N2} and M_{Ar} show the concentrations of the produced gases (% mol), molar amount of the gas, the total mole of the produced gases, the molar amount of the Nitrogen and the molar amount of the Argon gas respectively).

$$C_i = M_i / (M_t - M_{N2} - M_{Ar}) \hspace{3cm} \text{(Equation 5.4)}$$

To calculate the total number of carbon atoms and hydrogen atoms of each product, the molar amount of each produced gas is multiplied to the carbon and

hydrogen atoms of that gas. For example for methane, the molar amount of the produced methane is multiplied to 1 for the carbon atoms and again its molar amount is multiplied to 4 to give the hydrogen atoms of this species. Then, all the carbon and hydrogen atoms produced were added up, and the final C/H ratio of the produced gases was calculated and shown in Table 5.2.

In order to calculate the total gas produced from each sample, the mass values of the gases (G_i) were added up except for Nitrogen and Argon (Equation 5.5) (G_t, G_i, G_{N2} and G_{Ar} are the total amounts of mass for all of the gases (g), for each gas group (g), for Nitrogen (g) and for Argon(g) respectively).

$$G_t = \sum G_i - G_{N2} - G_{Ar}$$ Equation (5.5)

To achieve the gas yield produced from the samples, the total gas produced for each sample was divided to the initial mass of the sample. The gas yield of the samples is shown in Table 5.2.

For each sample, at least three runs have been done and the stated calculations were operated for each run. As a result, for each data at least three numbers were available from which a standard deviation and an average value were calculated. All the average data and their standard deviations are shown in Table 5.2. Equation 5.6 and Equation 5.7 show the formula used for calculating the average values and the standard deviations.

$$Y_{ave} = (Y_1 + Y_2 + Y_3)/3$$ (Equation 5.6)

$$Y_{SD} = \left(\frac{[(Y_1 - Y_{ave})^2 + (Y_2 - Y_{ave})^2 + (Y_3 - Y_{ave})^2]}{3}\right)^{\wedge}0.5$$ (Equation 5.7)

5.3. Results and discussion:

After one hour pyrolysis in a micro reactor, the gas product was collected in a gas bag and was analyzed using GC (Gas Chromatography). There was an exception in collecting the gas products. The mixture of bitumen and $Cu(NO_3)_2.2.5H_2O$ was stopped in the first minutes of the pyrolysis, because as the pyrolysis was going to start, the reactor pressure suddenly increased to more than 6.8 MPa in less than 5 minutes. It was not safe to continue with that high pressure because basically that was the maximum pressure that the pressure gauge provided. The copper nitrate decomposed to produce NO_2 and that caused a sudden increase in pressure.

According to the previous sections, carbon to hydrogen ratios were calculated based on three replications, also the total gas that was produced after pyrolysis was collected after one hour of pyrolysis in a micro reactor. The results on the C/H ratio and the produced gas amounts are presented in the following tables.

Table 5.2. Gas yields and the C/H ratio of the samples and the standard deviations. (PB: Pyrolysed bitumen at 380 °C, PPOB: pyrolysed partially oxidized bitumen was pyrolysed in a micro reactor for one hour at 380 °C, PC: Cellulose was pyrolysed in a micro reactor for one hour at 380 °C, Plignin: lignin was pyrolysed in a micro reactor for one hour at 380 °C; Plignite: lignite was pyrolysed in a micro reactor for one hour at 380 °C. PBC: Bituminous coal was pyrolysed in a micro reactor for one hour at 380 °C, PSC: Subbituminous coal was pyrolysed in a micro reactor for one hour at 380 °C. PBat 390: Pyrolysed bitumen at 390 °C, P(B+POB): Pyrolysed mixture of (90% bitumen and 10% partially oxidized bitumen), P(B+C): Pyrolysed mixture of 90% bitumen and 10% cellulose, P(B+lignin): Pyrolysed mixture of 90% bitumen and 10% lignin, P(B+lignite): Pyrolysed mixture of(90% bitumen and 10% lignite), P(B+BC): Pyrolysed mixture of(90% bitumen and 10% bituminous coal), P(B+SC): Pyrolysed mixture of(90% bitumen and 10% subbituminous coal, S.D: Standard Deviation)

Sample*	Gas yield from LT pyrolysis (wt%)	SD for Gas yield	C/H (molar ratio)	SD for C/H
PB	3.00	0.08	0.42	0.01
PBat390	4.01	0.47	0.42	0.03
PPOB	5.52	0.26	0.68	0.01
PC	72.42	6.18	0.76	0.22
Plignin	26.36	0.84	2.35	0.38
Plignite	22.87	0.44	4.04	0.93
PBC	7.60	0.74	3.96	0.92
PSC	13.03	0.28	2.74	0.59
P(B+POB)	2.78	0.16	0.420	0.009
P(B+C)	7.77	0.45	0.585	0.026
P(B+lignin)	4.75	0.54	0.497	0.024
P(B+lignite)	3.94	0.27	0.445	0.023
P(B+BC)	2.34	0.47	0.433	0.007
P(B+SC)	2.93	0.17	0.446	0.009

*This information was not collected for the pyrolysed asphaltene and the mixture of bitumen and asphaltene.

The pyrolysed mixture of bitumen and partially oxidized bitumen had a similar C/H ratio as the pyrolysed bitumen. The other additives seem to increase the C/H ratio of the produced gases.

According to Table 5.2, the C/H ratio of the pyrolysed cellulose was the highest one among the other individual pyrolysed materials. The mixture of the bitumen and cellulose had also a high amount of C/H ratio among the other mixtures. According to Table 5.2, it was observed that cellulose has the highest CO_2 and CO production; therefore, large amounts of carbon and oxygen were rejected in the form of non-hydrocarbon gases and this is the reason of the high value of the carbon to hydrogen ratio.

According to Table 5.2, although the gas productions for the individual pyrolysed bituminous coal and subbituminous coal were higher than for the pyrolysed bitumen, their mixture with bitumen produced less gas than the

pyrolysed bitumen. According to Table 4.5 in Chapter 4, the total liquid and gas produced by the P(B+BC) and P(B+SC) were also lower than the total liquid and gas produced by the pyrolysed bitumen. Therefore, according to Table 4.5, obviously the Effective MCR of low temperature pyrolysis (LT) for P(B+BC) and P(B+SC) were higher than for the pyrolysed bitumen.

Table 5.2 also shows the gas yields of the pyrolysed samples. Comparison between the pyrolysed bitumen at 380 °C and pyrolysed bitumen at 390 °C indicates that for an increase in the temperature, the gas yields increased. As it was indicated in the previous chapter, the gas yields for the mixtures of pyrolysed bitumen and cellulose, pyrolysed bitumen and lignin, pyrolysed bitumen and lignite are higher than the gas yield for the pyrolysed bitumen at 380 °C. The gas yield for the pyrolysed mixture of bitumen and partially oxidized bitumen is in the same range as for the pyrolysed bitumen at 380 °C. The gas yield for the mixture of bitumen and cellulose was highest gas yield among all the other additives.

Table 5.2 shows the gas composition of the individual pyrolysed samples. Tables 5.3 and 5.4 show the gas compositions of the copyrolysed mixtures. Obviously, there were some other gases which were produced during pyrolysis but are not shown in Tables 5.1, 5.2, 5.3, 5.4 and 5.5. For instance, when oxygenate rich materials are copyrolysed with bitumen, definitely some dehydration happens, as well as production of some sulfur containing gas groups (e.g. SO_2 and H_2S). However, the detectors that were used in this study did not observe those gases and at this step we have not put much attention to those gases.

According to the following tables, the concentration of carbon dioxide production increased when an additive was added to bitumen. The highest amount of carbon dioxide production was caused by the addition of lignite, cellulose and lignin to bitumen. The GC results elucidate that some of the components such as ethylene and propylene has not been produced in all of the

experiments. As a result, the standard deviations for these components are relatively high.

The lowest ethane production was caused from the plain bitumen pyrolysis. Other mixtures gave approximately same amounts for ethane. Among the other components, n-butane, i-pentane and n-pentane show considerable amounts; however, the rest of the components were produced in negligible quantities. The pyrolysed mixture of cellulose and bitumen and the pyrolysed mixture of lignin and bitumen generated the lowest amounts of n-butane and i-pentane. Lignin and lignite decreased the carbon monoxide (CO) production when they were pyrolysed with bitumen. Cellulose increased the CO production for about 54.2% when it was pyrolysed with bitumen.

Table 5.3. Gas components of the individual pyrolysed materials and the Standard deviations (SD). (PB: Pyrolysed bitumen at 380 ℃, PPOB: partially oxidized bitumen was pyrolysed in a micro reactor for one hour at 380 ℃, PC: Cellulose was pyrolysed in a micro reactor for one hour at 380 ℃, Plignin: lignin was pyrolysed in a micro reactor for one hour at 380 ℃; Plignite: lignite was pyrolysed in a micro reactor for one hour at 380 ℃. PBC: Bituminous coal was pyrolysed in a micro reactor for one hour at 380 ℃, PSC: Subbituminous coal was pyrolysed in a micro reactor for one hour at 380 ℃. PBat 390: Pyrolysed bitumen at 390 ℃)

Sample Gas Group*	PBC	PC	PLignin	PLignite	PPOB	PSC
CH_4	3.26	13.11	8.08	2.74	9.86	3.76
SD CH_4	0.54	0.51	0.63	0.37	0.75	0.97
CO_2	68.11	46.66	77.83	82.84	40.89	73.16
SD CO_2	1.01	1.34	1.25	1.16	2.05	1.64
C2H4 (ethylene)	0	0.76	0.10	0.29	0	0.41
SD C2H4	0	0.03	0.15	0.04	0	0.06
C2H6 (ethane)	0.59	4.19	0.46	0	2.06	0.51
SD C2H6	0.59	0.26	0.35	0	2.06	0.04
C3H6 (propylene)	0	0	0	0	0	0
SD C3H6	0	0	0	0	0	0
C3H8 (propane)	0.25	0.01	0.14	0.05	1.88	0.26
SD C3H8	0.18	<0.01	0.09	0.08	0.17	0.02
C4H10 (i-butane)	0	0.64	0.10	0	0	0
SD C4H10	0	0.04	0.13	0	0	0
C4H10 (n-butane)	0.21	0.02	0.06	0.11	1.72	0.24
SD C4H10	0.02	0.01	0.06	0.07	0.09	0.10
C4H8 (cis-2-butene)	0.21	<0.01	0.05	0.09	1.68	0.11
SD C4H8	0.07	<0.01	0.01	0.06	1.33	0.11
C5H12 (i-pentane)	0.50	2.74	0.10	0.38	2.82	0.12
SD C5H12	0.11	<0.01	0.02	0.18	0.35	0.10
C5H12 (n-pentane)	0	5.73	0.32	0.30	7.93	1.11
SD C5H12	0	3.93	0.24	0.30	0.81	0.23
C6H12 (i-hexene)	0.19	0.21	0.17	0.02	1.70	0.04
SD C6H12	0.01	<0.01	0.05	0.01	0.18	0.03
C6H14 (n-hexane)	0	0.11	0	0.03	0.32	0.07
SD C6H14	0	<0.01	0	0.04	0.02	0.06
CO (carbon monoxide)	26.67	22.32	12.56	12.49	29.13	20.21
SD CO	2.55	9.51	2.59	0.01	0.76	2.19

*This information was not collected for the pyrolysed asphaltene.

Table 5.4. Gas components of the mixed pyrolysed materials and the Standard deviations (SD). (P(B+POB): Pyrolysed mixture of (90% bitumen and 10% partially oxidized bitumen), P(B+C): Pyrolysed mixture of (90% bitumen and 10% cellulose), P(B+lignin): Pyrolysed mixture of (90% bitumen and 10% lignin), P(B+lignite): Pyrolysed mixture of (90% bitumen and 10% lignite)

Sample* Gas Group (mol %)	P(B+POB)	P(B+C)	P(b+lignin)	P(B+lignite)
CH$_4$	22.52	15.17	22.51	17.90
SD CH$_4$	0.84	0.48	3.06	1.11
CO$_2$	14.14	42.63	40.46	45.12
SD CO$_2$	3.07	1.29	2.70	3.44
C2H4 (ethylene)	1.17	0.56	0.84	0.48
SD C2H4	0.09	0.40	0.19	0.34
C2H6 (ethane)	10.56	7.46	8.10	8.13
SD C2H6	0.51	0.38	0.53	0.79
C3H6 (propylene)	1.20	0	0	0
SD C3H6	1.70	0	0	0
C3H8 (propane)	5.24	0.76	0.89	0.86
SD C3H8	2.91	0.07	0.08	0.02
C4H10 (i-butane)	0.43	0.82	0.95	1.08
SD C4H10	6.04	0.11	0.05	0.16
C4H10 (n-butane)	6.03	3.92	4.77	5.23
SD C4H10	0.10	0.33	0.12	0.53
C4H8 (cis-2-butene)	0.59	0.35	0.43	0.39
SD C4H8	<0.01	0.03	0.04	0.04
C5H12 (i-pentane)	6.85	2.10	2.88	3.33
SD C5H12	0.29	0.24	0.37	0.36
C5H12 (n-pentane)	20.82	7.22	9.63	11.90
SD C5H12	0.80	1.10	1.38	1.41
C6H12 (i-hexene)	0.61	0.21	0.39	0.54
SD C6H12	0.56	0.03	0.10	0.05
C6H14 (n-hexane)	1.00	0.30	0.41	0.53
SD C6H14	0.41	0.06	0.09	0.07
CO (carbon monoxide)	8.82	18.5	7.73	4.52
SD CO	3.06	1.47	1.62	1.73

*This information was not collected for the pyrolysed mixture of bitumen and asphaltene.

Table 5.5. Gas components of the mixed pyrolysed materials and the Standard deviations (SD) (PB: Pyrolysed bitumen at 380 ℃, PBat390: Pyrolysed bitumen at 390 ℃, P(B+BC): Pyrolysed mixture of (90% bitumen and 10% bituminous coal), P(B+SC): Pyrolysed mixture of (90% bitumen and 10% subbituminous coal)

Sample Gas Group (mol%)	P(B+ BC)	P(B+ SC)	PB	Bat390
CH_4	22.99	24.70	19.36	29.36
SD CH_4	0.96	1.79	5.02	7.60
CO_2	18.50	27.84	12.93	15.80
SD CO_2	2.09	1.45	0.74	9.30
C2H4 (ethylene)	0.37	0.72	1.12	0.75
SD C2H4	0.53	5.11	0.26	0.54
C2H6 (ethane)	11.14	12.13	10.65	7.77
SD C2H6	0.53	0.88	2.04	5.55
C3H6 (propylene)	1.14	0	1.00	0
SD C3H6	0.24	0	1.25	0
C3H8 (propane)	1.14	1.24	3.32	2.22
SD C3H8	0.24	0.03	2.56	0.93
C4H10 (i-butane)	1.19	1.47	1.32	1.94
SD C4H10	0.33	0.09	0.45	0.76
C4H10 (n-butane)	7.78	6.49	7.86	8.17
SD C4H10	0.62	0.15	2.18	2.90
C4H8 (cis-2-butene)	0.59	0.50	0.72	0.53
SD C4H8	0.23	0.08	0.15	0.06
C5H12 (i-pentane)	4.57	3.69	7.66	5.29
SD C5H12	0.07	0.14	2.24	1.45
C5H12 (n-pentane)	18.37	11.45	20.41	17.42
SD C5H12	2.82	0.53	4.63	5.38
C6H12 (i-hexene)	0.69	0.53	0.85	0
SD C6H12	0.09	0.05	0.52	0
C6H14 (n-hexane)	0.82	0.47	0.84	0.57
SD C6H14	0.23	0.02	0.42	0.21
CO (carbon monoxide)	11.84	8.74	12.00	10.16
SD CO	1.53	0.92	1.97	3.79

This chapter shows that the C/H ratio of the total produced gas increased when an oxygenate containing material was added to bitumen. Zhao et el (Zhao, et al. 2010) studied the change in the gas C/H ratio by the change in temperature and the reaction time. They found that by an increase in temperature and the reaction time, the C/H decreased for gas and coke products. In our study, it was shown that the addition of the oxygenate containing additives to bitumen had the opposite effect on the C/H ratio as the increase in the temperature and the increase in the retention time had in Zhao et al work.

It was also shown that the addition of an oxygenate containing material increased the total amount of the produced gas except for bituminous coal.

According to Ma et al. when temperature is increased in the range of 380-480 °C, the gas yield also increased (Ma, 2012), this idea was proved in our study and pyrolysis at higher temperature gave higher gas yield. Also, it was shown in our study, that the addition of the oxygenate containing materials also have the same effect as the increase in the temperature. The produced gas distribution showed that the carbon dioxide production increased when oxygenate containing materials were added, while the carbon monoxide production decreased.

5.4. References:

Ma, Y.; S. Li. The pyrolysis, extraction and kinetics of Buton oil sand bitumen. *Fuel Processing Technology*. **2012,** *100*, 11-15.

Zhao, Y., F.; Wei, et al. Effects of reaction time and temperature on carbonization in asphaltene pyrolysis. *Journal of Petroleum Science and Engineering*. **2010.** *74(1-2)*, 20-25

6. CHAPTER 6: SIMULATED DISTILLATION ANALYSIS OF THE COPYROLYSED BITUMEN WITH OXYGENATE CONTAINING MATERIAL

6.1. Introduction

Cold Lake bitumen was pyrolysed with oxygenate containing materials in a microreactor at relatively low temperature and initial pressure of 4 MPa of Nitrogen (The procedure of feed preparation was discussed in chapter two, section 2.2). After pyrolysis was done in a micro reactor, the liquid residue was collected for further analysis (The residue collecting procedure was discussed in chapter two, section 2.2.4). In order to compare the pyrolysed results with the raw ones, raw bitumen and raw partially oxidized bitumen were analyzed by simulated distillation analysis instrument (Sim-Dis). The raw mixtures could not be used for analysis with Sim-Dis because in order to prepare the samples for Sim-Dis analysis, they need to be solved in carbon disulfide but the solid additives that we studied were not soluble in carbon disulfide. So the samples used for this study were the liquid residue remained after pyrolysis. The raw bitumen and the derivatives of bitumen were also studied.

The objective of using Sim-Dis was to have a better understanding of the effect that each additive could have on the amount of the distilled cuts. It was hypothesized that the addition of the oxygenate containing material can improve the lighter products and would decrease the heavy fractions. By comparing the distributed cuts of the raw bitumen and the distributed cuts of mixtures, it was figured out that how each additive shifted the products to lighter or heavier fractions. It was yet obvious that all the advantageous results can not direct to a single result in choosing the best additive.

Ukwuoma studied the simulated distillation of the Nigerian tar sand bitumen on Gas Liquid Chromatography (GLC), they showed that up to 538 °C the total distillable amount was 65.2%. According to the table they brought in their work for the simulated distillation of tar sand, it was shown that only less than 5% of the tar sand bitumen distilled at temperatures lower than 260 °C. They showed that the highest distilled amounts happen at temperature ranges of 275-305 °C and 425-490 °C (Ukwuoma, 1999).

The technique of Gas chromatography simulated distillation (GCSD) was initially not so applicable for oil samples. Later, use of metal columns in GCSD allowed analysis of residue samples with that equipment (Carbognani, et al. 2007). Carbognani et al. studied the analysis of Athabasca vacuum residue (VR) and its visbreaking products with different operational conversion yields (VB) by High Temperature Simulated Distillation (HTSD). They studied samples' crackability and "on-column" HTSD crackings. They provided the distillation fractions of the samples and their data showed that an important difference is observed in the light fraction of the VB products' distillations. They showed that the yields of high distillate products for VB products are higher than the vacuum residue (feed) and there was an increase in the amount of total distillate fraction from 26% (at 545 °C) for the vacuum residue to 59.2% (at 545 °C) for one of their VB fractions. In their study they showed that the cracking reactions are not only restricted to temperatures above 350 °C and at temperatures lower than this amount, some cracking also happen.

Nigerian bitumen was hydrotreated at low temperatures and the liquid products were then analyzed by use of gas chromatography simulated distillation (Ukwuoma, 2002). They showed that an increase in temperature generally increased the conversion of bitumen to distillable products. They believed that figuring out the boiling point distribution by use of the simulated distillation methods made a revolution in crude oil characterization. They conducted some

experiments at a constant temperature but with different pressures and vice versa. It was observed that at 525 °C, the distillation yield increased with an increase in temperature. The distillation yield at 525 °C increased from 60% of feed to 86%, 94% and 96.5% with the operating temperatures of 250 °C, 300 °C and 350 °C respectively. They divided the boiling points into three ranges; light fraction (< 250 °C), intermediate distillation fraction (250- 400 °C) and the heavy distillates (400- 538 °C). They showed that the light fraction increased from 20% to 40% when temperature increased from 250 °C to 300 °C and another 43% when temperature increased from 300 °C to 350 °C at 1500 psig. The intermediate fraction also increased from 33% to 34% and 34.5% at the stated temperatures at 1500 psig. However, the heavy distillation fraction decreased from 34.5% to 19.5% and 17.5% when temperature increased from 250 °C to 300 °C and 350 °C respectively at the same operating pressure (1500 psig). They observed that an increase in the operating temperature and a decrease in the initial hydrogen pressure favored the light fraction production but the governing parameter in controlling the increase in light production is the temperature rather than the pressure. In general, by the study of the Nigerian tar sand bitumen upgrading in a laboratory reactor they showed that the production of high quality liquid is practical by bitumen hydrotreating at low temperatures even without the presence of any catalyst.

Bitumen distillation was studied in some literature but the coprocessed mixtures of bitumen and oxygenate containing materials have not been studied yet. Also, only distillation of raw materials has been studied in literature. It was needed to study the pyrolysed samples as well to see the effects of the pyrolysis on distribution of light, intermediate and heavy fractions. Also, in this study the role of some additives (which are oxygenate containing materials) on the distilled products was studied. From the data analyzed in this study, it can be observed how much each additive changes the distilled amounts after the copyrolysis of the bitumen and the additives.

6.2. Calculations

Sim-Dis gives the total amount of distilled cuts in different temperatures. In order to find out how much of the sample is distilled in different temperature ranges, the cumulative amounts can be deducted from each other (Equation 6.1).

$$Cum_{atT1} - Cum_{at\ T2} = Dist_{T1-T2} \qquad\qquad \text{(Equation 6.1)}$$

$Cum_{atT1} = Cumulative\ amount\ at\ T2$

$Cum_{atT2} = Cumulative\ amount\ at\ T2$

$Dist_{T1-T2} = Distilled\ amount\ between\ T1\ and\ T2$

6.3. Results and discussions

Tables 6.1 and Table 6.2 show the distilled and cumulative amounts for bitumen and bitumen derived mixtures. According to Table 6.2, the amounts of cumulative pyrolysed bitumen was higher than the data for the cumulative raw bitumen at almost all temperature ranges and the amount of difference is about 3-4%, in other words, at each temperature range the value of cumulative distilled bitumen was about three to four percent higher than the cumulative amount for the raw bitumen (Figure 6.2). The slopes of the RB and PB graphs are almost the same, yet one graph is upper than the other. Now, by looking at the distilled amounts of the named products, it is observed that at various temperature ranges, the distilled amounts of both are almost equal except at temperature ranges up to 250 °C. The main difference between the amounts of the cumulative raw and pyrolysed bitumen was mainly at the low temperature distillation range.

111

Although the mass % of the distilled samples are not as practical and important as vol% is for refiners, in this study we looked through the mass% of the distilled samples in order to compare the amount of the products. The realistic density values of the products were not available for this study so the vol% was not calculated. As a comparative study, the increase and decrease in the mass% of the products can demonstrate the same changes in the vol% of the products

Table 6.1. Distilled and cumulative distilled amounts for bitumen and bitumen derivatives. (CPT: Cut point temperature, D_PB: Distilled Pyrolysed Bitumen at 380 ℃, C_PB: Cumulative Pyrolysed Bitumen at 380 ℃, D_RB: Distilled_Raw Bitumen, C_RB: Cumulative_Raw Bitumen, D_PBat390: Distilled_Pyrolysed Bitumen at 390 ℃, C_PBat390: Cumulative_Pyrolysed Bitumen at 390 ℃)

| CPT (° C)	D_PB (wt%)	C_PB (wt%)	D_RB (wt%)	C_RB (wt%)	D_PBat 390 ° C (wt%)	C_PBat 390 ° C (wt%)
200	1.5	1.5	<1	<1	4.5	4.5
225	0.5	2	<1	<1	1.5	6
250	1	3	<1	<1	1.5	7.5
275	1.5	4.5	1.5	1.5	2.5	10
300	1.5	6	1.5	3	2.5	12.5
325	3	9	2.5	5.5	4	16.5
350	4	13	3.5	9	4	20.5
375	4	17	4	13	4	24.5
400	5	22	5	18	5	29.5
425	5.5	27.5	5.5	23.5	5	34.5
450	5.5	33	5.5	29	4.5	39
475	5	38	5	34	4	43
500	5	43	5	39	4	47
525	4	47	4.5	43.5	3	50
550	4.5	51.5	4.5	48	3	53
575	4	55.5	4	52	3	56
600	4.5	60	4	56	2.5	58.5
625	4	64	4	60	2.5	61
650	3	67	4	64	2.5	63.5
675	3.5	70.5	4.5	68.5	1.5	65
700	2.5	73	1.5	70	1.5	66.5

Table 6.2. Distilled and cumulative distilled amounts for bitumen and bitumen derivatives. (CPT: Cut point temperature. (D_RPOB: Distilled raw partially oxidized bitumen at 380 ℃, C_RPOB: Cumulative raw partially oxidized bitumen at 380 ℃, D_P(B+POB): Distilled pyrolysed (bitumen and partially oxidized bitumen) at 380 ℃, C_P(B+POB): Cumulative pyrolysed (bitumen and partially oxidized bitumen) at 380 ℃; D_R(B+POB): Distilled raw (Bitumen+ partially oxidized bitumen at 380 ℃); C_R(B+POB): Cumulative raw (Bitumen+ partially oxidized bitumen at 380 ℃))

CPT (℃)	D_RPOB (%)	C_RPOB (%)	D_P(B+POB) (%)	C_P(B+POB) (%)	D_R(B+POB)	C_R(B+POB)
200	6	6	3	3	<1	<1
225	2.5	8.5	1	4	<1	<1
250	2.5	11	1.5	5.5	<1	<1
275	4.5	15.5	2	7.5	1.5	1.5
300	4.5	20	2.5	10	1.5	3
325	4.5	24.5	3.5	13.5	2.5	5.5
350	5	29.5	4.5	18	3.5	9
375	6	35.5	5.5	23.5	4.5	13.5
400	4	39.5	5	28.5	4.5	18
425	6	45.5	6	34.5	5	23
450	4.5	50	5.5	40	5.5	28.5
475	4.5	54.5	5.5	45.5	5	33.5
500	4.5	59	5	50.5	4.5	38
525	5	64	4.5	55	4.5	42.5
550	5	69	4	59	4.5	47
575	4	73	4	63	4.5	51.5
600	2.5	75.5	4	67	3	54.5
625	3	78.5	3.5	70.5	4.5	59
650	3	81.5	3.5	74	3.5	62.5
675	2.5	84	3	77	3	65.5
700	3	87	2	79	3	68.5

The distillation profiles of bitumen pyrolysed at 380 and 390 ℃ were compared by looking at the amount of material that distilled over successive 25 ℃ intervals. At cut point temperatures below 350 ℃, it was noticed that for each 25 ℃ distillation interval more material was obtained in the fractions from PBat390 than that of pyrolysed bitumen at 380 ℃. In the temperature range between 350 ℃ and 400 ℃, the distilled amounts for both are the same. At temperature cuts higher than 400 ℃, more material was obtained in each of the fractions from pyrolysed bitumen at 380 ℃ than in the fractions obtained from pyrolysed bitumen at 390 ℃.
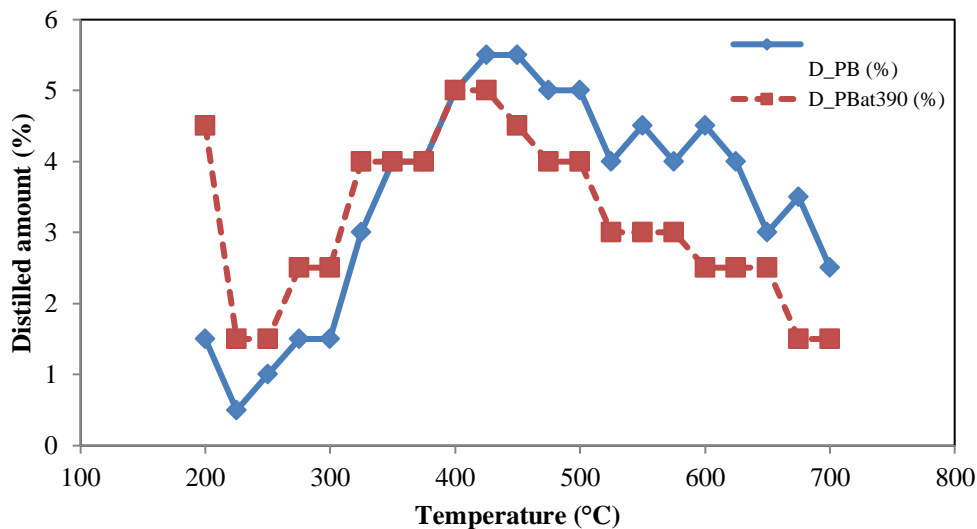
Figure 6.1. Distillation data for PB and PBat390 (D_PB: Distilled bitumen that was pyrolysed at 380 ℃ for one hour in a micro reactor, D_PBat390: Distilled bitumen that was pyrolysed at 390 ℃ for one hour in a micro reactor)

It was noticed that the raw partially oxidized bitumen had more low temperature distilled fractions than raw bitumen. The comparison between two columns of D_POB and D-RB in Table 6.2 showed that below 450 ℃, D_POB presented higher amounts of distilled fractions.

Figure 6.1 shows the cumulative distilled data on all the samples. According to this figure, P(B+POB) and P(B+SC) show very similar trends. The mixture of pyrolysed bitumen and bituminous coal showed the lowest amount of distilled fractions under 700 ℃, about 59% of this mixture distilled below 700 ℃, yet about all the mixture of bitumen and cellulose distilled below 700 ℃.

Table 6.3. Distilled and cumulative amounts for bitumen and the mixtures. (CPT: Cut point temperature, D_P(B+lignite): Distilled amounts for pyrolysed mixture of bitumen and lignite at 380 ℃; C_P(B+lignite): Cumulative amounts for pyrolysed mixture of bitumen and lignite at 380 ℃ (%); D_P(B+C): Distilled amounts for pyrolysed mixture of bitumen and cellulose at 380 ℃ ; C_P(B+C): Cumulative amounts for pyrolysed mixture of bitumen and cellulose at 380 ℃; D_P(B+BC): Distilled amounts for pyrolysed mixture of bitumen and bituminous coal at 380 ℃; C_P(B+BC): Cumulative amounts for pyrolysed mixture of bitumen and bituminous coal at 380 ℃)

CPT (℃)	D_P(B+lignite) (%)	C_P(B+lignite) (%)	D_P(B+C) (%)	C_P(B+C) (%)	D_P(B+BC) (%)	C_P(B+BC) (%)
200	2.5	2.5	4.5	4.5	2	2
225	0.5	3	1.5	6	0.5	2.5
250	1.5	4.5	2	8	1	3.5
275	1.5	6	2	10	1.5	5
300	2	8	3.5	13.5	1.5	6.5
325	3.5	11.5	4.5	18	2.5	9
350	3.5	15	5	23	3.5	12.5
375	5	20	6	29	3.5	16
400	5.5	25.5	7.5	36.5	4	20
425	5.5	31	7	43.5	4.5	24.5
450	5.5	36.5	7	50.5	4.5	29
475	5.5	42	7	57.5	4	33
500	5	47	6	63.5	4	37
525	4	51	6	69.5	3.5	40.5
550	4.5	55.5	5	74.5	3.5	44
575	4	59.5	5	79.5	3	47
600	4.5	64	5	84.5	3	50
625	4	68	4	88.5	2.5	52.5
650	3.5	71.5	4	92.5	3	55.5
675	3	74.5	3	95.5	2	57.5
700	2.5	77	3	98.5	1.5	59

Table 6.4. Distilled and cumulative amounts for bitumen and the mixtures. (D_P(B+lignin): Distilled amounts for pyrolysed mixture of bitumen and lignin at 380 ℃; C_P(B+lignin): Cumulative amounts for pyrolysed bitumen and lignin at 380 ℃; D_P(B+SC): Distilled amounts for pyrolysed bitumen and Subbituminous Coal at 380 ℃; C_P(B+SC): Cumulative amounts for pyrolysed mixture of bitumen and Subbituminous Coal) at 380 ℃)

CPT (℃)	D_P(B+lignin) (%)	C_P(B+lignin) (%)	D_P(B+SC) (%)	C_P(B+SC) (%)
200	3	3	4	4
225	1	4	1	5
250	1	5	1.5	6.5
275	1.5	6.5	2	8.5
300	3	9.5	2.5	11
325	3	12.5	3.5	14.5
350	4	16.5	4.5	19
375	5.5	22	4.5	23.5
400	5	27	6	29.5
425	6	33	6	35.5
450	5.5	38.5	5.5	41
475	5	43.5	5.5	46.5
500	5	48.5	5	51.5
525	5	53.5	4.5	56
550	4	57.5	4	60
575	4	61.5	4.5	64.5
600	4	65.5	4	68.5
625	3	68.5	4	72.5
650	3	71.5	3.5	76
675	3	74.5	3	79
700	1.5	76	2.5	81.5

According to Table 6.2, all the distilled amounts of the samples can be categorized into the same groups in an atmospheric pressure. The distributions of the samples are brought in Table 6.5. The samples used in this study were mainly heavy oils; therefore, the starting distillation point for these samples were about 200 ℃ and less than 5% of the samples was distilled below this temperature. The first group of the distribution is considered to be Heavy naphtha, yet for some samples no heavy naphtha was observed.

For all the samples except for the raw bitumen, not all of the original feed was subjected to distillation. Therefore, in order to calculate the equivalent of "yield" for the distillation products, the data on the amount of the original feed that was subjected to distillation was provided in the last column in Table 6.5. In other words, the numbers in the first ten rows in Table 6.5 show the selectivity of the products and the last column shows the conversion. In order to calculate the yield of each product, the selectivity should be multiplied by the conversion

(Equation 6.2). Table 6.6 shows the yields of the products calculated by Equation 6.2.

Conversion × Selectivity= Yield   Equation (6.2)

The amount of the feed that was subjected to distillation is achieved by Equation (6.3).

Amount of the feed subjected to distillation= 100%- Amount of the gas product from one hour pyrolysis at 380 °C(%)   Equation (6.3)

Basically, the feed that was subjected to distillation is the non-gas product that was collected after one hour pyrolysis of the feed in a micro reactor at 380 °C. The gas product yield was provided in Table (5.2) in Chapter five.

Table 6.5. The distribution of the products according to their distillation points. (PB: pyrolysed bitumen at 380 °C, RB: raw bitumen, PBat390 °C: pyrolysed bitumen at 390 °C, RPOB: raw partially oxidized bitumen at 380 °C, P(B+POB): mixture of pyrolysed bitumen and partially oxidized bitumen, R(B+POB): mixture of raw bitumen and partially oxidized bitumen, P(B+lignite): mixture of pyrolysed bitumen and lignite, P(B+C): mixture of pyrolysed bitumen and cellulose, P(B+BC): mixture of pyrolysed bitumen and bituminous coal, P(B+lignin): mixture of pyrolysed bitumen and lignin, P(B+SC): mixture of pyrolysed bitumen and Subbituminous coal)

Hydrocarbon range (°C)	Heavy naphtha (121-191 °C) (%)	Kerosene (191-277 °C) (%)	Distillate fuel oil (277-343 °C) (%)	Gas oil or lube stock (343-566 °C) (%)	Residuum (>566 °C) (%)	Amount of the feed that was subjected to distillation (%) (Conversion)
PB	1.5	3	7.5	42	46	97
RB	<1	1	6.5	42.5	50	100
PBat390 °C	4	6	9.5	35.5	45	95.99
RPOB*	6	10	11.5	44	28.5	100
P(B+POB)	<1	4.5	10.5	45	37	97.22
R(B+POB)	<1	1	6.5	41.5	51	100
P(B+lignite)	2.5	3.5	8.5	43.5	42	96.06
P(B+C)	4.5	6	9.5	56	24	92.23
P(B+BC)	2	3	6.5	34.5	54	97.66
P(B+lignin)	3	4	9	44	40	95.25
P(B+SC)	4	5	9	45	37	97.07

*The information on the pyrolysed partially oxidized bitumen was not collected.

Table 6.6. Product yields according to their distillation points. (PB: pyrolysed bitumen at 380 ℃, RB: raw bitumen, PBat390: pyrolysed bitumen at 390 ℃, RPOB: raw partially oxidized bitumen at 380 ℃, P(B+POB): mixture of pyrolysed bitumen and partially oxidized bitumen, R(B+POB): mixture of raw bitumen and partially oxidized bitumen, P(B+lignite): mixture of pyrolysed bitumen and lignite, P(B+C): mixture of pyrolysed bitumen and cellulose, P(B+BC): mixture of pyrolysed bitumen and bituminous coal, P(B+lignin): mixture of pyrolysed bitumen and lignin, P(B+SC): mixture of pyrolysed bitumen and subbituminous coal)

Hydrocarbon range (° C)	Heavy naphtha (121-191 ° C) (%)	Kerosene (191-277 ° C) (%)	Distillate fuel oil (277-343 ° C) (%)	Gas oil or lube stock (343-566 ° C) (%)	Residuum (>566 ° C) (%)
PB	1.4	2.9	7.3	40.7	44.6
RB	<1	1	6.5	42.5	50
PBat390 ° C	3.8	5.7	9.1	34.1	43.2
RPOB*	6	10	11.5	44	28.5
P(B+POB)	<1	4.4	10.2	43.7	36
R(B+POB)	<1	1	6.5	41.5	51
P(B+lignite)	2.4	3.4	8.2	41.8	40.3
P(B+C)	4.1	5.5	8.8	51.6	22.1
P(B+BC)	1.9	2.9	6.3	33.7	52.7
P(B+lignin)	2.8	3.8	8.6	41.9	38.1
P(B+SC)	3.9	4.8	8.7	43.7	35.9

*The information on the pyrolysed partially oxidized bitumen was not collected.

According to Table 6.6, it is observed that the addition of the oxygenate containing materials increased the amount of the light products (Heavy naphtha, Kerosene, Distillate fuel oil) and decreased the residuum. The mixture of bitumen and cellulose pyrolysed at 380 °C seem to be the most effective additive in increasing the heavy naphtha and Kerosene yield. In average, the main product of pyrolysis in this study is Gas oil which stands for about 50% of the total product.

As it was discussed before, it can also be noticed from Table 6.4 that the gas oil amount of the mixture of bitumen and cellulose is the highest amount, while P(B+BC) showed the lowest amount of the gas oil fraction. The amounts of the residuum and the distillate fuel oil were almost similar for various samples. However, the high amount of heavy naphtha and kerosene fractions for POB differentiates it from the other additives.
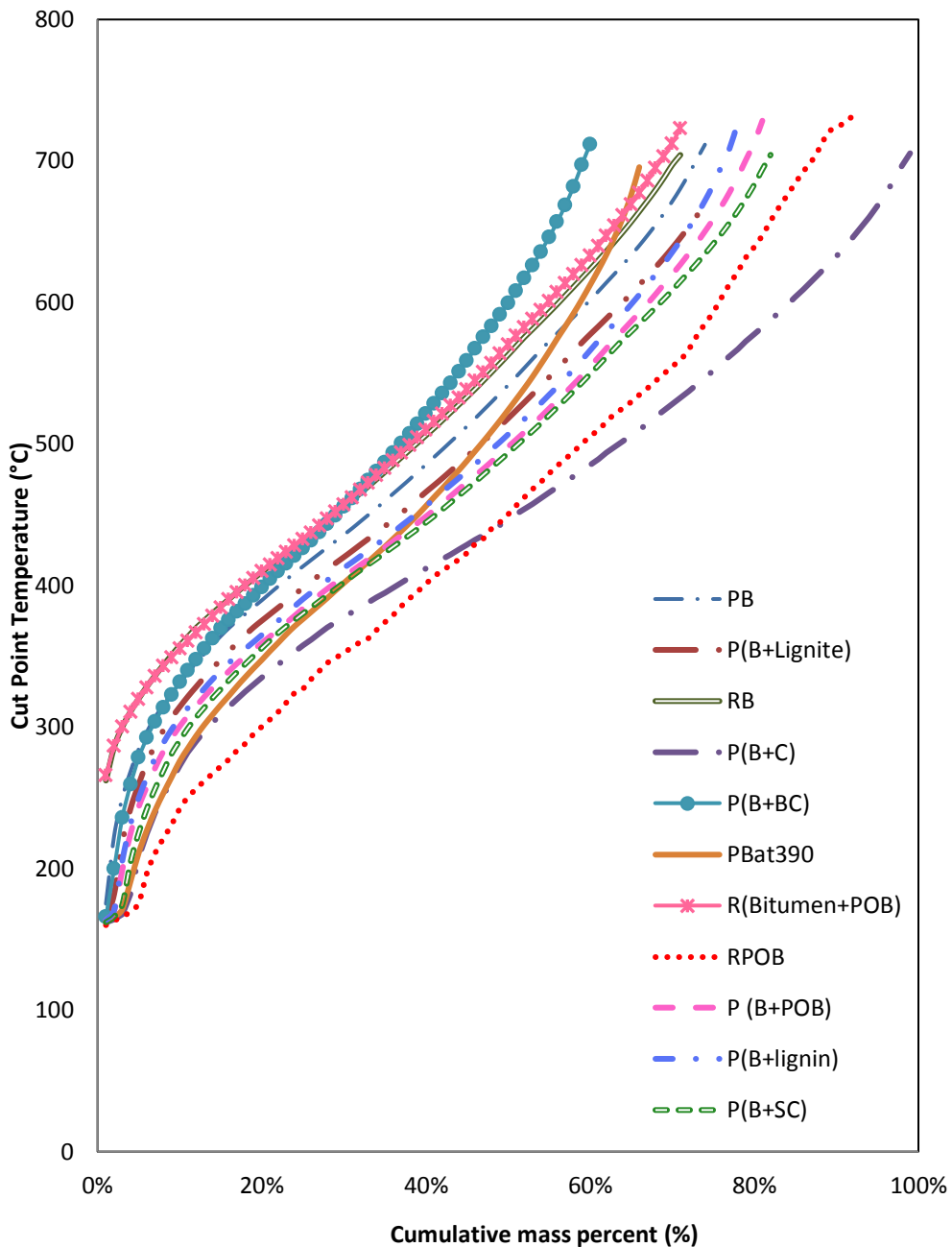
Figure 6.2. Cut point temperature versus cumulative mass percent. (PB: pyrolysed Bitumen at 380 °C, RB: raw bitumen, PBat390: pyrolysed bitumen at 390 °C, RPOB: raw partially oxidized bitumen at 380 °C, P(B+POB): pyrolysed bitumen and partially oxidized bitumen at 380 °C; R(B+POB): raw bitumen and Partially Oxidized Bitumen at 380 °C; P(B+lignite): pyrolysed bitumen and lignite at 380 °C; P(B+C): pyrolysed bitumen and cellulose at 380 °C; P(B+BC): pyrolysed bitumen and bituminous Coal at 380 °C; P(B+lignin): pyrolysed bitumen and lignin at 380 °C; P(B+SC): pyrolysed bitumen and subbituminous Coal at 380 °C)

Figure 6.3 shows the distillation data of the samples (not cumulative). According to this figure, there is a range in temperature in which all the samples possess the highest amount of distilled fraction. All the samples present a peak in the range

119

of 350 °C to 550 °C which presents the gas oil or lube stock fraction (as presented in Table 6.4). For all the samples the peaks are at about 400 °C.
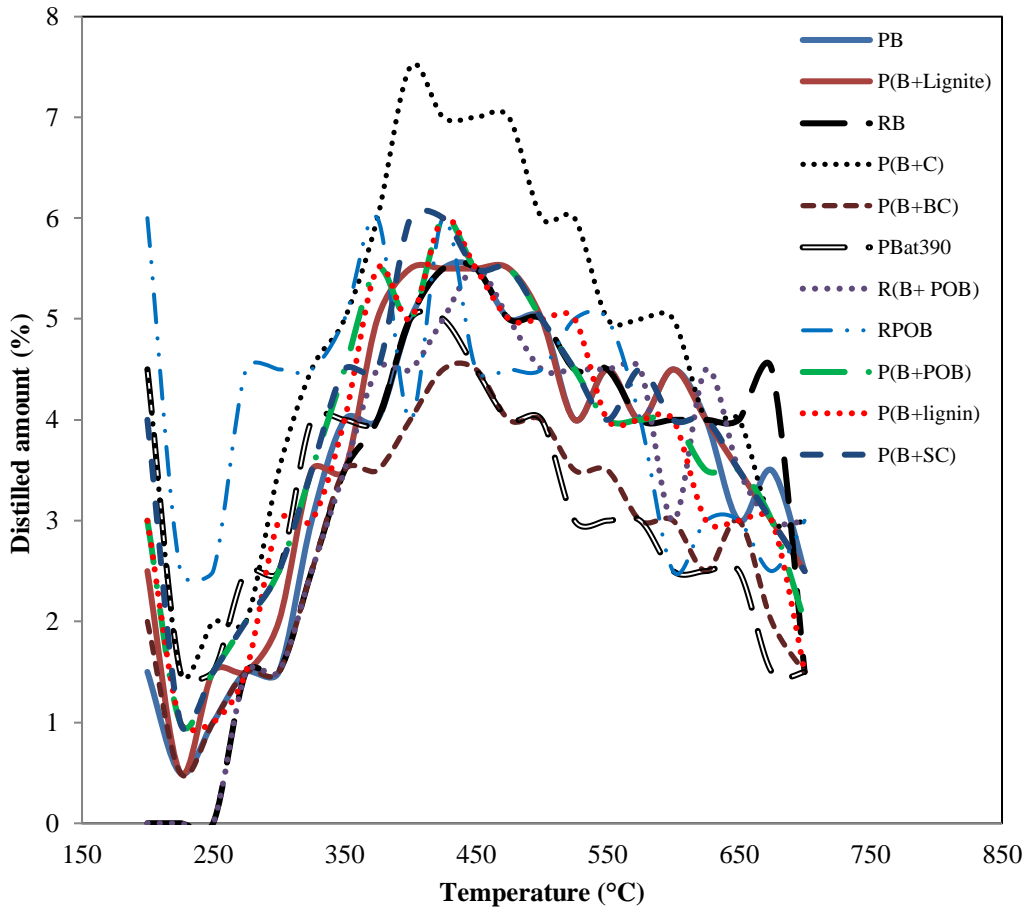
Figure 6.3. Distilled amounts of the samples versus temperature. (PB: pyrolysed bitumen at 380 °C, RB: raw bitumen, PBat390: pyrolysed bitumen at 390 °C, RPOB: raw Partially Oxidized Bitumen at 380 °C, P(B+POB): pyrolysed mixture of bitumen and partially oxidized bitumen at 380 °C; R(B+POB): raw mixture of bitumen and partially oxidized bitumen at 380 °C; P(B+lignite): pyrolysed mixture of bitumen and lignite at 380 °C; P(B+C): pyrolysed mixture of bitumen and cellulose at 380 °C; P(B+BC): pyrolysed mixture of bitumen and bituminous Coal at 380 °C; P(B+lignin): pyrolysed mixture of bitumen and lignin at 380 °C; P(B+SC): pyrolysed mixture of bitumen and subbituminous coal at 380 °C)

Unlike Ukwuoma work (Ukwuoma, 1999) who showed that the Nigerian tar sand distills cumulatively for about 5% up to 260 °C, Table 6.1, Table 6.2, Table 6.3 and Table 6.4 shows that the raw Cold Lake bitumen distilled only about 1% up to 260 °C and the pyrolysed bitumen at 380 °C distilled about 4% up to 260 °C. The comparison of the distilled raw and distilled pyrolysed bitumen show similar amounts in each temperature range except for temperature ranges up to 260 °C. The raw partially oxidized bitumen shows the highest amount of

distillation up to 260 °C and it is observed that about 13% of the raw partially oxidized bitumen is distilled below 260 °C.

According to Figure 6.3 and Table 6.4, one major peak is observed in the temperature range of 400-500 °C which is similar to Ukwuoma work (Ukwuoma, 1999) in which there was an increase in the distillation amount in the range of 425- 490 °C. According to Figure 6.3, Table 6.2, Table 6.3 and Table 6.4 the distillation amount increased in this temperature range for all the samples.

The comparison of the raw bitumen distillation amounts to other sample distillation amounts in Table 6.1 show that at low temperatures (<275 °C) the raw bitumen has the lowest amount of distillation amount in comparison to the pyrolysed bitumen samples at 380 °C and 390 °C. This shows some cracking happened at low temperatures and this idea is similar to Carbognani, *et al.* work which showed that cracking reactions can happen at temperatures lower than 350 °C (Carbognani, et al. 2007).

According to Table 6.2, Table 6.3 and Table 6.4, the cumulative distilled amounts increased a lot after addition of the additives. In temperature range of 400- 500 °C, the mixture of bitumen and cellulose showed the largest distilled amounts.

Ukwuoma, et al. (Ukwuoma, et al. 2002) showed that by increasing the temperature, the light fractions also increased from 20% to 40 and 43% at the operating temperatures of 250 °C, 300 °C and 350 °C. The amount of the intermediate fractions also increased, yet the amount of the heavy fractions decreased by an increase in temperature. According to Table 6.5, the amount of the light fractions (Heavy naphtha, Kerosene and Distilled fuel oil) increased to a great extent after the pyrolysis of the additive and the bitumen. The comparison

of the distillation distribution of the raw bitumen and the distillation distribution of the raw mixture of bitumen and partially oxidized bitumen show that although the raw mixture was well mixed, it still demonstrated almost the same distribution that was resulted for the raw bitumen. The comparison of the pyrolysed bitumen at 380 °C and 390 °C showed similar results with the results of Ukwuoma work which showed that when the operating temperature increased, the yield of heavy distilled products decreased. The residue and Gas oil distilled amounts of the pyrolysed bitumen at 390 °C are lower than the same products for the pyrolysed bitumen at 380 °C. Among the mixtures, the mixtures of bitumen and cellulose and the mixture of bitumen and partially oxidized bitumen showed the highest amounts of Kerosene and Distillate fuel oil. The mixture of pyrolysed bitumen and bituminous coal seemed to be the only mixture which showed a distinct difference in the amount of the Kerosene and Distillate fuel oil production in comparison to the production of the named two groups distilled from the raw bitumen (Table 6.5).

6.4. References

Carbognani, L.; Lubkowitz, J.; Gonzalez, M. F.; Pereira-Almao, P. High Temperature simulated Distillation of Athabasca Vacuum Residue Fractions. Bimodal Distributions and Evidence for Secondary "On-Column" Cracking of Heavy Hydrocarbons. *Energy Fuel*. **2007**, *21*, 2831-2839

Ukwuoma, O. Comparative study of the compositional characteristics of liquids derived by hydrotreating of Nigerian tar sand bitumen. I. simulated distillation. *Petroleum Science and Technology*. **2002**, *20*, 525-534

Ukwuoma, O. Study of composition of Nigerian tar sand bitumen. *Petroledum science and technology*. **1999**, *17*, 57-65

7. CHAPTER 7: ELEMENTAL ANALYSYS OF THE OXYGENATE CONTAINING MATERILALS AND THEIR COPYROLYSED MIXTURE WITH BITUMEN

7.1. Introduction

Today's world pays much attention to refining and upgrading the residues and heavy vacuums to lighter fractions because the world's supply for the light oil is decreasing every day. Generally, the oil sand derivatives contain high level of nitrogen and sulfur amount which are environmentally hazardous and cause air pollution when are combusted and also have poisoning effects on catalyst cracking (Ferdous, *et al.* 2006). Therefore, finding the quality improving methods which can both provide light liquid fraction production with less amount of heteroatoms would be of importance. And of course, one of the other preliminary goals of upgrading is to minimize the carbon to hydrogen ratio of the products which directs to production of lighter products.

One of the main objectives of this thesis, which was also discussed in previous chapters, was to improve the liquid yield from bitumen pyrolysis at low temperature, yet the main problem which rose was the low kinetic rate of the reactions at low temperatures. It was hypothesized in the previous chapters that the addition of oxygenate containing materials would help increase the rates. However, this chapter discusses the addition of the additive in another aspect. It looks through the products by the elemental component ratios of the products. For example, if an additive possesses low nitrogen content individually, it might be a proper additive in lowering the total product's nitrogen content. In this study, the carbon, hydrogen, nitrogen and sulfur amounts of each sample individually and the mixture compounds were studied and the advantageous of adding the oxygenate containing materials were discussed from the elemental analysis point of view.

One aspect of the coprocessing technology that has not been much studied before is the effects that coprocessing has on the products' elements. Medina *et al.* showed that when coal is copyrolysed with bitumen, there would be less amount of heteroatoms in light products and also higher amount of heteroatomns in heavier products (Medina, *et al.* 1989). Eamsiri, *et al.* tried using a catalyst named presulfied nickel molebdate while coprocessing oil and coal and they showed that the elemental analysis of the products had similar results when coal and oil were coprocessed with catalyst and when they were coprocessed without the presence of any catalyst (Eamsiri. et al, 1991). They observed that the addition of the aromatic compressed oil Kuwait atmoshpheric residue (KAR) and Koppers creosote oil (KC300) to coal, increased the hydrogen content of the products. The simulated distillation results showed that the addition of the coal to all the three types of the oils resulted an increase in the amount of the material with boiling point below 200 °C. They have studied the asphaltenes produced from the reaction of the oils with coal and observed that due to the presence of coal-derived products, some condensations have occurred to the heavy oil. However, this idea is adverse to the idea of Steer, *et al.* who believed that only a very small percentage of the carbon in the oil is coal derived (Steer, *et al.* 1987). Colombe *et al.* showed that the addition of the subbituminous coal to Cold Lake vacuum bottoms caused an increase in the C/H atomic ratio, sulfur amount and vanadium and increased the oxygen and nitrogen content (Colombe, et al. 1985).

Chakma, *et al.* studied coprocessing of a subbituminous coal with Pentane soluble maltene Athabasca bitumen fractions (e.g; saturates, polyaromatics and mono/di aromatics) and also with the Athabasca virgin bitumen (Chakma, 1993). They showed that the first group mixtures give higher coal conversion and less coke formation. Among the first group solvents, polyaromatics and mono/di aromatics provided the highest liquid yield respectively. Polyaromatics also showed the highest coke yield and provided the lowest C/H ratio for the products. Surprisingly, the addition of saturates to bitumen increased the C/H ratio, although the saturates are mainly rich in hydrogen. They suggested that the increase in the C/H ratio after the addition of saturates to bitumen is because of

the increase in the gas yield. They observed that by the addition of the saturates to bitumen, the gas yield increased and much of the hydrogen content of the feeds is released in the format of gas and that is basically the reason of the increase in C/H ratio in the liquid product.

Pan, et al. studied the effect of copyrolysis of low rank coals and biomass and did not observe many interactions between the two feeds (Pan, et al. 1996). Garcia et al. suggested that when biomass and petroleum residue were coprocessed, biomass reduced the sulphur content and the ash content of the petroleum residue and increased the low PH value of the bio-oil. Biomass could also improve the reactor feeding process by increasing the maximum capacity of the feed (Garcia, *et al.* 2001). They suggested that the most thermal reactions that happen in lignin is the cracking of the α and β alkyl aryl ether bonds. They summarized the general thermolysis reactions which happen among polysaccharides as "cleavage of glycosidic, C-H, C-O, and C-C bonds, dehydration, decarboxylation, decarbonylation reactions, formation C-C, C=C, C-O bonds as well as carbonyl and carboxyl groups."

Many works were done on different variables which affect the amount of light and heavy product yields after pyrolysis, for example the effect of temperature and the other variables on pyrolysis have long been studied, yet there is not much study done on the quality implications such as the amount of decrease in C/H ratio, sulfur and nitrogen amount. This study shows the elemental analysis on the raw and pyrolysed individual samples and also studies the same analysis on the raw and pyrolysed mixtures. It gives an idea of how different oxygenate containing material changed the total carbon, hydrogen, nitrogen and sulfur amount of the mixture.

7.2. Calculations

For the elemental analysis of the samples, in order to have the exact results, each number that is presented in this study is an average amount of minimum three runs. To have a clear idea of a diversity of the results, the standard deviation is calculated for the results. The average result is calculated by Equation 7.1 and the standard deviation is obtained by Equation 7.2.

$$X_{ave} = (X_1 + X_2 + X_3)/3 \qquad \text{(Equation 7.1)}$$

$$X_{SD} = ([(X_1 - X_{ave})^2 + (X_2 - X_{ave})^2 + (X_3 - X_{ave})^2]/3)^{0.5}$$

$$\text{(Equation 7.2)}$$

The average data and the standard deviations derived from the elemental analysis of the samples are brought in Table 7.1.

7.3. Results and discussions

Table 7.1 shows the elemental analysis of the raw and pyrolysed samples used in this study. The weight percentages of the C, H, N and S were given by the CHNS analyzer. The last column in Table 7.1 shows the oxygen wt% and is calculated by Equation 7.3.

O wt%= 100- C wt% - H wt% - N wt%- S wt% $\qquad$ (Equation 7.3)

It was observed that sum of the weight percentages of C, H, N and S for the raw bitumen and for the mixture of raw bitumen and partially oxidized bitumen were more than 100%. The analysis for each sample was done three times and for all the three times the sum of the elemental amounts for the named two samples were about 1% more than 100%. Although for each sample minimum three runs were done, having many runs for an experiment is not a proof of accuracy. The number of the runs is only an indication of the repeatability. This error that the sum of the element percentages is more than 100% could be caused by random errors such as errors in the equipment software.

Although the standard deviations were calculated for each sample, it is not of much importance to compare the absolute values of the elements with each other and the effect of a bias in the absolute value would be reduced by taking the ratios. In order to have a more reliable data to compare the changes in the elements of the samples, the molar ratio of H/C, N/C and S/C were calculated and are brought in Table 7.2.

Table 7.1. Elemental (C, H, N, S, O) analysis of the samples and the standard deviations. (RB: raw bitumen, PB: bitumen pyrolysed at 380 °C for one hour, PBat390: bitumen pyrolysed at 390 °C for one hour, RPOB: raw partially oxidized bitumen, RC: raw cellulose, Rlignin: raw lignin, Rlignite: raw lignite, RBC: raw bituminous coal, RSC: raw subbituminous coal, PC: cellulose pyrolysed at 380 °C for one hour, Plignin: lignin pyrolysed at 380 °C for one hour, Plignite: lignite pyrolysed at 380 °C for one hour, PBC: bituminous coal pyrolysed at 380 °C for one hour, PSC: subbituminous coal pyrolysed at 380 C for one hour, R(B+POB): mixture of raw bitumen and partially oxidized bitumen, P(B+POB): mixture of bitumen and partially oxidized bitumen pyrolysed at 380 °C for one hour. R(B+C): Raw mixture of bitumen and cellulose, P(B+C): mixture of bitumen and cellulose pyrolysed at 380 °C for one hour, R(B+lignin): Raw mixture of bitumen and lignin, P(B+lignin): mixture of bitumen and lignin pyrolysed at 380 °C for one hour, R(B+lignite): Raw mixture of bitumen and lignite, P(B+lignite): mixture of bitumen and lignite pyrolysed at 380 °C for one hour, R(B+BC): Raw mixture of bitumen and bituminous coal, P(B+BC): mixture of bitumen and bituminous coal pyrolysed at 380 °C for one hour, R(B+SC): Raw mixture of bitumen and subbituminous coal, P(B+SC): mixture of bitumen and subbituminous coal pyrolysed at 380 °C for one hour)

Sample	C (wt %)	*SD C%	H (wt %)	SD H%	N (wt %)	SD N%	S (wt %)	SD S%	O (wt %)
RB	85.07	0.12	9.95	0.02	0.84	0.33	5.32	<0.01	0
PB	84.36	0.62	9.61	0.06	0.64	0.07	5.03	0.04	0.36
PBat390	84.91	0.31	9.39	0.09	0.73	0.14	4.68	0.03	0.29
RPOB*	84.83	0.69	9.23	0.08	0.68	0.05	4.62	0.05	0.64
RC	43.68	0.10	5.98	0.05	0	_	0.15	0.04	50.19
Rlignin	49.05	0.02	4.73	<0.01	0.06	<0.01	4.42	0.07	41.74
Rlignite	58.73	0.05	4.43	0.03	0.93	<0.01	0.79	0.05	65.12
RBC	84.28	0.10	4.56	0.7	1.37	<0.01	0.72	0.03	9.07
RSC	65.40	0.13	4.22	<0.01	0.82	0.01	0.37	0.01	29.19
PC	79.49	0.39	4.08	0.02	0	_	0.13	0.04	16.3
Plignin	52.40	1.73	2.99	0.12	0.10	0.01	3.87	0.07	40.64
Plignite	62.48	0.38	3.69	0.02	1.05	0.01	0.76	0.03	32.02
PBC	77.17	2.52	4.01	0.08	1.24	0.03	0.76	0.07	16.82
PSC	68.33	0.23	3.48	0.04	0.90	<0.01	0.41	<0.01	26.88
R(B+POB)	84.98	0.22	9.80	0.04	0.80	0.25	5.28	0.03	0
P(B+POB)	84.14	0.69	9.51	0.08	0.61	0.02	4.79	0.02	0.95
R(B+C)	81.42	0.68	9.54	0.10	0.64	0.16	4.80	0.06	3.6
P(B+C)	84.69	1.13	9.24	0.14	0.55	0.03	4.76	0.06	0.76
R(B+lignin)	82.04	0.45	9.43	0.07	0.76	0.04	5.20	0.01	2.57
P(B+lignin)	83.02	0.53	9.28	0.21	0.70	<0.01	5.00	0.14	2
R(B+lignite)	82.25	0.65	9.32	0.07	0.72	0.14	4.84	0.07	2.87
P(B+lignite)	83.51	0.32	9.21	0.08	0.66	0.03	4.71	0.06	1.91
R(B+BC)	84.28	0.20	9.81	0.06	0.55	0.03	5.17	0.03	0.19
P(B+BC)	83.85	0.52	9.36	0.04	0.71	0.13	4.68	0.07	1.4
R(B+SC)	83.78	0.25	9.68	0.05	0.56	0.07	5.10	0.06	0.88
P(B+SC)	84.14	0.50	9.29	0.07	0.65	0.09	4.66	0.03	1.26

*The information on the pyrolysed partially oxidized bitumen was not collected.

Table 7.2. Molar ratio of H/C, N/C, S/C and O/C. (RB: raw bitumen, PB: bitumen pyrolysed at 380 ℃ for one hour, PBat390: bitumen pyrolysed at 390 ℃ for one hour, RPOB: partially oxidized bitumen, RC: Raw Cellulose, Rlignin: raw lignin, Rlignite: raw lignite, RBC: raw bituminous coal, RSC: raw subbituminous coal, PC: cellulose pyrolysed at 380 ℃ for one hour, Plignin: lignin pyrolysed at 380 ℃ for one hour, Plignite: lignite pyrolysed at 380 ℃ for one hour, PBC: bituminous coal pyrolysed at 380 ℃ for one hour, PSC: subbituminous coal pyrolysed at 380 ℃ for one hour, R(B+POB): mixture of raw bitumen and partially oxidized bitumen, P(B+POB): mixture of bitumen and partially oxidized bitumen pyrolysed at 380 ℃ for one hour. R(B+C): Raw mixture of bitumen and cellulose, P(B+C): mixture of bitumen and cellulose pyrolysed at 380 ℃ for one hour, R(B+lignin): Raw mixture of bitumen and lignin, P(B+lignin): mixture of bitumen and lignin pyrolysed at 380 ℃ for one hour, R(B+lignite): Raw mixture of bitumen and lignite, P(B+lignite): mixture of bitumen and lignite pyrolysed at 380 ℃ for one hour, R(B+BC): Raw mixture of bitumen and bituminous coal, P(B+BC): mixture of bitumen and bituminous coal pyrolysed at 380 ℃ for one hour, R(B+SC): Raw mixture of bitumen and subbituminous coal, P(B+SC): mixture of bitumen and subbituminous coal pyrolysed at 380 ℃ for one hour)

Sample	H/C (molar ratio)	N/C (molar ratio)	S/C (molar ratio)	O/C (molar ratio)
RB	1.40	<0.01	0.02	0
PB	1.37	<0.01	0.02	<0.01
PBat390	1.33	<0.01	0.02	<0.01
RPOB	1.30	<0.01	0.02	<0.01
RC	1.64	0	<0.01	0.86
Rlignin	1.16	<0.01	0.03	0.64
Rlignite	0.90	0.01	<0.01	0.45
RBC	0.65	0.01	<0.01	0.08
RSC	0.77	0.01	<0.01	0.33
PC	0.61	0	<0.01	0.15
Plignin	0.68	<0.01	0.03	0.58
Plignite	0.71	0.01	<0.01	0.38
PBC	0.62	0.01	<0.01	0.16
PSC	0.61	0.01	<0.01	0.29
R(B+POB)	1.38	<0.01	0.02	0
P(B+POB)	1.36	<0.01	0.02	<0.01
R(B+C)	1.41	<0.01	0.02	0.03
P(B+C)	1.31	<0.01	0.02	<0.01
R(B+lignin)	1.38	<0.01	0.02	0.02
P(B+lignin)	1.34	<0.01	0.02	0.02
R(B+lignite)	1.36	<0.01	0.02	0.02
P(B+lignite)	1.32	<0.01	0.02	0.02
R(B+BC)	1.40	<0.01	0.02	<0.01
P(B+BC)	1.34	<0.01	0.02	0.01
R(B+SC)	1.39	<0.01	0.02	<0.01
P(B+SC)	1.32	<0.01	0.02	0.01

*The information on the pyrolysed partially oxidized bitumen was not collected.

The data in Table 7.2 show that obviously the H/C ratios are lower for coal samples than for bitumen. Cellulose has clearly higher H/C ratio than raw bitumen. The N/C ratios are very low for all the samples. It is observed that the S/C ratios of the raw additives (except for raw lignin) are lower than the same ratio for the raw bitumen. As it was expected, the molar ratio of O/C for the raw

additives are much higher than for the raw bitumen. Adding the oxygenate containing materials to bitumen have increased the O/C ratio of the samples.

Unlike Eamsiri et al work (Eamsiri, 1991)., who showed that after the copyrolysis of the oil and coal, the hydrogen content of the products increased, this study showed that when the additives were added to bitumen the H/C remained almost the same and some decreasing was also monitored in the H/C ratio. Eamsiri et al. believed that when coal was added to oil, some condensations happened to oil (Eamsiri, et al. 1991) but Colombe et al. disagreed with this idea and believed that not much percentage of the carbon in the copyrolysed samples was coal derived (Colombe, et al. 1985). The present study supported the Colombe et al. idea and showed that after the raw mixtures of coal and bitumen were pyrolysed, not much difference happened to the carbon content of the mixture (Colombe, et al. 1985). They also showed that when subbituminous coal was added to Cold Lake bitumen, the amount of sulfur and the H/C ratio decreased (Colombe, et al. 1985).

Table 7.3 gives the relative changes that happen in the H/C, N/C, S/C and O/C ratios after copyrolysis. The change is given per ratio of the raw mixed sample (Equation 7.4).

Relative change in X/C (%)= [(X/C) of raw sample – (X/C) of pyrolysed sample] ×100/ (X/C) of raw sample   (Equation 7.4)

Although the values of the ratios are small for all the ratios (especially for N/C and S/C which the ratios are <0.1 and about 0.02 respectively), the relative changes in the ratios are considerable for some of the samples.

Table 7.3. Relative changes in H/C, N/C, S/C and O/C ratios after pyrolysis

Samples	H/C (relative %)	N/C (relative %)	S/C (relative %)	O/C (relative %)
Bitumen	2.60	23.17	4.65	130.76
bitumen and partially oxidized bitumen	1.99	22.99	8.37	211.57
bitumen and cellulose	6.88	17.38	4.66	79.70
bitumen and lignin	2.75	8.98	4.98	23.10
bitumen and lignite	2.67	9.72	4.15	34.45
bitumen and bituminous coal	4.10	-29.75	9.01	-640.62
bitumen and subbituminous coal	4.44	-15.57	9.01	-42.57

According to Table 7.3, cellulose makes the highest difference to the H/C ratio. It is observed that all the additives, decrease the H/C and S/C ratio after pyrolysis. However, the mixtures of bituminous coal and bitumen and the mixture of subbituminous coal and bitumen increased the S/C and O/C values after pyrolysis.

Garcia et al. observed that after coprocessing biomass and petroleum residue, the sulfur amount was reduced (Garcia, et al. 2001). Our study showed that the addition of whether cellulose and lignin to bitumen increased the S/C ratio because the S/C ratio sign is positive in Table 7.3.

In the previous chapter it was observed that about 90% of the most samples are Gas oil and Residuum which are heavy fractions so the main products of the copyrolysis operations can be assumed as heavy fractions. Medina et al. showed that when coal is pyrolysed with bitumen, there was a higher amount of heteroatoms in the heavy product (Medina, et al. 1989). This idea was half proved in our study. Our study showed that when coal and bitumen were copyrolysed, the N/C ratio increased while the S/C ratio decreased.

7.4. References

Chakma, A. Coprocessing of a sub-bituminous coal with liquid fractions derived from Athabasca bitumen. *Fuel Processing Technology*. **1993,** *36*, 147-153.

Colombe, S.; Rahmani, P.; Fouda, S.; Ikura, M.; Sawatzky, H. Influence of reducing gas in the coprocessing of coal and bitumen. *Preprints of the American Chemical Society*. **1985,** *30 (4),* 366-370

Eamsiri, A.; Larkins, F. P; Jackson, W. R. Studies related to the structure and reactivity of coals: 20. Coprocessing of Victorian brown coal with petroleum residues and with a coal tar distillate. *Fuel Processing Technology*. **1991**, *27*, 149-160.

Ferdous, D.; Dalai, A.K.; Adjaye, J. Comparison of product selectivity during hydroprocessing of bitumen derived gas oil in the presence of $NiMo/Al_2O_3$ catalyst containing Boron and Phosphorus. *Fuel*. **2006**, *85*, 1286-1297.

Garcia-Perez, M.; Chaala, A.; Yang, J.; Roy, C. Co-pyrolysis of sugarcane bagasse with petroleum residue. Part I: thermogravimetric analysis. *Fuel*. **2001**, *80*, 1245-1258

Medina, R. J.; Keogh, R.; Davis, B. H. Co-Processing coal and tar-sand resid: a new approach to alternative transportation fuels. *Sixth Annual International Pittsburgh Coal Conference*, Pittsburgh, Sept 25-29, 1989, cd 483

Pan, Y. G.; Velo. E,; Puigjaner, L. Pyrolysis of blends of biomass with poor coals. *Fuel*. **1996**, *75(4)*, 412-418

Steer, J.G.; Ohuchi, T.; Muehlenbachs, K. Efficacy of coal-bitumen co-processing as determined by isotopic mass balance calculations. *Fuel Processing Technology*. **1987**, *15*, 429-438.

8. CHAPER 8: CONCLUSIONS

Low temperature pyrolysis of bitumen was studied in the presence of various oxygenate containing materials. This was of interest, because it was reported that higher liquid yields are possible by thermal conversion at less severe conditions. However, when the reaction temperature is decreased, the reaction rate is also decreased. It was hypothesized that by co-feeding oxygenate containing materials the reaction rate can be increased during low temperature pyrolysis due to the weaker bonds between oxygen and carbon atoms in oxygenate containing materials. In summary, it was studied that whether the oxygenate containing materials can increase the conversion rates and if they can improve the quality of the bitumen pyrolysis products.

In the previous chapters all the results and discussions were brought in details. This chapter points out to a brief summary of all the previous results.

- In Chapter four, it was shown that the addition of the oxygenate containing materials did not lower the onset temperature. The changes that happened to the onset temperatures after the addition were negligible (less than 1 °C). Among all of the raw mixtures, only the mixture of bitumen and partially oxidized bitumen presented a lower onset temperature than for raw bitumen. However, whether the additives accelerate the reaction rates or not cannot be only judged by the changes in the onset temperatures. Therefore, the mass loss rates were studied to discuss the rates during the whole process of the pyrolysis time.

- The mass loss rates of the samples were studied at low temperatures (less than 425 °C). It was shown that the mass loss rates for the pyrolysed mixtures were higher than the mass loss rates for the raw bitumen. The higher mass loss rates for the pyrolysed mixtures show that more

compounds were able to lose mass at low temperature range. As it was discussed in Chapter four, these compounds are mainly low and medium molecular weight compounds including; alkanes, alkenes, benzene, toluene, styrene and other products with bonds that would break with providing low amount of energy at low temperature ranges. It was proved that there was higher amount of these compounds in the products of the pyrolysed mixtures. Thus, the goal of having more amount of light products by co-pyrolysis of the bitumen and oxygenate containing materials was achieved.

- It was also shown that the mass loss rates for the raw mixtures were higher than the mass loss rate for the raw bitumen at temperature range of 325-425 ℃. In this study, configuring the precise reaction rates was not the objective. However, the mass loss rate indicates some important points about the reactivity of the samples. In Chapter four, it was stated that the volatilizations and demoisturization were completed below 250 ℃. It can be concluded that in temperature range of 325-425 ℃, the higher mass loss rates for the raw mixtures shows the faster ability of the mixtures to take part in the reactions.

- The comparison between the mass loss rates for the raw bitumen and pyrolysed bitumen, shows that the mass loss rate for the raw bitumen is higher than the mass loss rate for the pyrolysed bitumen only at temperature range of 375-425 ℃. This is because the pyrolysed bitumen lost its organic compounds, which are mostly produced at 380 ℃, when it was pyrolysed in a micro batch reactor at 380 ℃ for one hour.

- The mass loss rates for the pyrolysed mixtures were less than the mass loss rates for the pyrolysed bitumen at temperature range of 375-425 ℃. According to the results discussed in Chapter five, the gas production was higher for the pyrolysed samples than for the pyrolysed bitumen.

These products were resulted by pyrolysis in a batch micro reactor at 380 °C. Therefore, the pyrolysed mixture already lost much of its products in the gas format so the mass loss rates for the mixtures are less than the pyrolysed bitumen at 375-425 °C.

- By comparing the experimental and the theoretical coke yields in Chapter four, it was shown that the pyrolysed mixture of bitumen and lignin and the pyrolysed mixture of bitumen and bituminous coal have the highest amount difference between the two coke yield amounts. Comparatively, these two mixtures produced less amount of coke yields after the pyrolysis. Because of the special features of lignin and bituminous coal (Section 4.2.3, chapter four), these two additives are able to produce low and medium molecular weight compounds at low temperature pyrolysis situations which were resulted mostly in the phases of gas and liquid and not coke.

- Besides the liquid components which were produced from pyrolysis, the gas products should also be considered. It would be beneficial to eliminate the hazardous gas compounds. The pyrolysis gas products were studied in Chapter five. This chapter showed the concentration of different gas components produced from pyrolysis. It was shown that the addition of partially oxidized bitumen and bituminous coal to bitumen kept the CO_2 production in almost the same mol% in comparison to the CO_2 produced from the pyrolysed bitumen at the same temperature. However, it was found that the addition of other oxygenate containing materials increased the CO_2 production more than twice of the same gas that was produced from only pyrolysed bitumen at the same temperature. The addition of the oxygenate containing materials decreased the total CO production (except for cellulose). By comparing the gas components produced from each sample, it was noticed that the amounts of almost all of the gas components (except CO and CO_2) that were produced from

mixtures were less than the same components that were produced only by bitumen. This idea shows that the addition of the oxygenate containing materials do not basically help bitumen to produce more light gas fractions.

- In Chapter six, it was found that the main product of the pyrolysis of all the samples is the gas oil which was about half of the total mass of the products. It was figured out that the addition of the oxygenate containing materials increased the production of heavy naphtha, kerosene and distillate fuel oil and decreased the amount of the residuum production.

- One of the goals of bitumen upgrading is improving the qualities of the products. Decreasing the heteroatoms existing in the bitumen can be considered as one of the improvements of bitumen upgrading. The elemental analyses of the samples were studied in Chapter seven. In this chapter, it was observed that all the additives decreased the amount of S/C ratio of the mixture when they were pyrolysed with bitumen. All (except bituminous coal and subbituminous coal) have also decreased the N/C.

All in all, although all the results never combine to help choose one or some of the additives as the best options for copyrolysis with bitumen, they show important advantages which let them be proper choices for copyrolysis. The additions of the oxygenate containing materials to bitumen have synergistic effect in accelerating the decomposition reactions, increasing the total gas and liquid production, less carbon monoxide production and less S/C and N/C.